AN EXPERIMENTAL INVESTIGATION INTO EXPLOSIVE FORMING OF SHEETS

by

MAJOR M. B. S. REKHI

DEPARTMENT OF MECHANICAL ENGINEERING

INDIAN INSTITUTE OF TECHNOLOGY KANPUR

APRIL, 1977

AN EXPERIMENTAL INVESTIGATION INTO EXPLOSIVE FORMING OF SHEETS

A Thesis Submitted
In Partial Fulfilment of the Requirements
for the Degree of
MASTER OF TECHNOLOGY

by

MAJOR M. B. S. REKHI

to the

DEPARTMENT OF MECHANICAL ENGINEERING

INDIAN INSTITUTE OF TECHNOLOGY KANPUR
APRIL, 1977

ME-1977-M-REK-EXP

DEDICATED TO

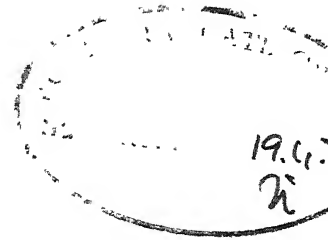   THE LOVING MEMORY OF

    MY REVEREND FATHER AND MY

    ELDEST SON, WHOM I LOST DURING
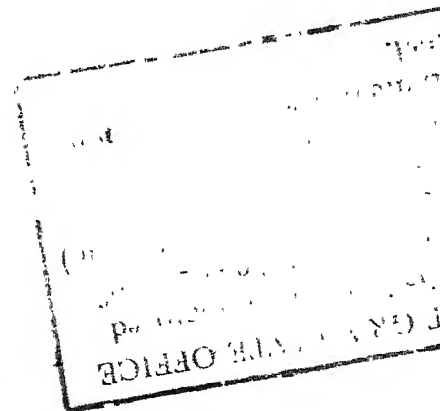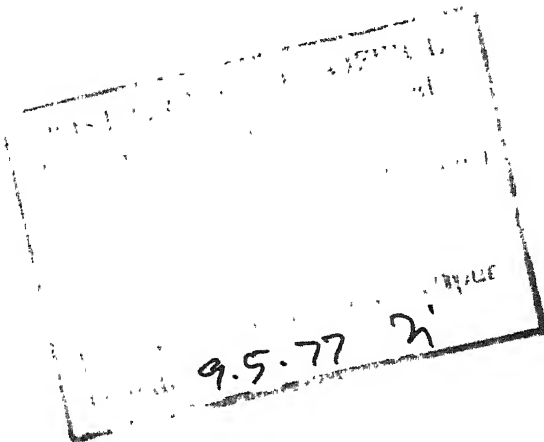
    THE COURSE OF THIS STUDY

CERTIFICATE

This is to certify that the work entitled "An Experimental Investigation Into Explosive Forming of Sheets" has been carried out under my supervision and has not been submitted elsewhere for the award of a degree.

G.S. KAINTH 19/4/77
Assistant Professor
Department of Mechanical Engineering
Indian Institute of Technology Kanpur

ACKNOWLEDGEMENT

TABLE OF CONTENTS

LIST OF FIGURES

ABSTRACT

The present work concerns with experimental investigation into stretch forming of sheet using explosive charge. To carry out stand-off under-water explosive forming operations using open-system, a ferrocement tank 1.525 M dia. and 1.55 M deep and supporting structure is designed and fabricated. Die-assembly, to accommodate a die of 150 mm dia., with supporting cradle is designed and fabricated. Details of experimental set-up are given in Chapter III.

Explosive forming tests are carried out on Brass, Stainless Steel and Aluminium sheets of various thicknesses using Cordtex explosive charge and No. 6 electric ICI - detonators.

A large number of experiments are carried out to study the effect of charge weight, stand-off distance, draw radius of die and annealing heat treatment on i) profile and polar deflection of blank, ii) thickness strain distribution and iii) radial strain distribution. The details of experimental conditions and measuring procedures are given in Chapter IV.

Results of the experimental investigation are
followed by discussion and are recorded in Chapter V.
A simple theoretical analysis proposed by Noble and Oxley[18]
is applied. Theoretically estimated values of polar deflec-
tion are found to be in agreement with experimental results
of the present investigation..

Broad conclusions and suggestions for further work
are outlined in Chapter VI.

CHAPTER I

INTRODUCTION

1.1. GENERAL

Sheet metal components are being extensively used in various applications, viz., pressure vessels, chemical plants, ship building, aviation and missiles; where the size is fairly large and the number of pieces required is small. Conventional methods of shaping sheet metal employ matched metal dies requiring expensive equipment and tooling which could be justified only with large quantities. Eventhough, the conventional process has very good reproducibility, however, it is uneconomical for production of a few pieces of large size.

Production of sheet metal components by unconventional methods of forming using high explosives has aroused tremendous interest since early fifties. Explosive forming has considerable applications in space industry, primarily, in the manufacture of complex shapes in high strength sheet materials such as Titanium, Rene 41 and Stainless steel which are difficult to form by conventional processes.

Methods of explosive forming can be classified as under.

1. Confined or Closed System

Confined system generally employes split dies which completely enclose the work piece as shown in Fig. 1.1(a). The explosion takes place in a confined space. The closed system has been used for sizing of thin walled tubing and preformed parts. This system is suitable for small sized parts only.

2. Unconfined or Open System

In unconfined system, Fig. 1.1(b), the explosion takes place in open space such that the whole of energy of explosion is not available for forming. The system is useful for large components where high loads are required for deforming sheets.

Explosive metal working operations can be divided into two main types.

1. Contact operations where explosive charge is placed in direct contact with work piece.

In contact operations, the pressure of several million lb f/in^2 is developed at the interface. Contact operations are employed in explosive welding, cladding, metal cutting, hardening and powder compaction.

UPPER DIE   PREFORM   EXPLOSIVE CHARGE   DETONATOR

FIRING LEADS

LOWER DIE   DIE CAVITY

(a)   Confined or closed system

TRANSMITTING FLUID

EXPLOSIVE CHARGE

H
S

HOLD DOWN RING

BLANK

DIE

VACUUM LINE
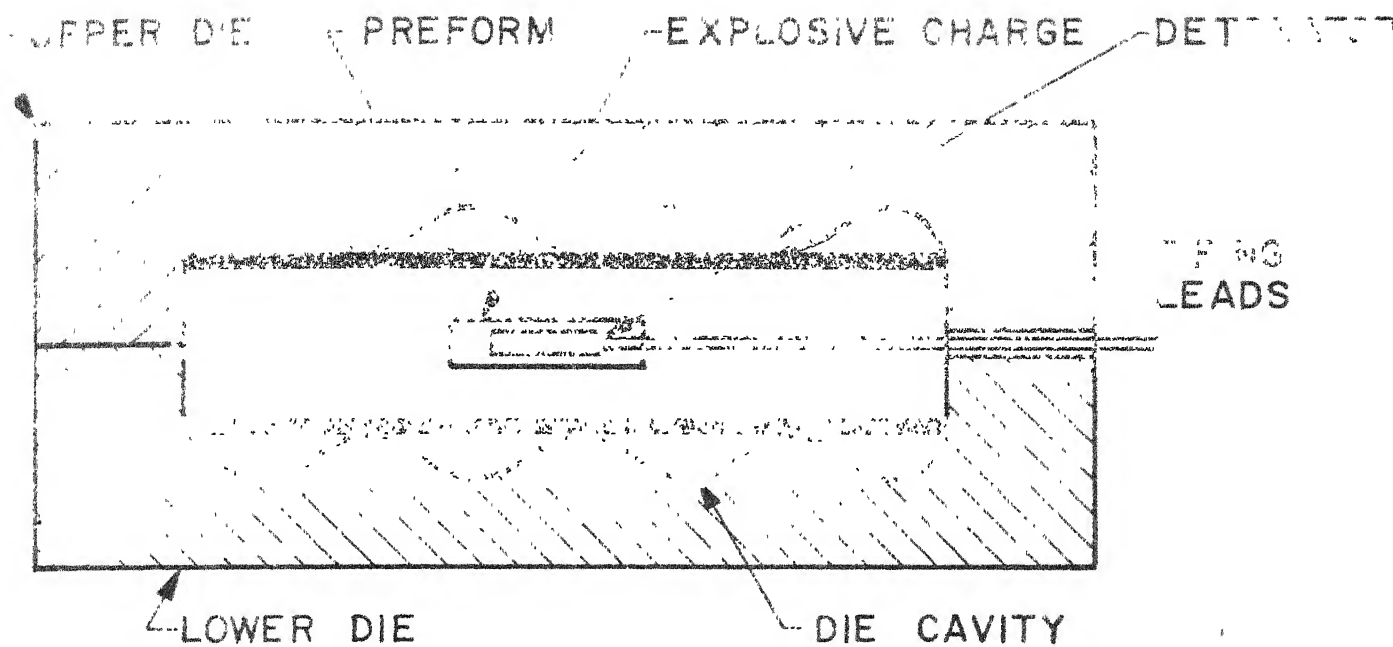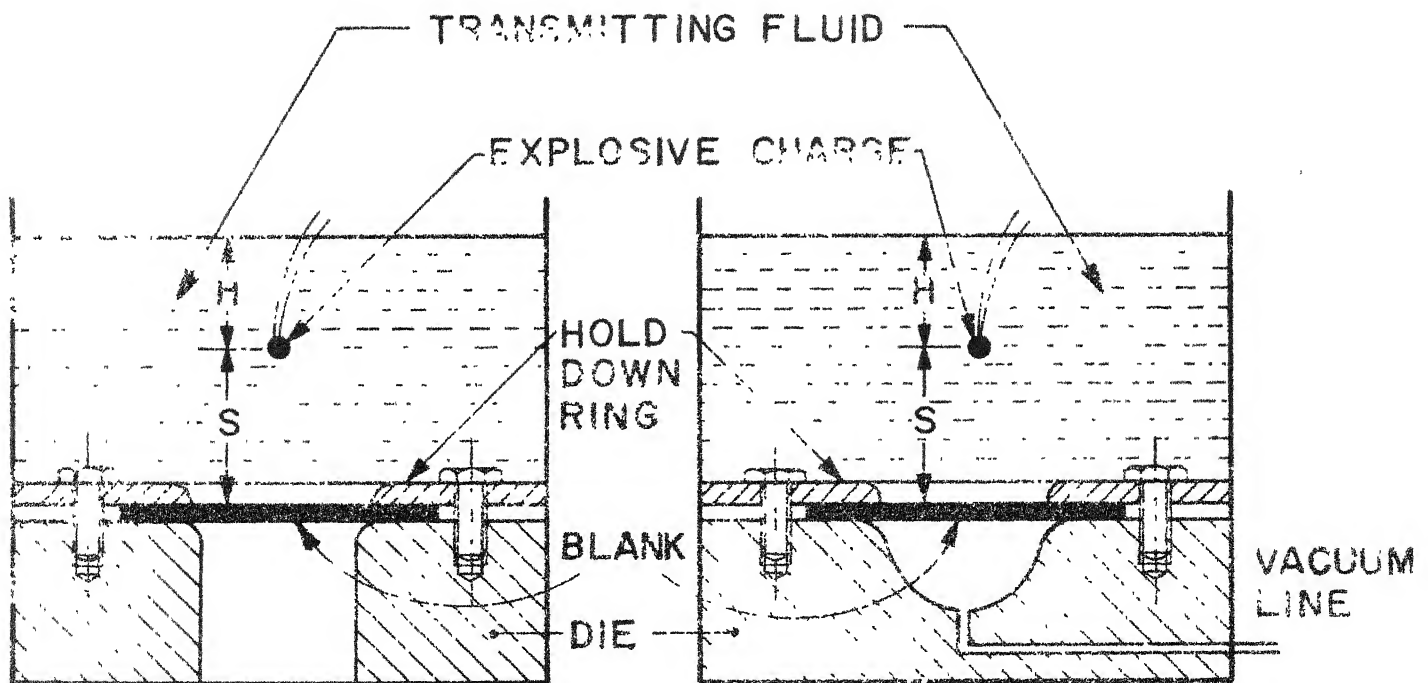
FREE FORMING   DIE FORMING

H = Hydrostatic head
S = Stand off Distance

(b)   Unconfined or open system

Systems of explosive forming

Fig. 1.1

2. Stand-off operations where charge is located some distance away from workpiece and the energy is transmitted through some intervening medium such as air or water.

In stand-off operations, the peak pressure decays as the shock wave travels through the trans-mitting medium, and consequently, the pressure exerted on the work piece is much less than that in contact operations. The pressure is of the order of several thousands lb f/in^2.

The nature of explosives and basic aspects of shock wave theory are given in the next two sections.

1.2 CHEMICAL EXPLOSIVES[1]

Chemical explosives are substances which can undergo rapid chemical reactions during which large quantities of heat and gaseous products are evolved.

Explosives can be divided into two main types viz, (i) detonating or high explosives and (ii) deflagrating or low explosives.

High explosives are characterised by very high rates of reaction and high pressure. They are divided into primary and secondary explosives. A primary or initiating explosive can usually be detonated by simple ignition by

means of spark, flame, impact or any other primary heat source. Secondary high explosives need initiators for detonation and can-not be exploded by ignition or impact. Primary explosives are used in detonators for initiating detonation in secondary explosives.

Most of the high explosives contain nitro compounds and complex esters of nitric acid. The high explosives in common use depend for their energy of reaction upon the fact that when oxygen is combined with nitrogen the reaction energy is almost zero, whereas, when oxygen combines with carbon or hydrogen the reaction is highly exothermic. When the explosive is detonated, the oxygen changes its affinity from nitrogen to carbon and hydrogen, thereby, forming CO, CO_2, water vapours, and free nitrogen. This reaction produces a large volume of gaseous products. The energy released depends upon the type of explosive used. The volume of gaseous products liberated is of the order of 1000 cm^3/gm. at N.T.P.

1.2.1 Properties of Explosives

Brief details of some of the explosives, in general use, are given below.

a) TNT C_1 H_5 N_3 O_6 (Trinitro-toluene) is a pale yellow crystalline solid. It possesses high strength and very low sensitivity to friction and impact. It

has a melting point of 81 ^{o}C and thus it can be cast to required shape. Its velocity of detonation is 6800 m/sec.

b) Tetryl or CE $C_7 H_5 O_8 N_5$ (Trinitro-Phenyl methyl nitromine) is a yellow crystalline solid explosive of high strength and *it has* rather high sensitivity to initiation by friction and impact. It is used as a base charge for detonators. Pressed tetryl pellets having a density of 1.5 to 1.6 gm/cm^3 are sometimes used in explosive forming operations, where these form a convenient point charge. Detonation velocity of tetryl is 7510 m/sec.

c) P E T N $C_5 H_8 N_{12} O_4$ (Penta-erythritol Tetranitrate) is a white crystalline compound having a melting point of 141 ^{o}C. and high thermal stability. It has a detonation velocity of 6500 m/sec. It has very high strength but is also highly sensitive to friction and impact. It is used as a base charge in detonators and is widely used in detonating fuses such as 'Cordtex', a strong waterproof fuse that detonates at 6500 m/sec. Cordtex is widely used in explosive forming processes because it can be coiled into desired shape.

d) Plastic explosives consist of a high brisant explosive such as R D X, $C_3 H_6 N_6 O_6$, (Cyclo-trimethylene trinitromine) and a bonding agent that forms a putty like mass. The explosive can be hand moulded and it is frequently used in metal working operations. Detonation velocity of R D X is 7810 m/sec.

e) Plastic sheet explosives have a P E T N base with other gradients to give tough flexible properties. Metabel (ICI) was originally developed for explosive hardening, but it has been used for other metal working operations such as welding and cladding of sheets.

1.2.2 Transmission of Energy of Detonation

When detonation is initiated in an explosive charge, the chemical reaction usually starts at a point and the detonation wave moves outwards in all directions at constant velocity leading to a spherical detonation front. Fig. 1.2(a) shows the detonation of an explosive charge immersed in a fluid medium. As the detonation front spreads through the charge, it leaves hot compressed gases which are in motion and capable of doing work. When the front reaches the boundary of the charge it interacts with the surrounding medium thereby generating shock waves in the medium. At the

same time waves are reflected from the boundary into the
gaseous products. The energy released by the detonating
explosive is transmitted through the surrounding fluid by
shock waves and expansion of gaseous products.

Fig. 1.2(b) illustrates the propagation of shock-
wave front when the explosive charge is in intimate contact
with a metal slab. At the explosive air boundary, the
behaviour of the shock wave is same as shown in Fig. 1.2(a).
At the metal-explosive interface, the detonation wave induces
a shock wave in the metal. Ahead of the shock wave, the
metal is undisturbed, however, behind the shockwave the
metal is highly compressed and attains a high particle velo-
city in the direction of shock wave.

Although arrangement for explosive forming is not
difficult to set up, but the associated deformation mecha-
nism is one of extreme complexity and involves the following
phenomena[2]:

a) Shock wave propagation through fluids and its
    interaction at the workpiece surface,

b) the reaction of metals to impulsive loading,

c) the subsequent interaction of the agitated fluid
    medium with the workpiece which includes the
    influence of gas bubble pulsation, cavitation   .
    and water hammer effect.

SHOCK WAVE FRONT AD AND ⬚
FRONT OF EXP⬚⬚ HOT GAS⬚
AF AND BG
UNEX⬚⬚ED HOT GA⬚S AH⬚
UNDETONATED EXPLOS⬚⬚
DETONATION FRONT AB
RELEASE WAVE FRONT ACB

(a)   Det⬚⬚⬚⬚ in atmosphere

SHOCK WAVE IN AIR
FRONT OF EXPANDING ⬚OT ⬚A⬚ES
⬚NEXPANDED HOT ⬚⬚⬚⬚
DETONATION ⬚⬚⬚⬚ AB
UNDETONATED EXPLOSIVE
RELEASE WAVE FRONT
COMPRESSED REGION OF METAL
METAL
SHOCK WAVE IN METAL
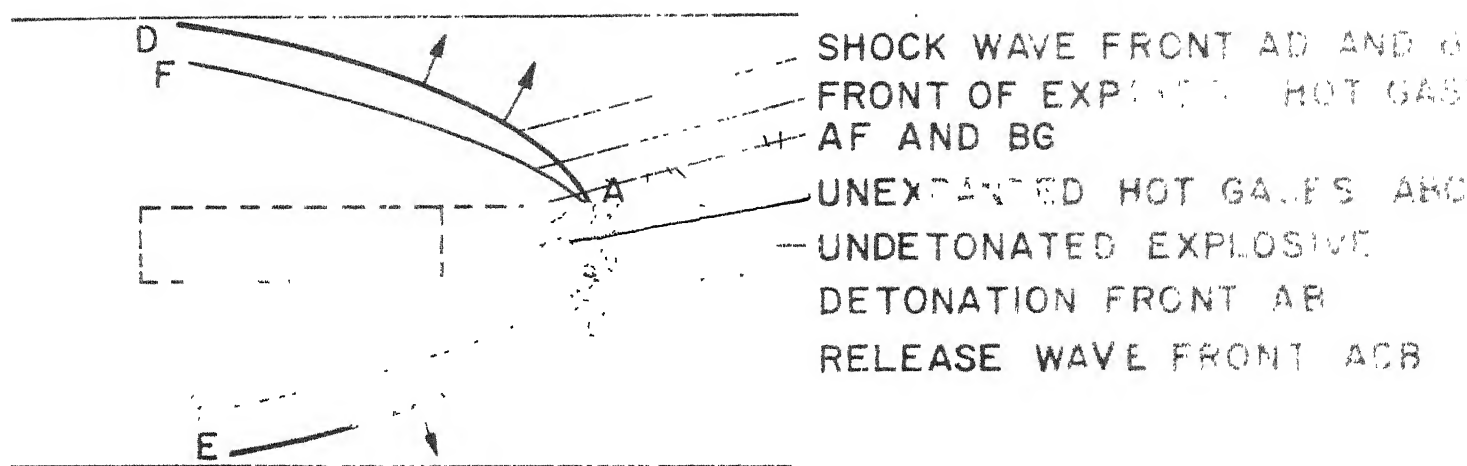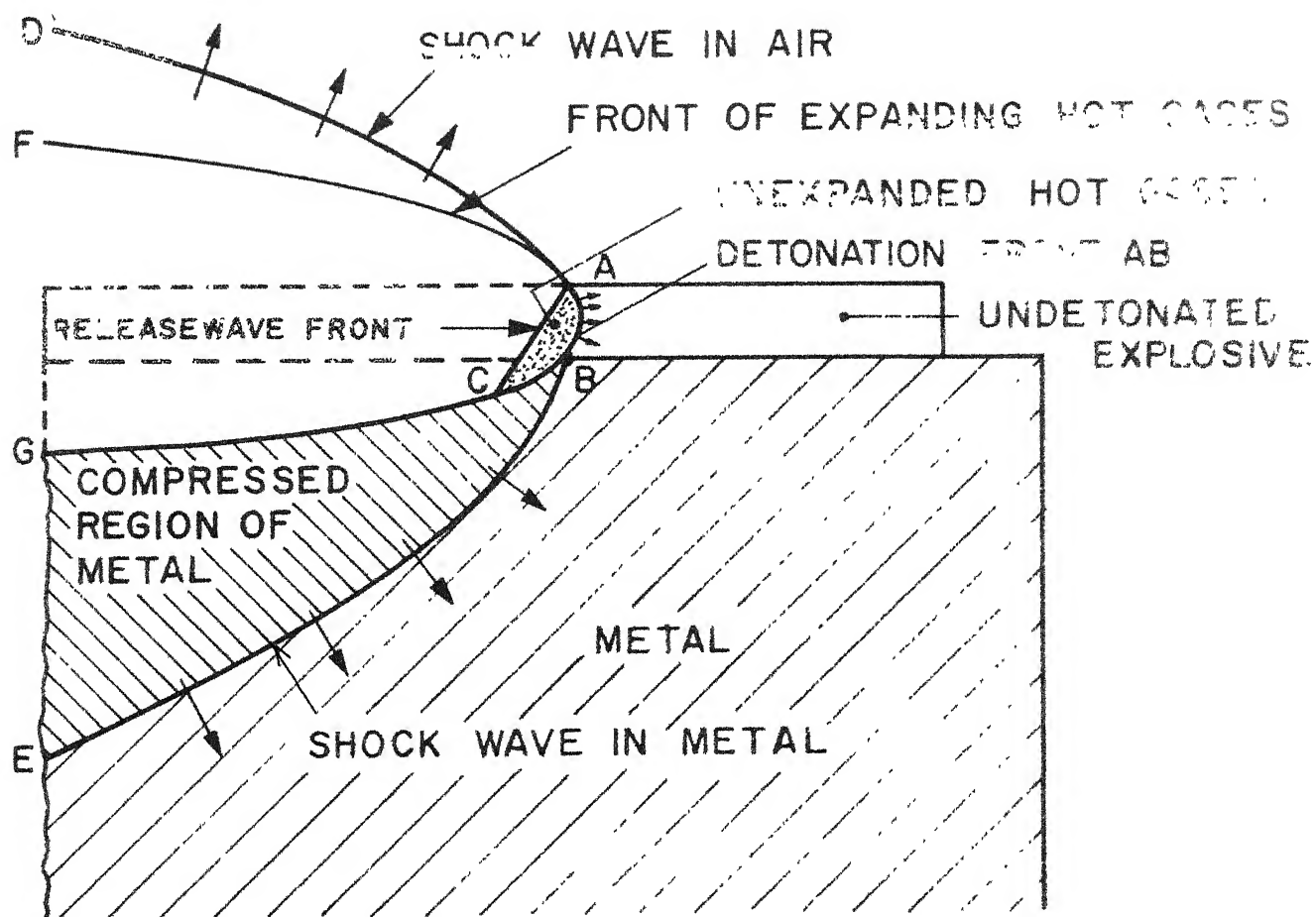
(b)   Detonation in contact with metal

Shock wave propagation.

Fig. 1.2

1.3 PROPAGATION OF SHOCK WAVE

When an explosive charge is detonated under water, it instantaneously generates gases at a very high pressure[3] of the order of 1×10^6 to 4×10^6 psi. Initially there is a complicated interplay of pressure waves inside the gas globe due to partial reflection of the detonation wave from explosive water interface back into the detonation products. It has not been possible to analyse the phenomena close to the charge because of high temperature and pressures involved and the lack of thermodynamic data of these extreme conditions. However, the explosion finally results in a pressure wave or primary shock wave which moves out spherically through the liquid. The gaseous products of the gas globe expand to a size several times its initial radius.

A unique relationship exists between the pressure in the shockwave front, its speed of propagation through the medium, and the velocity of a particle in the medium itself.[3] For small amplitude waves which move through a medium, initially at rest, the pressure across the shock front is given by Kolsky[4] as under,

$$p = \rho c u \qquad\qquad 1.1$$

where p = pressure across shock front

ρ = density of the medium

c = velocity of sound (shock waves move at the

velocity of sound in incompressible mediums)

u = velocity of a particle in the medium.

Bahrani and Crossland[5] explained the phenomena
of the energy release from the detonation of an explosive
charge. The nature of pressure pulse is shown in Fig. 1.3(a).
The primary shock wave is of 37 μ sec. duration and has a
sharp peak pressure of 17000 lb f/in^2. The secondary wave
which is due to pulsation of gas bubble is of 5 m. sec.
duration and has a peak pressure of 2100 lb f/in^2.

They mentioned that though the magnitude of peak
pressure produced by gas bubble is 10 to 20 percent of the
peak pressure of primary shock wave (Fig. 1.3(a)), however,
the duration of the secondary shock wave is much greater
than that of the primary shock wave. Hence, they concluded
that energy released due to pulsation of the gas bubble
contributes considerably in the deformation process.

Pearson[6] studied the effect of medium used for
transmitting the pressure pulse between the explosive and
the workpiece. Air and water are mediums normally used in
the explosive forming. Fig. 1.3(b) shows the variation of
peak pressure at workpiece as a function of stand-off
distance with two media, viz., air and water. The peak
shock pressure produced with air is lower than water because
air is much more compressible.

PRESSURE

$P = 17000 \text{ lbf/in}^2$

PRIMARY SHOCK WAVE

SECONDARY SHOCK WAVE

$P = 2100 \text{ lbf/in}^2$

37 μ sec

5 m. sec
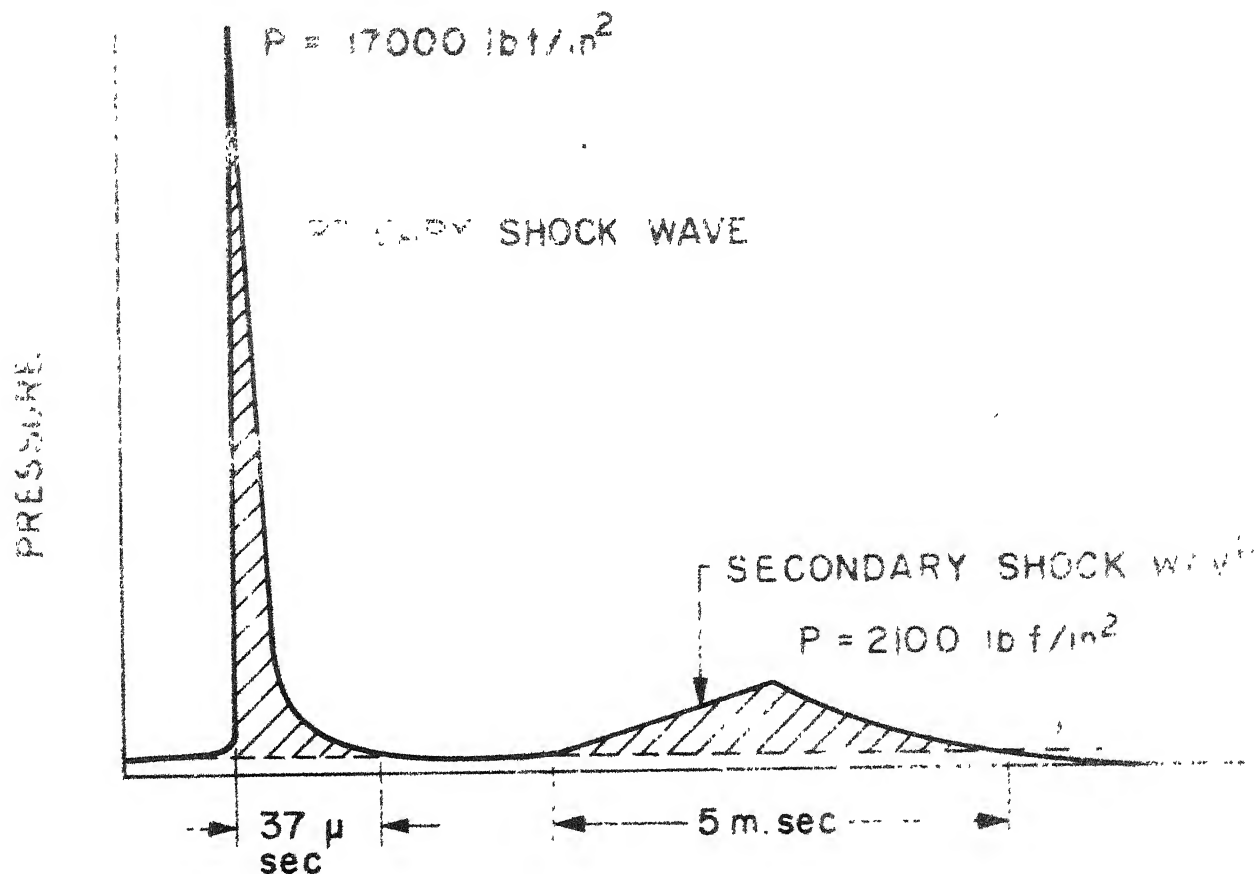
(a) Pressure versus time record 1.5 inch from 0.05 gm charge of tetryl exploded at depth of 3 feet (Reference 5)

$\text{X} \times 10^3$

PEAK PRESSURE

CHARGE 4 lb TNT

WATER

AIR

DISTANCE FROM CHARGE (feet)
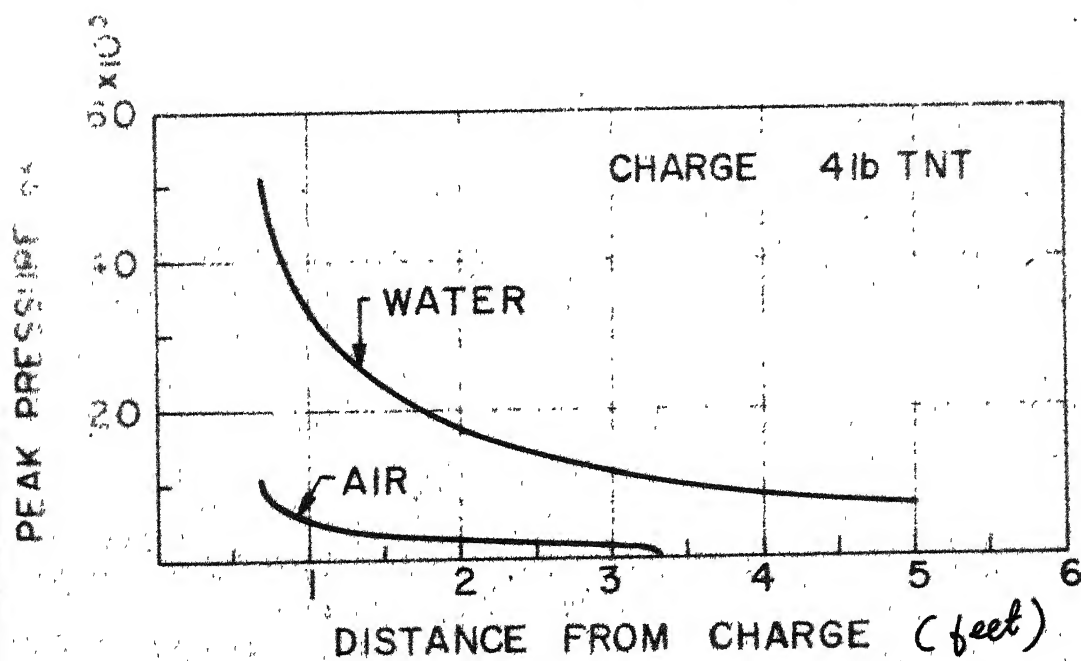
(b) Peak pressure versus stand off distance for explosive charges fired in water and air (Reference 6)

CHAPTER II

LITERATURE SURVEY

2.1 GENERAL

First ever recorded work on use of explosive is
that by Munroe[7] who described a technique for engraving
designs on metal by use of gunpowder in 1888.

During second world war, extensive studies were
made on effects of underwater explosions on materials. All
these records have been compiled by Cole[8]. Penny, et al[9].
compiled the studies on detonation mechanism of explosives
carried out during war.

Hudson[10] proposed a mechanism of deformation based
on the study of the damage done by underwater explosion on a
thin metal circular diaphragm. He mounted a small thin
lead diaphragm in a rigid closed container which was attached
to a structure. When an impulsive velocity was imparted to
the structure normal to the plane of diaphragm, the diaphragm
container moved and diaphragm material tended to remain
behind.

The various stages of deformation envisaged by
Hudson[10] are as under,   (Fig. 2.1 (a))

a) The diaphragm receives an initial impulsive velo-
     city. (shown by vertical arrows)

b) The material has a radial velocity distribution (shown by horizontal arrows) and material at periphery is restrained from moving.

c) The bending wave, shown by the sharp corners in the profile has progressed inward from edge.

d) As the diaphragm deforms further, the central region of diaphragm remains flat and moves with its initial velocity. The bending wave is travelling into central region progressively deforming the diaphragm.

e) As the bending wave nears the centre, deformation speeds up slightly.

f) The speeding up of the bending wave results in rounding off the apex of the conically deformed diaphragm.

Hudson[10] assumed that at zero time a uniform velocity normal to initial plane of diaphragm is impulsively acquired. At this stage radial velocity in the material is zero. The peripheral restraint is immediately felt resulting in two impulses being propagated as under.

a) a radial impulse travels inwards, leaving the central portion in a state of plane plastic flow with an induced radial velocity and

b) plastic bending impulse is generated near the edge,
because of the edge-restraint, and is propagated
slowly inwards.

These impulses tilt each annular element, thereby,
transfering the available kinetic energy to the central
region where the energy is converted into plastic work of
stretching. The final shape is essentially a cone with
rounded tip.

Johnson, et al.[11] have obtained a functional
relationship between the polar height of deformation and
the radial position of a particle. They assumed that the
shape of the deformed diaphragm is parabolic.

A circular blank is firmly clamped around its
periphery so that its initial position is defined by A_1
A_2 as shown in Fig. 2.1 (b). After being subjected to a
point explosive attack, the final shape of the blank is
described by $A_1 B_o A_2$. The maximum or polar height of the
bulge being h_o.

They[11] proposed that, in moving from its initial
to its final position, the blank assumes a series of forms
of increasing height as indicated by lighter lines. They
assumed that these intermediate blank shapes are described
by the following equation

$$y/h = 1 - \left(\frac{x}{a}\right)^m \qquad (2.1)$$
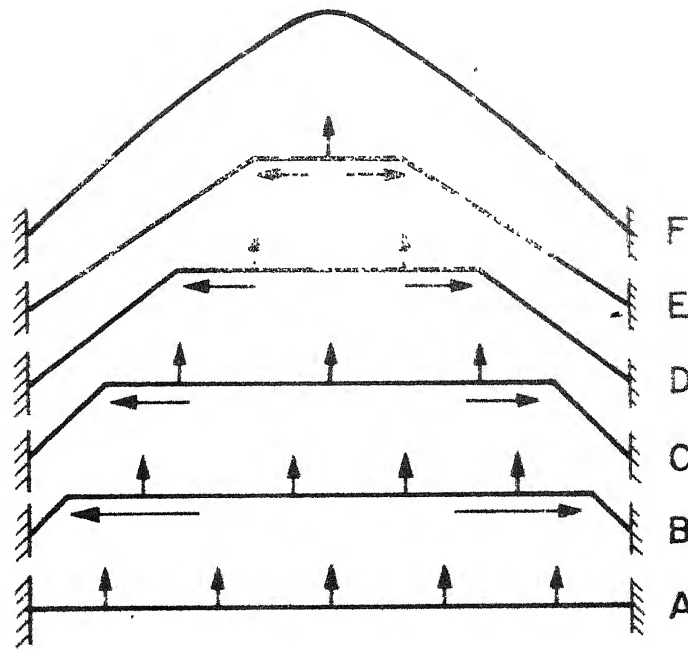
(a) Mode of deformation given by Hudson (Reference 10)
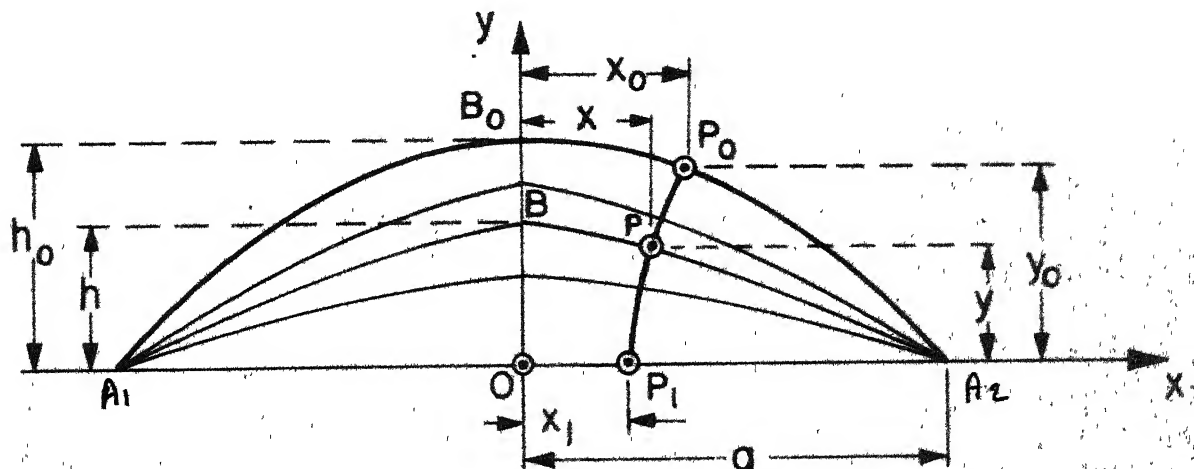
(b) Mode of deformation given by Johnson (Reference 11)

Fig 2.1

The parameters characterising the history of blank deflection being h and m. They proposed a mathematical model for the shape of the deformed blank, assuming that the points such as P_1 on blank follow orthogonal trajectories shown by points P and P_o in Fig. 2.1(b).

The history of deformation assumed by Johnson, et al.[11] is different from the one proposed by Hudson[10].

Boyd[12] carried out parametric investigation into large straining of membranes by explosive loading. He formulated a mathematical model assuming that

a) bending and shearing stresses are neglected so that a membrane theory can be used.

b) Work done by forces acting in the radial direction is neglected.

c) The elastic strains are negligible so that the general plastic theory of deformation is valid viz., material is incompressible and relations between octahedral shearing stress and octahedral shearing strain at a point is unique and single valued.

Johnson, et al.[2] have discussed the factors likely to influence the deformation in explosive forming. They propose that the deformation is not only due to primary shock wave but it is also due to subsequent energy transfer

arising from cavitation, water hammer and bubble pulsation effect. The primary shock wave impinging upon a stationary blank undergoes reflection at the blank face and it will be reflected either as a compression or rarefaction wave depending upon the rigidity of the blank. If the blank is assumed to be rigid, it will experience initially a pressure approximately twice that of the incident pulse. Once the blank begins to move, the pressure over the blank will be relieved.

The secondary shock wave produced by the pulsating gas bubble can also influence deformation depending upon the position of the bubble relative to the blank and water surface. The gas bubble continues to expand behind the primary shock wave and may undergo several oscillations before it finally breaks-up or migrates through the water. After each successive oscillation a secondary pulse is emitted, thereby, increasing the deformation.

Remmerswaal[14] conducted experiments on explosive forming of sheet metal. From his experimental results he reported that the deformation is affected by

a) the thickness of the material to be deformed,

b) vacuum between die and blank,

c) the weight of the explosive charge and its distance from the material to be formed.

Johnson, et, al.[15] conducted experiments for variable hydrostatic head upto seven feet keeping constant charge weight and stand-off distance. They observed that the polar deflection of the blank increased upto a hydrostatic head of 15 inch and thereafter remained constant.

Corbett and Bicker[16] studied the effect of peripheral constraint on polar deflection. They varied the torque on bolts holding down the clamping ring for a series of firings while all other parameters were kept constant. They observed that an increase in the pressure on the blank decreases deformation.

This is attributed to an increase in the resistant of the metal to flow owing to increased frictional forces on the contact surfaces of the blank.

Thurston[17] studied the effect of edge pull-in on explosive forming of domes. He observed that for a given draw depth, if the edge pull-in is prevented, tensile stresses can become large enough to tear the blank. If large edge pull-in is allowed, the resulting circumferential compressive stresses can cause excessive wrinkling near the edge.

Noble and Oxley[18] have given a simple analysis to estimate the weight of charge required in explosive forming. Considering a small element of sheet of original sides, x and y, the plastic work done is given by

W D = original volume x strain energy per unit volume

$$= t \, x \, y \, (\, Y \, \frac{\triangle x}{x} + Y \, \frac{\triangle y}{y} \,)$$

$$= t \, Y \triangle A \qquad\qquad (2.1)$$

where $\triangle x$ and $\triangle y$ are the extensions in the elemental

lengths x and y.

Y - yield stress of the material

$\triangle A$ is the change in surface area.

t is initial thickness of the blank

Assuming

a) for uniaxial tension, $\triangle A$ is taken as product of

the extension in the direction of the load and the

initial width of the element,

b) the change in area resulting from the drawing-in

at right angles to the load is neglected,

c) equation (2.1) holds good for biaxial state of

stress,

d) strains being small, engineering strain can be used

instead of natural strains in equation (2.1).

For work hardening material equation (2.1) becomes

$$W \, D = t \, \triangle A \, (Y + \frac{1}{2} \, \frac{\triangle A}{A} \, H) \qquad\qquad (2.2)$$

where H is slope of idealised stress strain curve.

e) The total explosive energy is represented by the

area of the spherical wave front.

Assuming that the clamped circular diaphragm of free radius 'a' deforms to a spherical cap of radius 'r' and central height h, then

$$\text{spherical surface area} = \pi \left(\frac{a^2}{4} \right) + h^2$$

$$\text{original surface area} = \pi \frac{a^2}{4}$$

$$\text{change in surface area} \quad \Delta A = \pi h^2$$

from equation (2.1), work of deformation is

$$W D = t Y \pi h^2 \tag{2.3}$$

By considering spherical sector of wave front falling on the blank the energy available for doing work is given by

$$E_W = W \gamma \theta^2 / 4 \tag{2.4}$$

where 2θ is the solid angle subtended by the blank at the centre of the charge.

W is chemical energy released by explosive charge on detonation.

γ is efficiency of energy transfer which will depend upon the transfer medium.

Equating equations (2.3) and (2.4)

$$t Y \pi h^2 = W \gamma \theta^2 / 4$$

which gives

$$h^2 = \frac{W \gamma \theta^2}{4 t \pi Y}$$

$$\text{or} \quad h^2 \propto W \theta^2 / t Y \tag{2.5}$$

CHAPTER III

EXPERIMENTAL SET UP

3.1 GENERAL

To carry out basic studies in explosive forming stand-off operations, a tank 1.525 M dia and 1.55 M deep is made. Experimental set-up consisting of die assembly, craddle and supporting structure is designed and fabricated.

3.2 EXPLOSIVE FORMING TANK

The tank used for explosive forming operations should be strong enough to withstand the repeated explosive blast loading. For this purpose a ferrocement shell developed at I.I.T. Kanpur[19] was utilised. An underground excavation 2.1 M deep x 2.4 M dia was made and the surfaces were properly levelled. At the bottom of the excavated pit, mass concreting (mixture ratio 1:2:4 with water cement ratio of 0.45 by weight) was done to get a base thickness of 600 mm (Fig. 3.1). A reinforcement cage of wire mesh prepared earlier was lowered into excavated pit so that it hung centrally over concerete base. The tank was then cast with rich cement mortar. The annular gap of 450 mm between the tank and surrounding ground was then concreted. Curing was done for 28 days.

A water lifting pump was used for evacuating the tank when required.
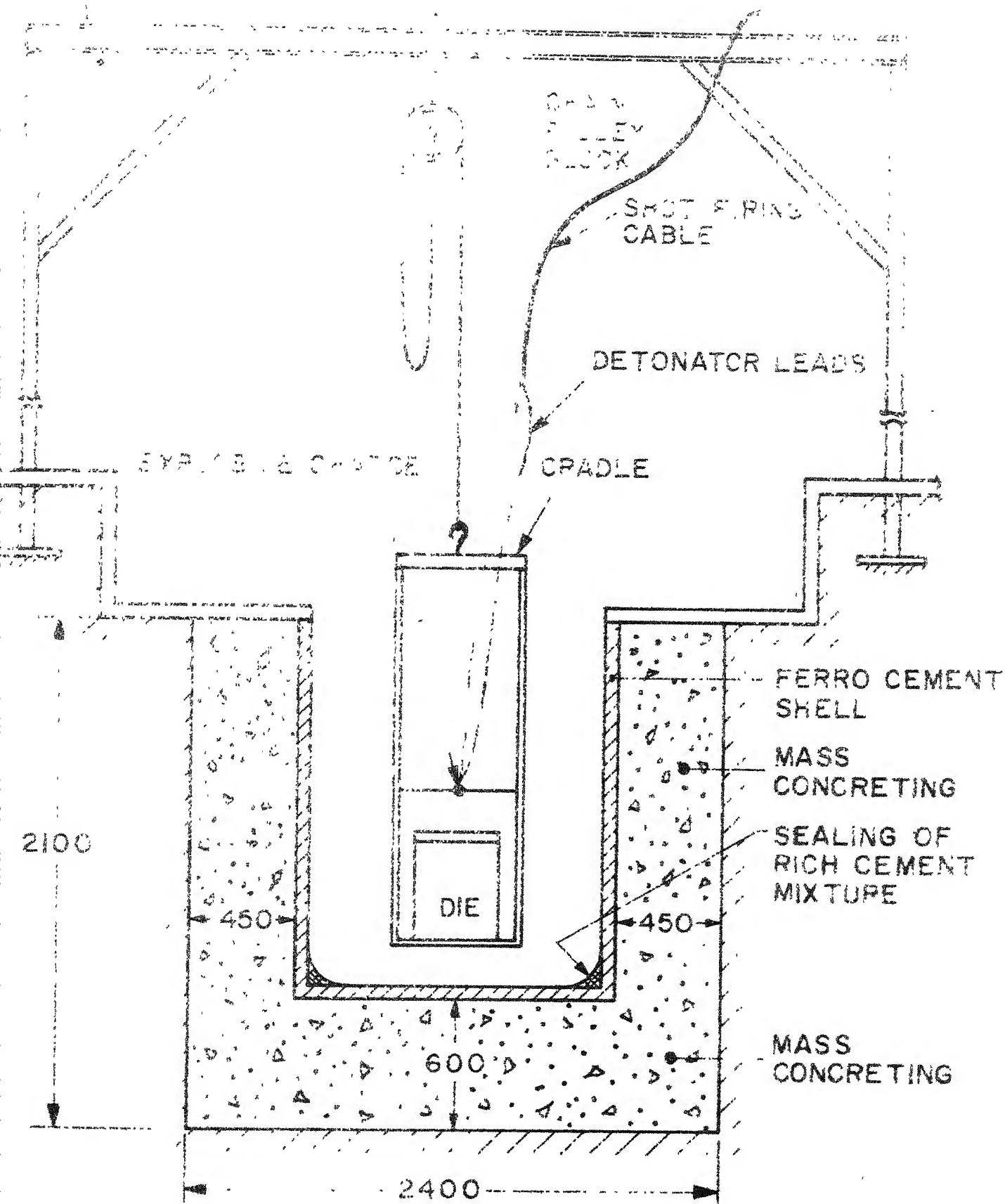
Explosive forming set-up

3.3 HOISTING EQUIPMENT

A steel super structure was fabricated as shown in Fig. 3.1 for suspending a chain pulley block. The chain pulley block was used to lower the die block assembly into the water tank.

3.4 DIE ASSEMBLY AND CRADLE

Die was designed to conduct stretch forming experiments for metals of various thicknesses. A step of 3 mm depth was provided in the die block for proper positioning of the blanks. An annular groove was provided for an 'O' ring for proper scaling of die cavity to prevent leakage of vacuum created in the die cavity.

To study the effect of draw radius on shaped and strain distribution, five draw rings were manufactured with different draw radius. A step was provided on die for seating these rings. A brass nozzle was fitted to the die block to connect vacuum pipe to the die cavity. Fig.3.2(a) shows assembled die. Design details of various parts are shown in Fig. 3.2(b).

Die was machined out of a grey cast iron casting. A layer of araldite was applied in the inner cavity to seal all blow holes to prevent any leakage of vacuum. Hold down ring was machined from MS plate. A 3 mm step was provided

HOLD DOWN RING

DRAW RING

O-SEAL

BLANK

DIE BL

VACUUM
NE

Die Assembly

Fig 3.2

5 rings with corner radii
R = 2, 4, 6, 8 and 10 mm
r = 2mm

Draw ring
M.S.

150 Φ
170 Φ $^{+0.014}_{-0.011}$
275 Φ

10 HOLES TAPPED, 1/2" BSW ON 235 P.C.D.
210 Φ
8.03" Φ
7.28" Φ

170 Φ $^{+0.040}_{-0.000}$
152 Φ

0.19"
3
30
25
170 Φ $^{+0.015}_{-0.000}$

Die B
C.I.

200

50

TO
VACUUM
LINE

20
15

4 HOLES TAPPED, 1/2" BSW ON
200 P.C.D.

20
150 Φ
210 Φ
275 Φ
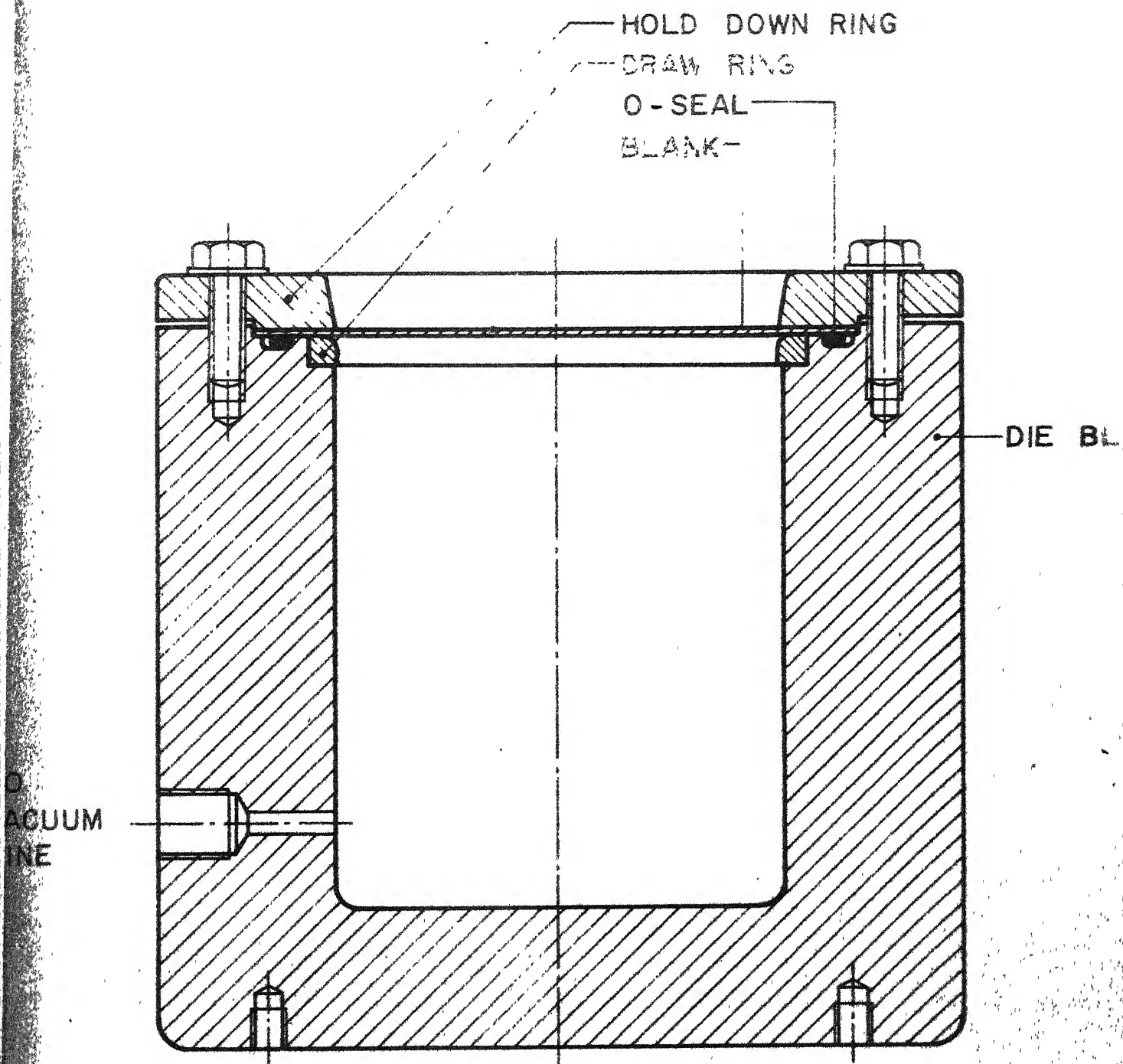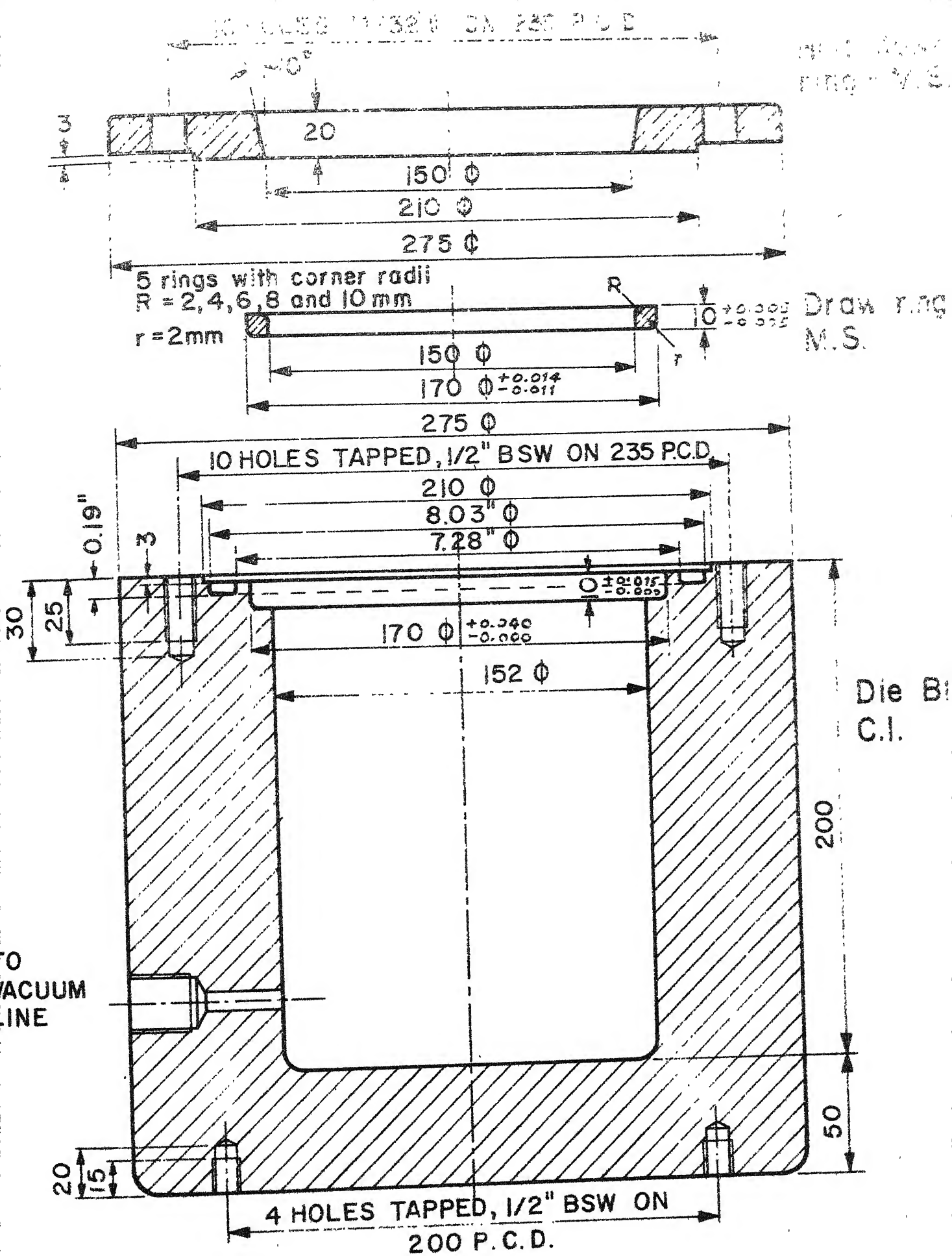
Details of die

Fig. 3.2

on face of the hold down ring to fit into the corresponding groove on die face. This ensured the application of uniform pressure on the blank.

A cradle was fabricated for supporting the die block. The die assembly was bolted on to base plate of the cradle (Fig. 3.3(a)) The cradle was suspended from chain pulley block as shown in Fig. 3.3 (b).

3.5 VACUUM PUMP

A rotary double action vacuum pump capable of creating a vacuum of 28" of Hg was used. A non-porous vacuum hose was used to connect the die block to vacuum pump. All joints in the vacuum line were sealed off with plasticine.

3.6 EXPLOSIVE EQUIPMENT

A Rhino type multishot electric exploder was used for initiating detonators. A twin-core low-resistance cable was used for connecting the detonator to the exploder.

CHAPTER IV

EXPERIMENTAL INVESTIGATION

4.1 GENERAL

Explosive stretch forming experiments are carried out on Brass, Aluminium and Stainless Steel 304 sheets by using Cordtex explosive. The effect of charge weight, stand-off distance, and draw radius on thickness strain distribution, radial strain distribution and profile of deformed blanks are studied. The effect of annealing of Brass sheets is also investigated.

4.2 EXPERIMENTAL PROCEDURE

a) Preparation of test pieces (blanks)

Blanks of Stainless Steel 304, 0.875 mm, 70-30 Brass, 1.555 mm, 0.73 mm and 0.576 mm, and Aluminium 1100.0 1.61 mm., 1.189 mm and 0.671 mm were machined to a dia. of 210 mm. To measure thickness and radial strains, concentric circles were inscribed on the blanks at diameters of 30, 50, 70, 90, 110, 130 and 150 mm. Four diametric lines were also inscribed at an interval of 45°.

b) The die, and the hold down ring were thoroughly cleaned using acetone to remove all traces of antirust oil to eliminate any film of lubricant at the interfaces between (i) die surface and blank and (ii) hold down ring and blank.

The blank was placed in the groove and clamped on to the die by the hold down ring using ten 1/2" BSW bolts. The bolts were uniformally tightened to a torque of 80 ft lb using a torque wrench.

Cordtex explosive was coiled and suspended at a chosen stand-off distance by cords attached to the four supports of the cradle. The charge was carefully positioned above the centre of the blank. A detonator was inserted into the coiled charge. The leads from the detonator were connected to the shot firing cable. The die assembly was lowered into the tank to maintain a water head of 600 mm above the charge so that the effect of reflected wave from water surface is minimised. The shot firing cable was attached to the exploder and the charge was detonated.

A couple of experiments were carried out by evacuating the die cavity to a vacuum of 28" of Hg. However, rest of the experiments were conducted under atmospheric pressure in the die as no significant difference was observed by using vacuum for the case of free stretch forming.

4.3 EXPERIMENTAL CONDITIONS

a) 'Cordtex' detonating fuse, consisting of a core of PETN surrounded by yarn and white plastic casing, was used. The explosive core contains 3.18 grams of explosive per foot and is potentially capable of releasing 4400

calories per foot. The cordtex explosive has a velocity of detonation of 6500 m/sec.

b) Explosion is initiated by an electric detonator (Indian Aluminium type No. 6) which has an energy potential of 375 calories equivalent to 26 mm of cordtex.

c) Die ring with 6 mm forming radius was used for all experiments except where different draw rings were used to study the effect of draw radius.

d) Water head (hydrostatic head) was kept constant at 600 mm above the charge for all experiments.

e) Brass blanks of thickness 1.555 mm and 0.576 mm were annealed in an electric furnace at 500 °C for eight hours. The blanks were gradually cooled to room temperature by putting off the furnace.

f) Properties of the material used are given below:

Material	UTS kg/mm^2	Yield Strength kg/mm^2
70-30 Brass	34.516	24.808
Stainless Steel 304	75.59	34.195
Aluminium 1100.0	11.32	9.482

4.4 EXPERIMENTAL DETAILS

The following sets of explosive forming tests were carried out on various materials to study the effect of charge weight, stand-off distance and draw radius of die as per the details given below.

1. Five blanks of Brass sheet of 0.73 mm thickness were formed keeping 150 mm stand-off distance and varying the charge weight from 0.795 gms to 3.975 gms.

2. Five blanks of Brass sheet of 0.73 mm thickness were formed using 3.18 gms charge weight and by varying stand-off distance from 75 mm to 375 mm.

3. Six blanks of Brass sheet of 1.555 mm thickness were formed, keeping 150 mm stand-off distance and varying the charge from 1.59 gms. to 7.95 gms.

4. Five blanks of Brass sheet of 0.576 mm thickness were formed, keeping 150 mm stand-off distance and varying the charge weight from 0.795 gms to 3.18 gms.

5. Seven blanks of Stainless Steel 304 sheet of 0.875 mm thickness were formed by keeping 150 mm stand-off distance and by varying the charge weight from 1.59 gms to 11.13 gms.

6. Eight blanks of Aluminium sheet of 1.189 mm thickness were formed by keeping 300 mm stand-off distance and varying the charge weight from 0.530 gms to 5.565 gms.

7. Five blanks of Aluminium sheet of 1.189 mm thickness were formed by keeping 150 mm stand-off distance and by varying the charge weight from 0.53 gms to 1.59 gms.

8. Six blanks of Aluminium sheet of 0.671 mm thickness were formed by keeping 300 mm stand-off distance and by varying charge weight from 0.795 gms to 3.18 gms.

9. Five blanks of Aluminium sheet of 1.615 mm thickness were formed by keeping 300 mm stand-off distance and by varying charge weight from 1.06 gms to 3.18 gms.

10. Five blanks of Aluminium sheet of 1.189 mm thickness were formed by keeping charge weight constant 5.565 gms and 300 mm stand-off distance and by varying the draw radius from 2 mm to 10 mm.

11. Four annealed blanks of Brass sheet of 0.576 mm thickness were formed by keeping 150 mm stand-off distance and by varying charge weight from 1.59 gms to 3.18 gms.

12. Four annealed blanks of Brass sheet of 1.555 mm thickness were formed keeping 150 m: stand-off distance and by varying charge weight from 1.59 gms to 6.36 gms.

13. Hardness test was carried out on Brass blanks of 0.576 mm thickness and annealed brass blanks of 0.576 mm thickness before forming and at pole after forming.

4.5   MEASURING TECHNIQUES

a.   Thickness Strain

Measurements of thickness were taken at each intercept of the concentric circle with the inscribed diameter as well as at the centre of the blanks. The set-up for the thickness measurement is shown in Fig. 4.1 (a).

A brass rod with a spherical end was held horizontally with the help of a magnetic clamp fixed on the surface. A dial gauge having a least count of .01 mm was mounted on a magnetic clamp fixed on the surface plate. The spindle of the dial gauge was kept in contact with spherical end of the rod. The deformed thickness of the blank was found by inserting the blank in between the rod and the dial gauge spindle. The lowest reading on the dial gauge was taken by manipulating the blanks.

Logrithmic thickness strain was calculated as $\epsilon_t = \ln \left(\dfrac{T_o}{T} \right)$ where T_o is original thickness of blank and T is thickness after deformation.

b.   Radial Strain

The measurement for radial strain were taken on tool makers microscope. These measurements were taken across the inscribed diameter. The set-up for radius measurement is shown in Fig. 4.1 (b).

Logrithmic radial strain was calculated as

$$\epsilon_r = \ln \left(\frac{D}{D_o} \right)$$

where

D_o - is original dia, and

D - dia of an inscribed circle after deformation.

c. Profile of Deformed Blank
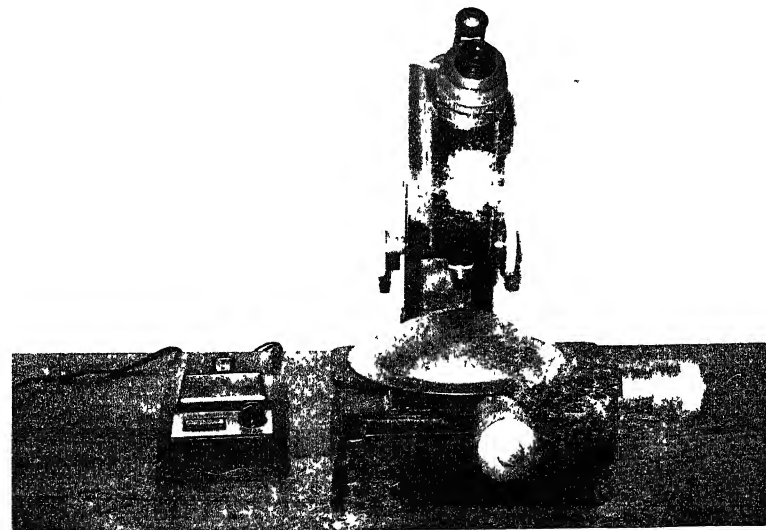
The profile of the deformed blank was obtained by means of a height gauge. The deformed blanks were held firmly on a surface plate and the location of each of the inscribed circles was determined (Fig. 4.1 (c)). Profiles of the deformed blanks are plotted in full scale.
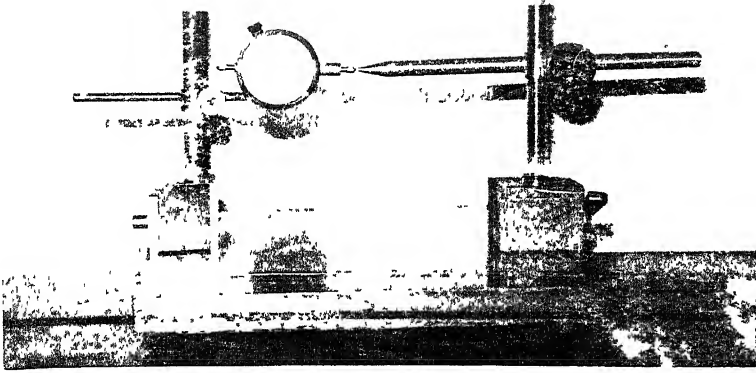
Thickness strain measurement
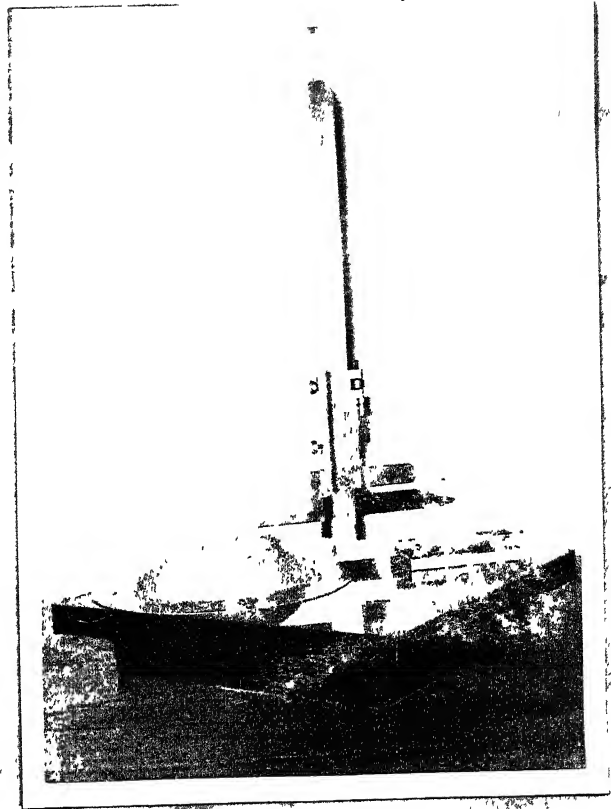
(c) Height measurement

Radial strain measurement

Measuring Techniques

Fig. 4.1

CHAPTER V

EXPERIMENTAL RESULTS AND DISCUSSIONS

5.1 EFFECT OF CHARGE WEIGHT

The effects of charge weight on thickness strain distribution, radial strain distribution and profile of the blanks are shown in Figs. 5.01 to 5.16.

5.1.1 Thickness Strain Distribution

Logrithmic thickness strain ϵ_t versus radial distance is plotted in Figs. 5.01 to 5.04 for various materials with explosive charge weight as a variable parameter.

Fig. 5.01 shows the thickness strain distribution with Brass blanks of 1.555, 0.73 and 0.576 mm thickness, keeping stand-off distance constant at 150 mm.

Fig. 5.02 shows the thickness strain distribution with Stainless Steel 304, 0.875 mm thickness at 150 mm stand-off distance.

Fig. 5.03 shows thickness strain distribution with Aluminium blanks of 1.189 and 0.671 mm thickness keeping 300 mm stand-off distance.

Fig. 5.04 shows the thickness strain distribution with Aluminium blanks of 1.189 and 1.61 mm thickness keeping 150 mm stand-off distance.

(a) Brass 555 mm

(b) Brass 0.73 mm

(c) Brass 0.576 mm
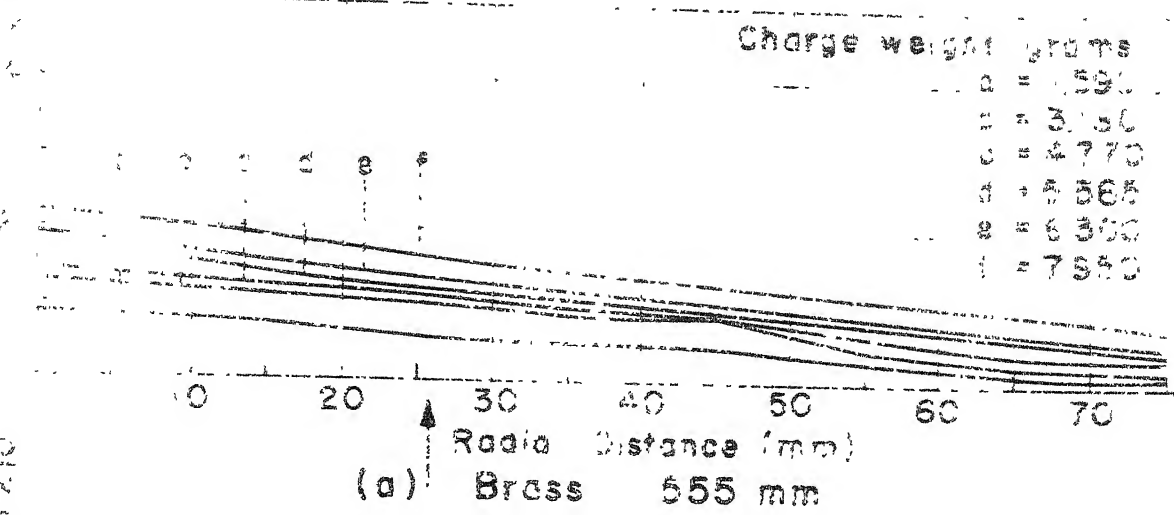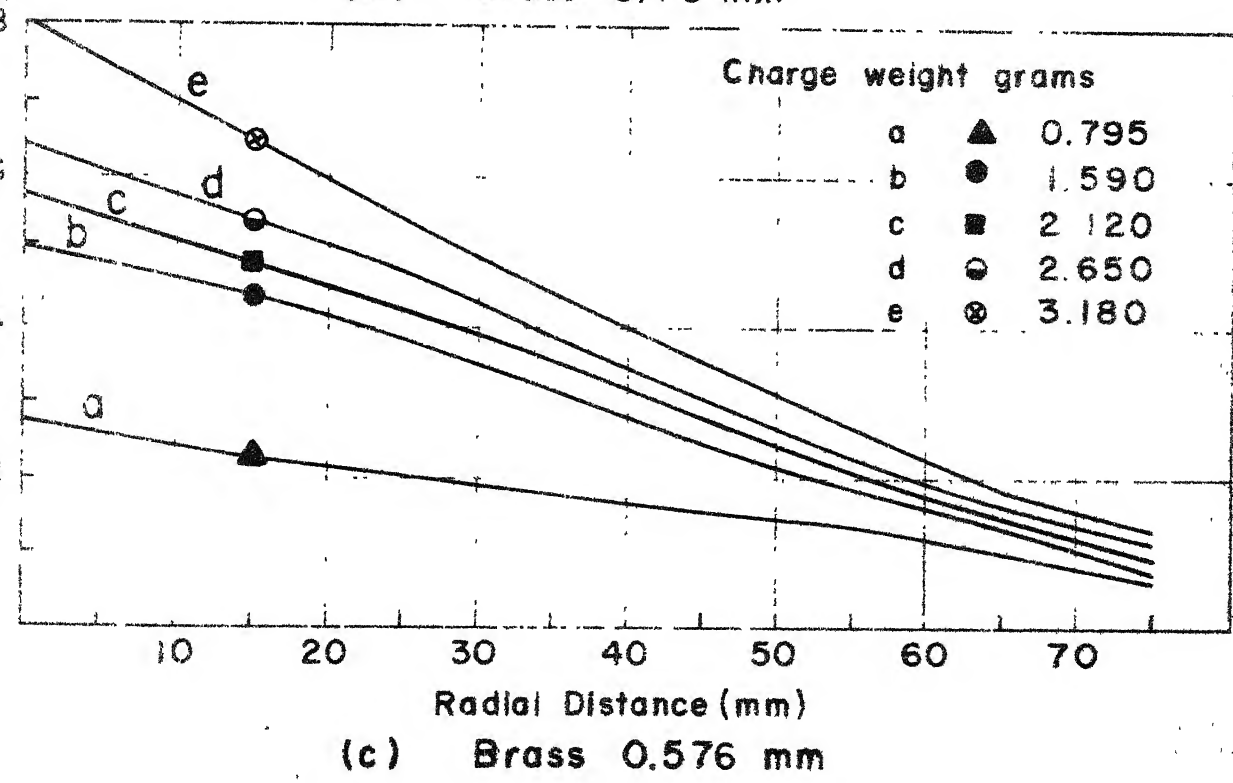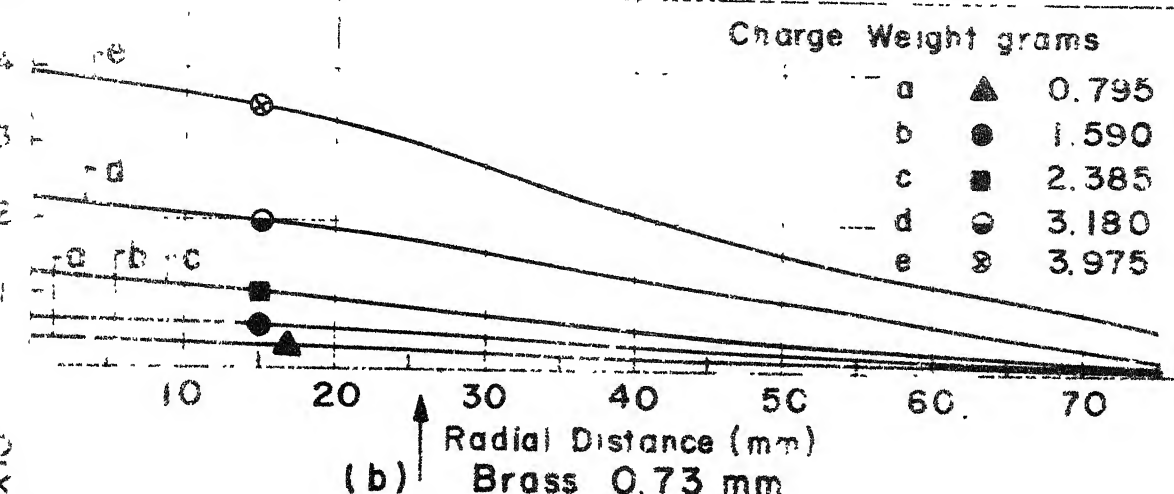
Thickness strain versus radial distance
Matl. Brass, Stand-off 150mm
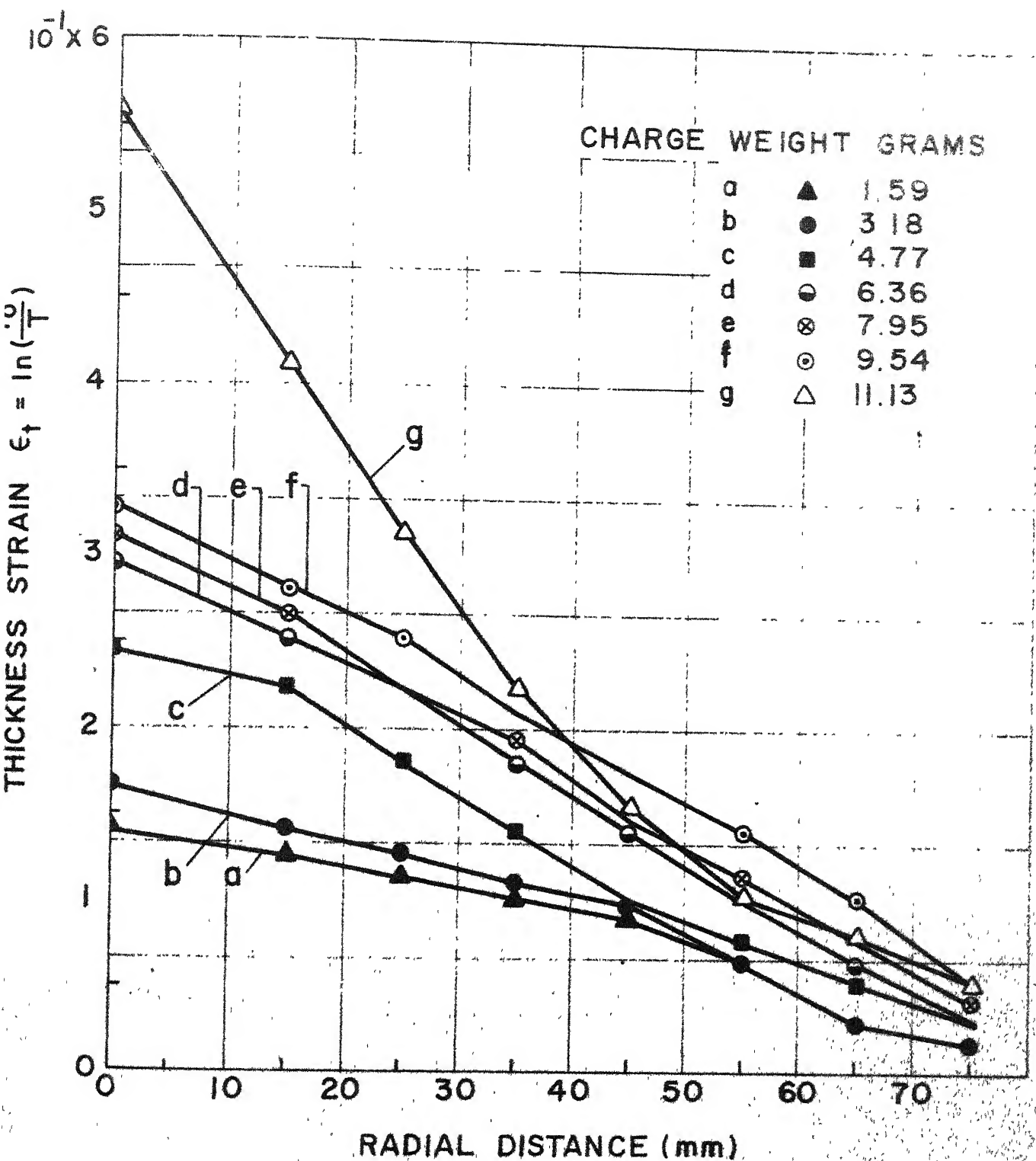
Thickness strain versus radial distance
Matl. stainless steel 304, 0.875 mm.
Stand-off = 150 mm

Fig. 5.02

	CHARGE WEIGHT GRAMS
a	0.530
b	1.060
c	1.590
d	2.120
e	2.650
f	3.975
g	4.770
h	5.565

RADIAL DISTANCE (mm)

(a) Matl. Aluminium 1.189 mm

	CHARGE WEIGHT GRAMS
a	0.795
b	1.590
c	2.385
d	2.783
e	3.180
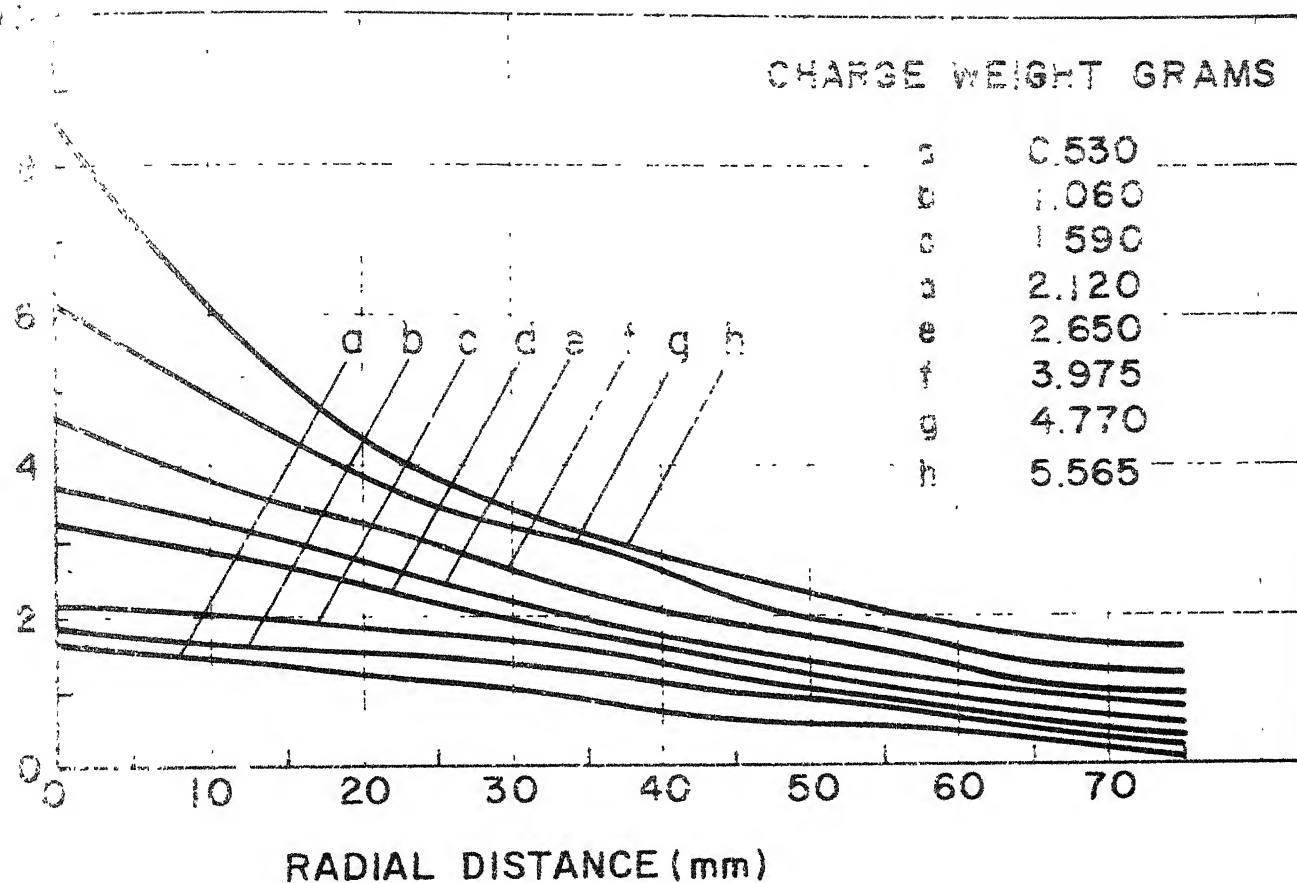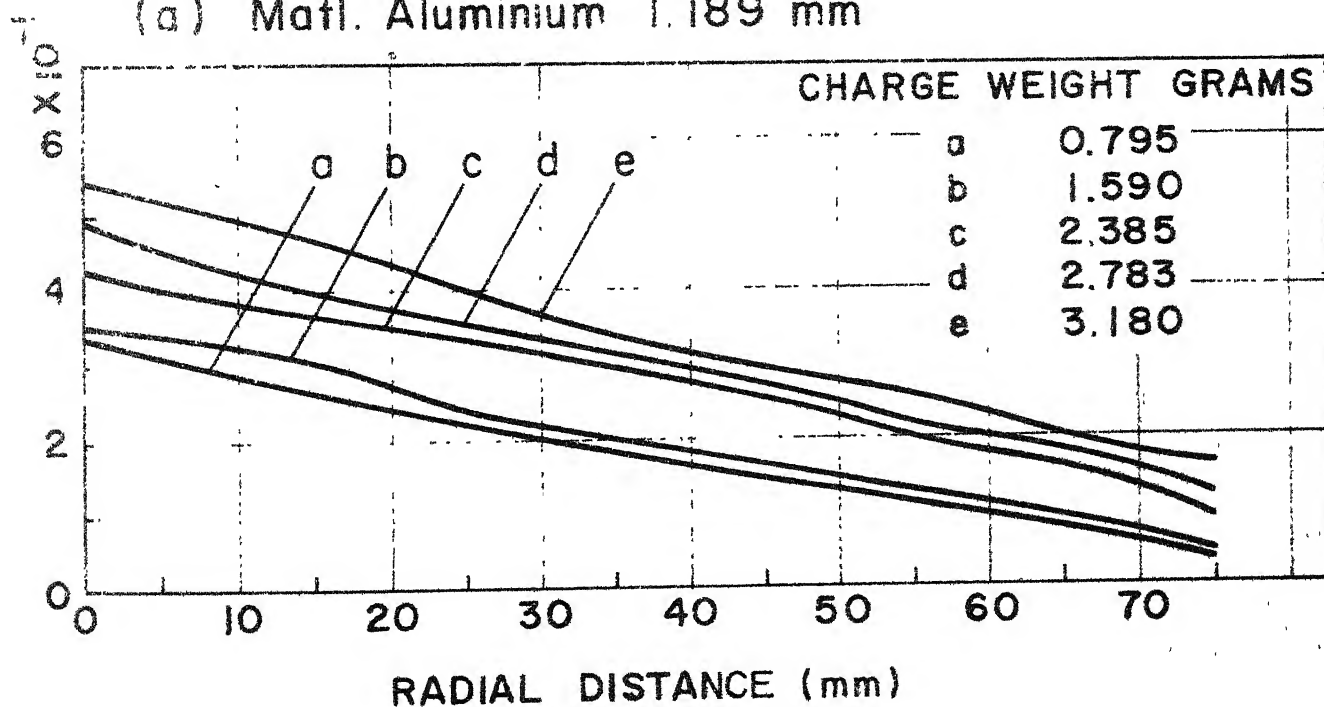
RADIAL DISTANCE (mm)

(b) Matl. Aluminium 0.671 mm

Thickness strain versus radial distance
Matl. Aluminium , Stand-off 300 mm

Fig. 5.03

(a) Matl. Aluminium 1.189 mm

CHARGE	WEIGHT	GRAMS
a		0.530
b		0.795
c		1.060
d		1.325
e		1.590

(b) Matl. Aluminium 1.61 mm
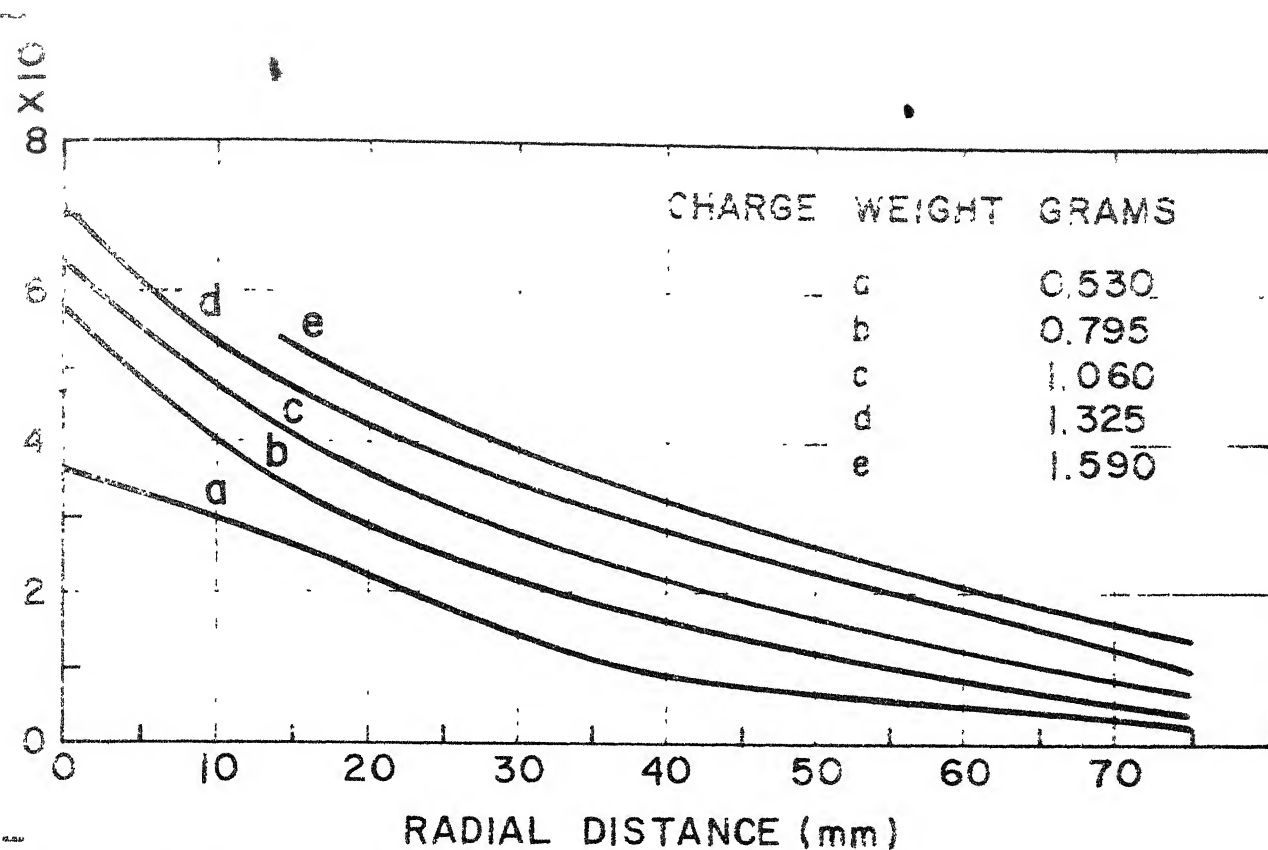
CHARGE	WEIGHT	GRAMS
a		1.06
b		1.59
c		2.12
d		2.65
e		3.18
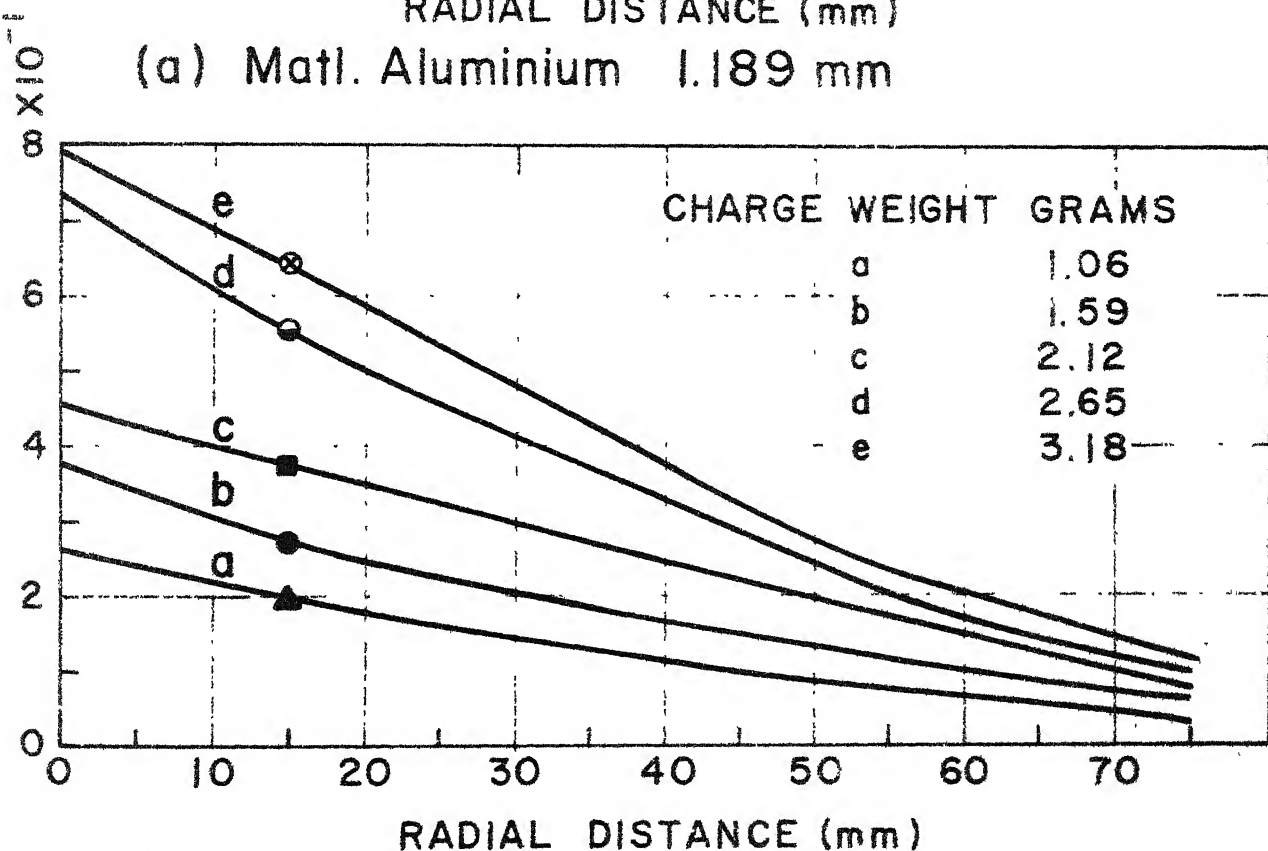
Thickness strain versus radial distance
Stand off = 150 mm

Fig. 5.04

5.1.2   Radial Strain Distribution

Logrithmic radial strain ϵ_r versus radial distance plots for variable charge weight are shown in Figs. 5.05 to 5.11 for different materials.

Figs. 5.05 to 5.07 show the radial strain distribution with Brass blanks of 0.576, 0.73 and 1.555 mm thickness respectively for a stand-off distance of 150 mm.

Fig. 5.08 shows the radial strain distribution with Stainless Steel 304, 0.875 mm thickness for a stand-off distance of 150 mm.

Fig. 5.09 shows the radial strain distribution in Aluminium 1.61 and 1.189 mm thickness for a stand-off distance of 150 mm.

Figs. 5.10 and 5.11 show the radial strain distribution in Aluminium blanks of 1.189 mm and 0.671 mm thickness for a stand-off distance of 300 mm.

5.1.3   Maximum Deflection and Profile of Blanks

The effect of charge weight on profile of blanks and maximum deflection are shown in Figs. 5.12 to 5.15.

Fig. 5.12 shows profiles of explosively formed Brass blanks of 1.555, 0.73 and 0.576 mm thickness for various charge weight at a stand-off distance of 150 mm.
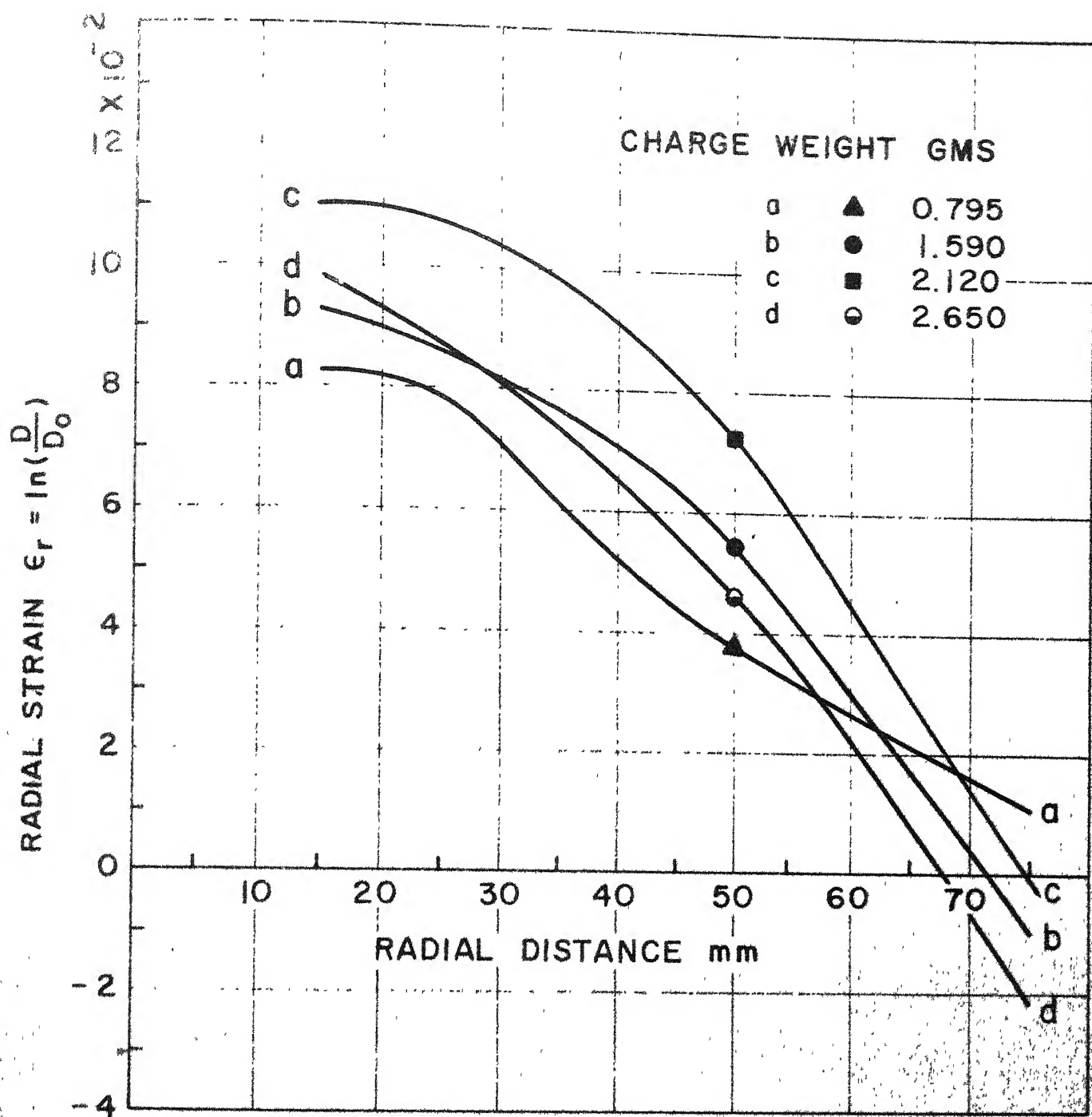
Radial strain versus radial distance
Matl. Brass 0.576 mm , Stand-off 150 mm

Fig 5.05
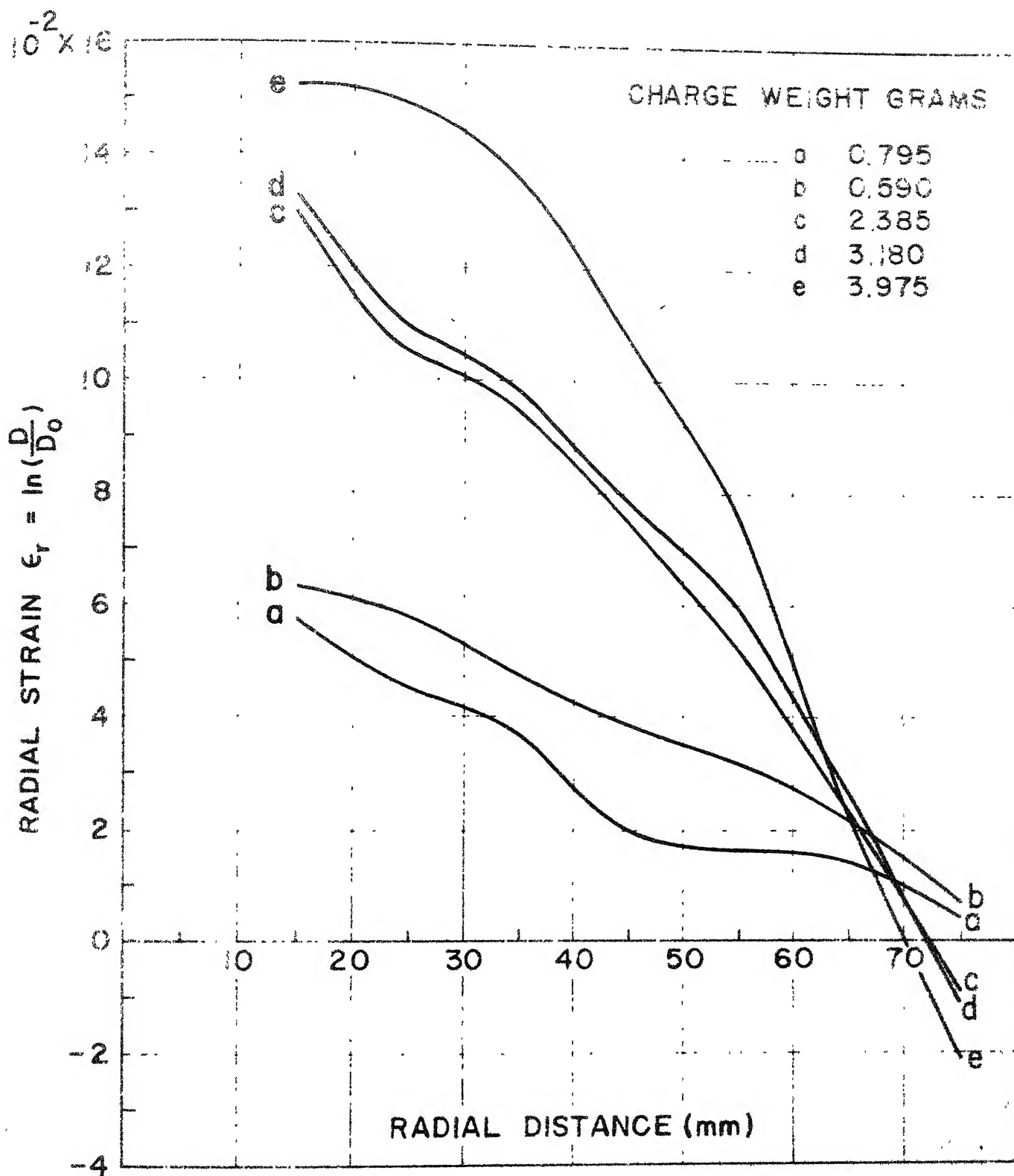
Radial strain versus radial distance
Matl. Brass 0.73 mm, Stand-off 150 mm

Fig. 5.06
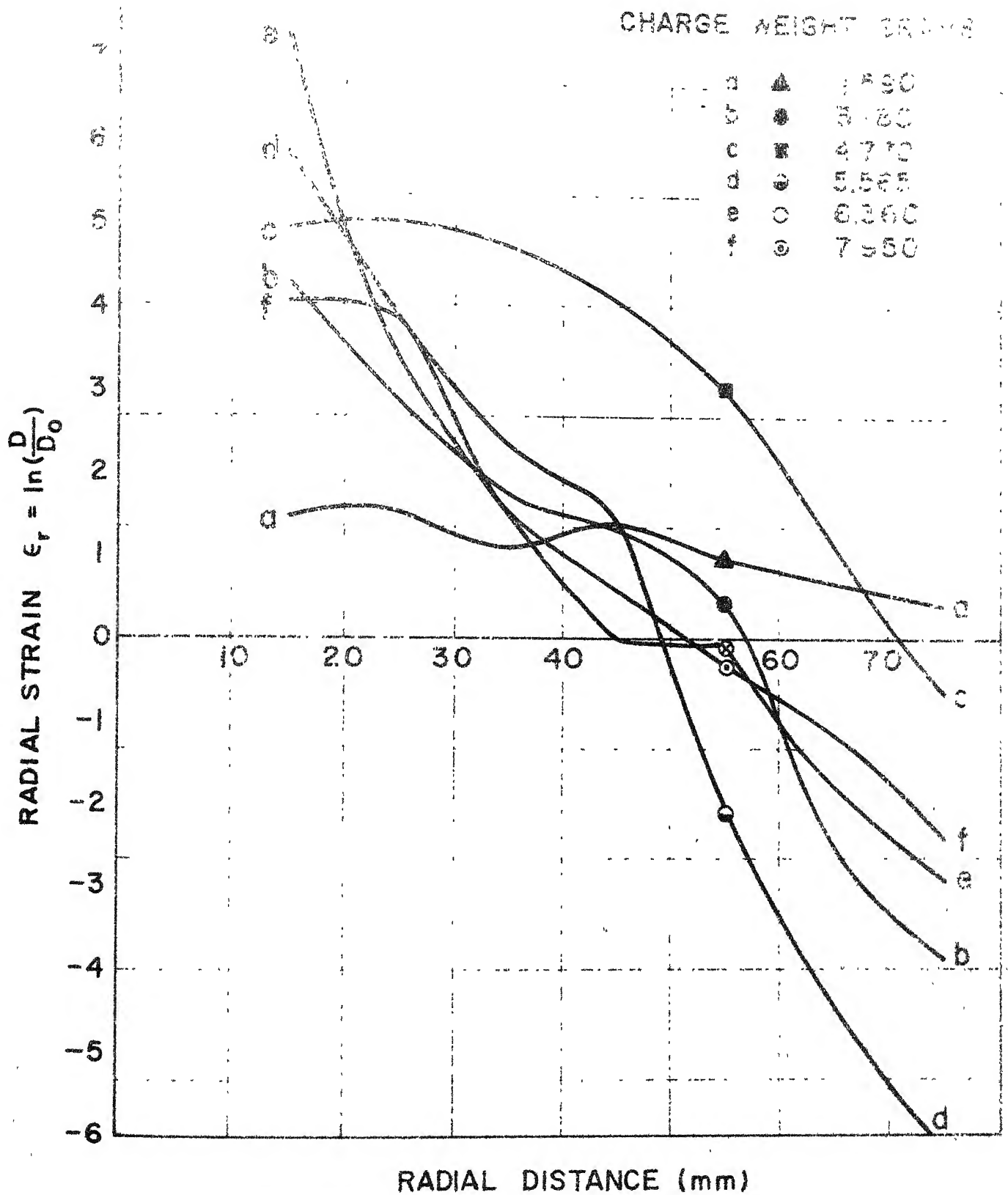
Radial strain versus radial distance
Matl. Brass 1.555 mm, Stand-off 150 mm
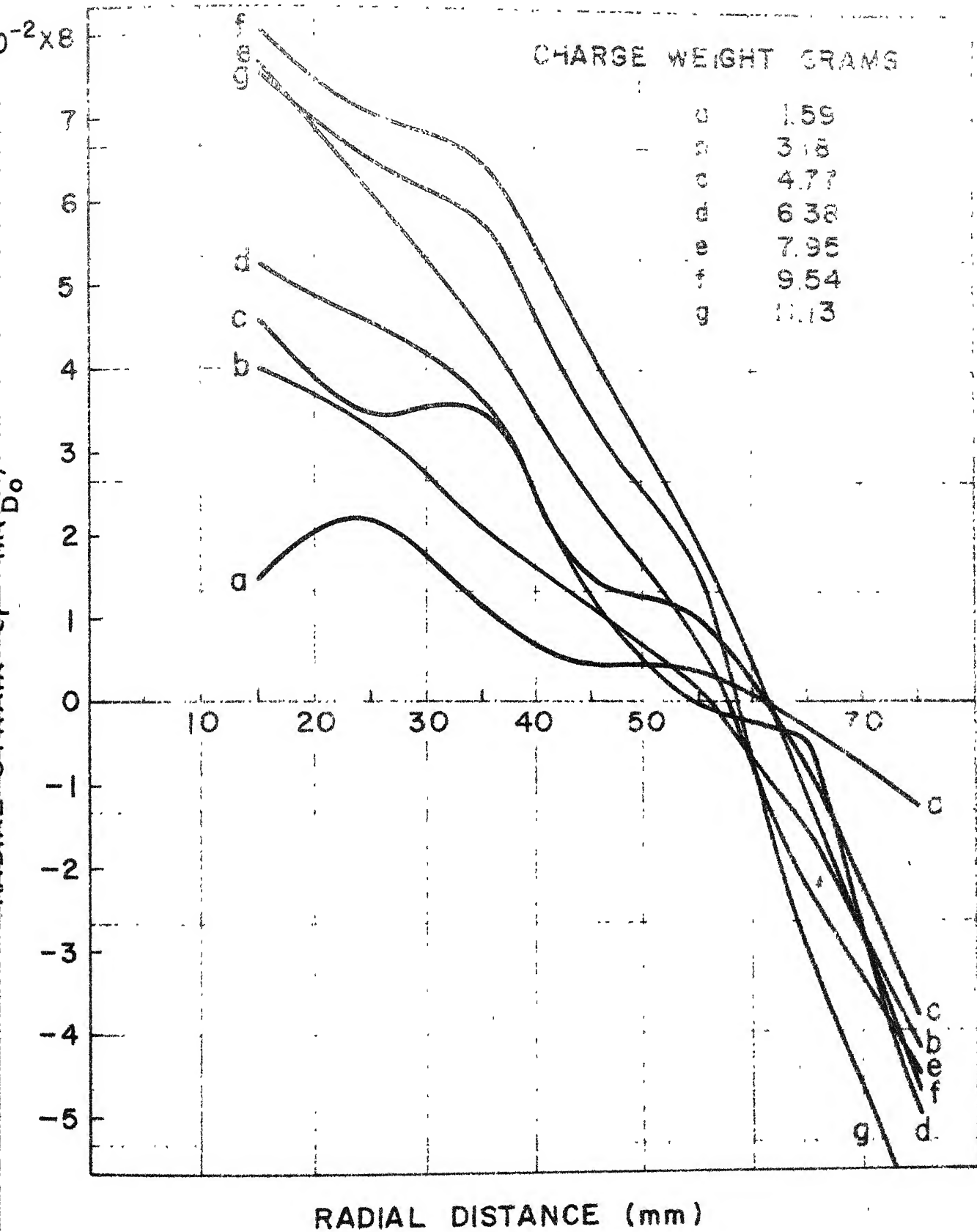
Fig. 5.07

CHARGE WEIGHT GRAMS

a	1.59
b	3.18
c	4.77
d	6.38
e	7.95
f	9.54
g	11.13

RADIAL DISTANCE (mm)

Radial strain versus radial distance
Matl. Stainless steel 304, 0.875mm., Stand-off 150mm

Fig. 5.08

Radial strain versus radial distance
Matl. Aluminium , Stand-off 150 mm

Fig. 5.09

$10^{-2} \times 20$

CHARGE WEIGHT GRAMS

a	▲	0.530
b	●	1.060
c	■	1.540
d	◐	2.120
e	⊗	2.650
f	⊙	3.975
g	△	4.770
h	○	5.565

RUPTURE
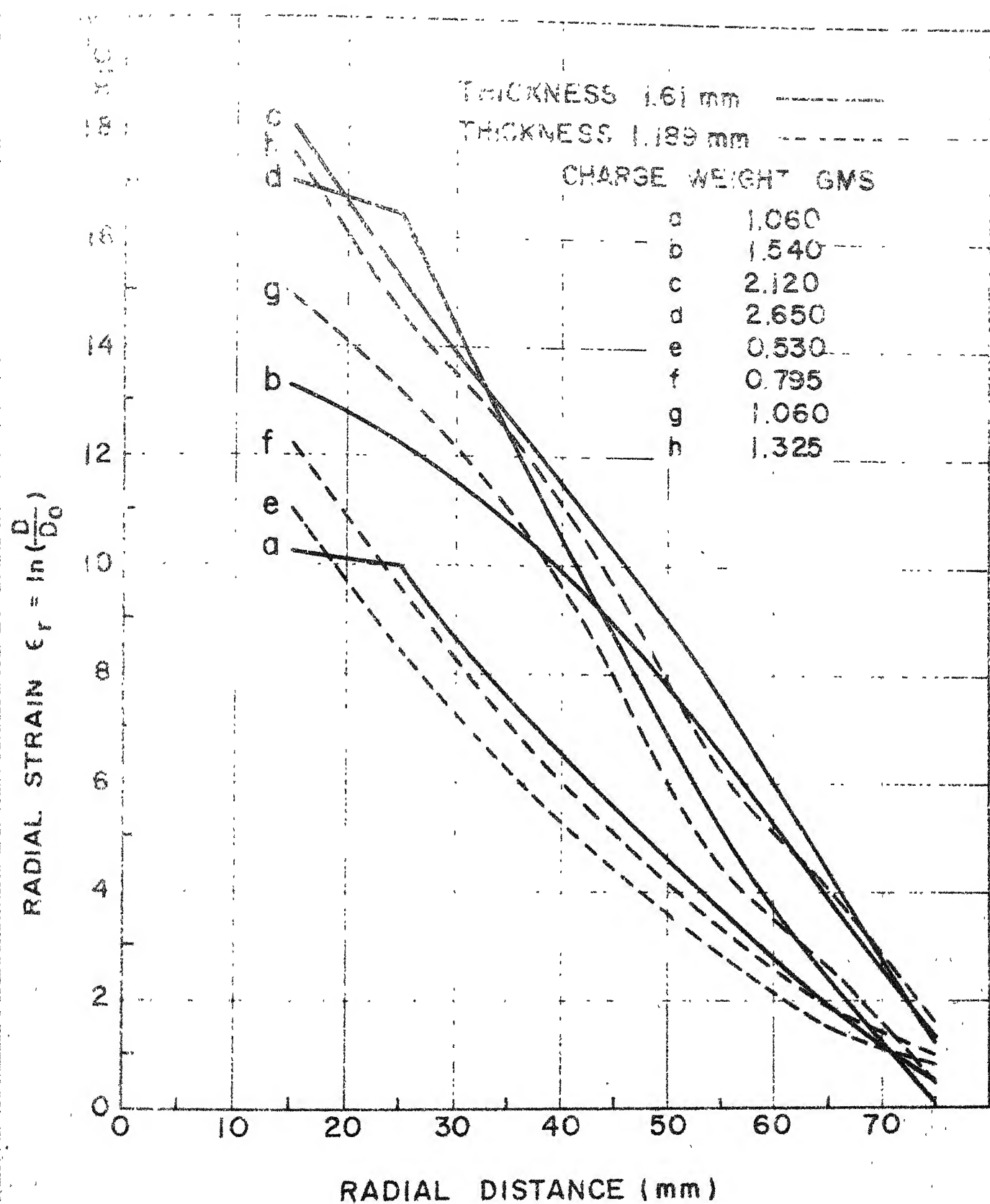
RADIAL STRAIN $\epsilon_r = \ln\left(\dfrac{D}{D_o}\right)$
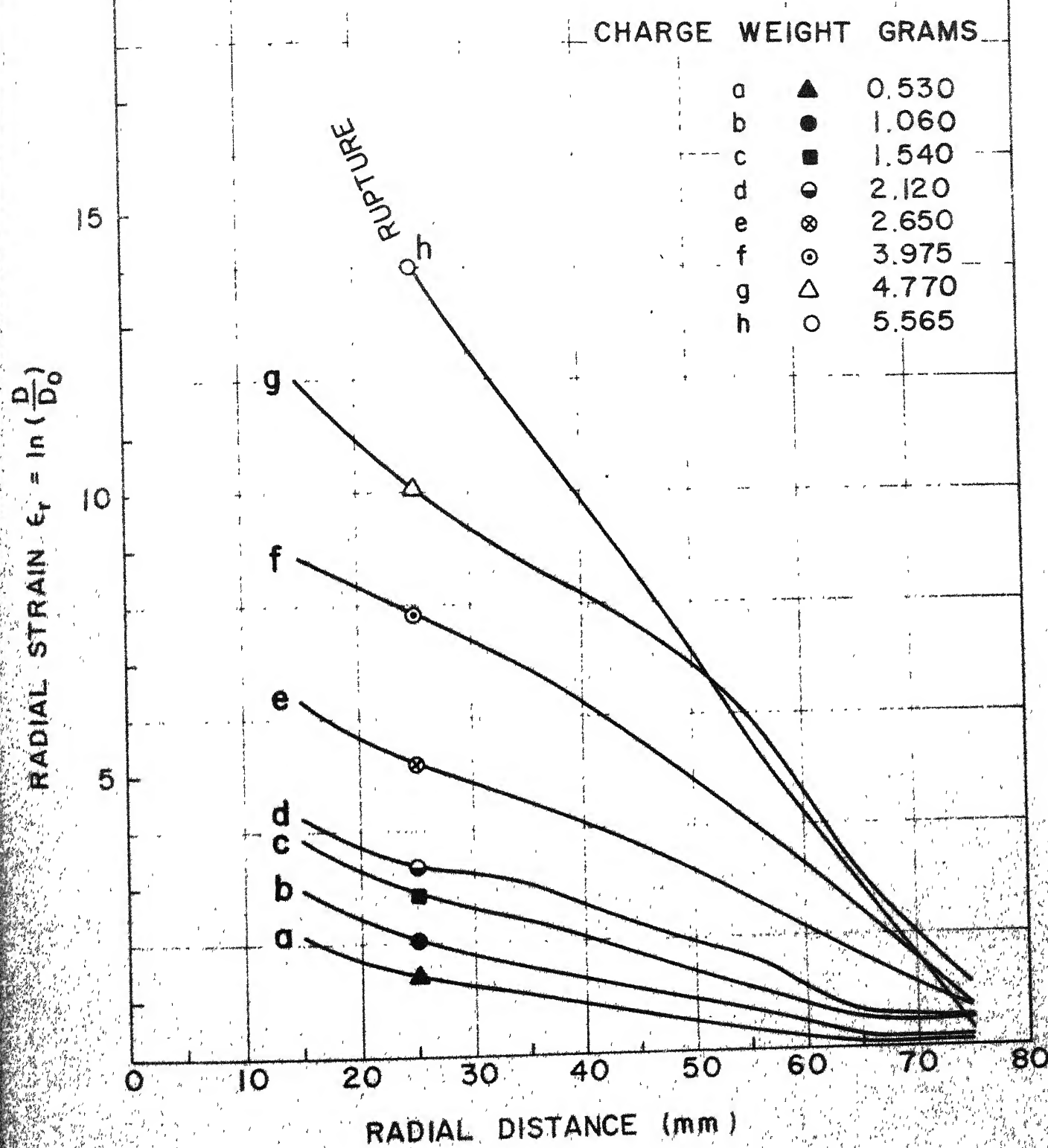
RADIAL DISTANCE (mm)

Radial strain versus radial distance
Matl. Al. 1.189 mm thick, Stand-off distance 300

Fig. 5.1
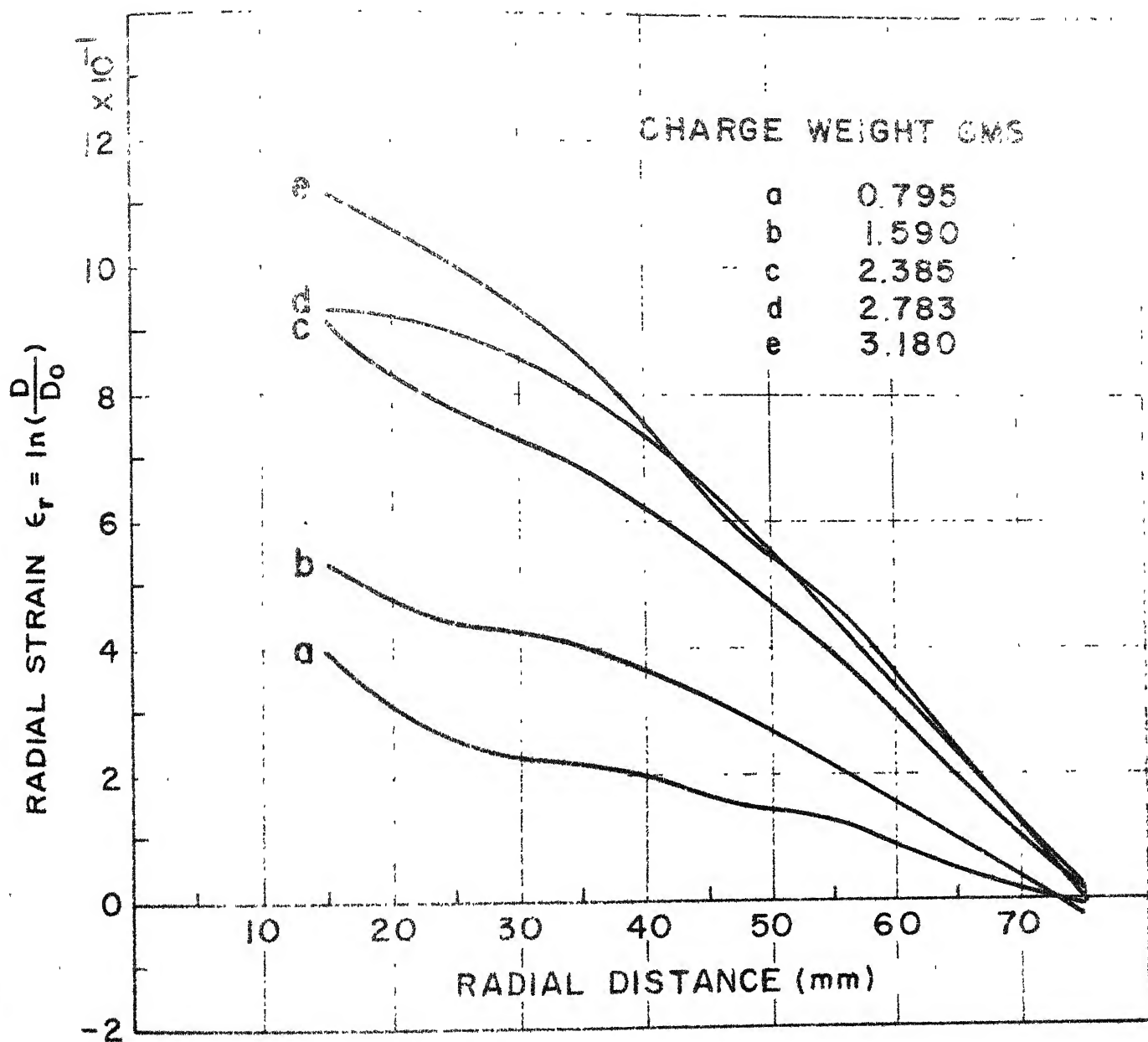
Radial strain versus radial distance
Matl. Aluminium 0.671mm, Stand-off 300 mm

Fig. 5.11

	CHARGE WEIGHT GRAMS
a	1.590
b	3.180
c	4.770
d	6.360
e	7.950

(a) Brass 1.555 mm

	CHARGE WEIGHT GRAM
a	0.795
b	1.590
c	2.120
d	2.650
e	3.180

(b) Brass 0.576 mm

	CHARGE WEIGHT GRAMS
a	0.795
b	1.590
c	2.385
d	3.180
e	3.975
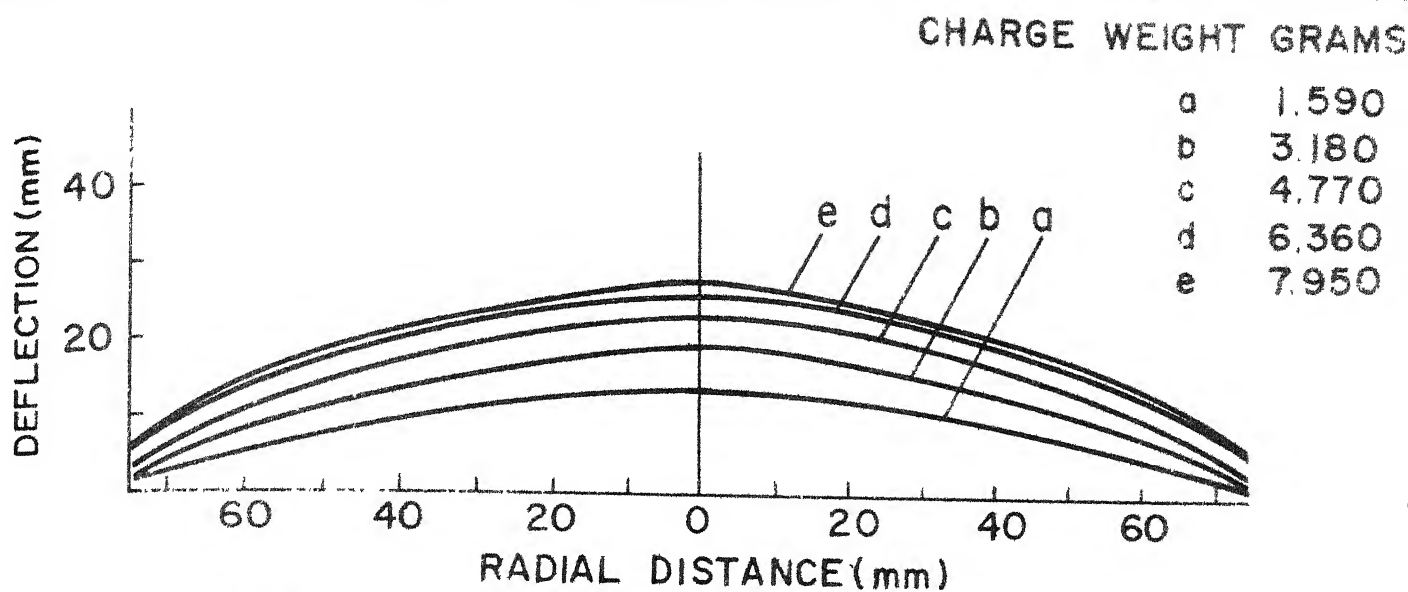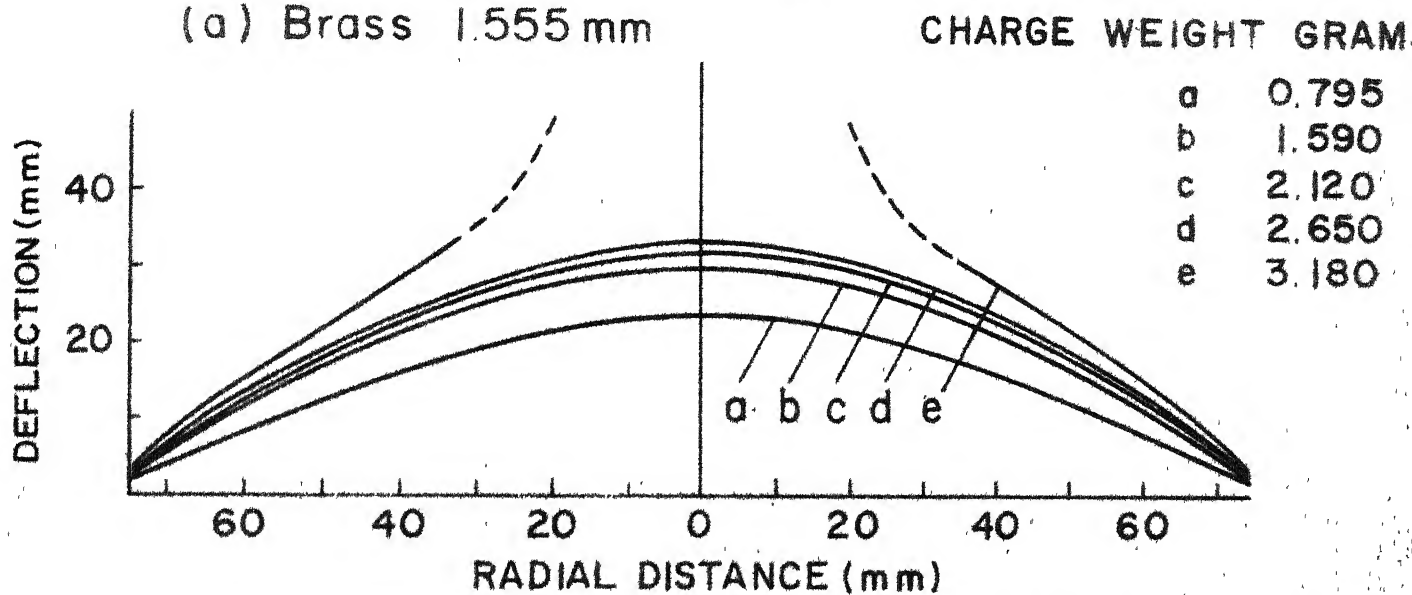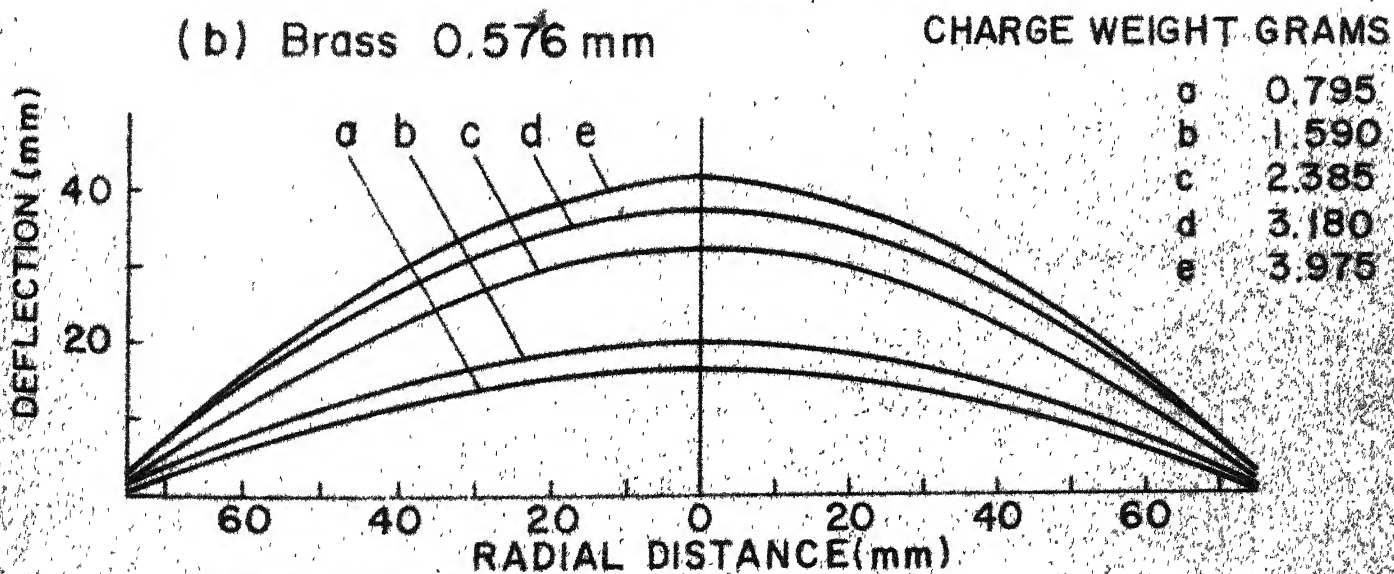
(c) Brass 0.73 mm

Profile of explosively formed blanks
Matl. Brass, Stand-off distance 150 mm

Fig 5.12

Fig. 5.13 shows plots of maximum polar deflection versus charge weight Brass blanks of 1.555, 0.73 and 0.576 mm thickness and annealed Brass blanks of 1.555 and 0.576 mm thickness, the stand-off distance being 150 mm.

Fig. 5.14 shows blank profile and maximum deformation versus charge weight curve for explosively formed Stainless Steel 304, 0.875 mm thickness.

Fig. 5.15 shows blank profiles and maximum deflection versus charge weight plots for Aluminium of 1.61 and 1.189 mm thickness with stand-off distance at 150 mm.

Fig. 5.16 shows explosively formed profiles and maximum deflection versus charge weight plots for Aluminium blanks of 1.189 and 0.671 mm thickness with stand-off distance of 300 mm.

5.2 EFFECT OF STAND-OFF DISTANCE

Tests were carried out on Brass blanks of 0.73 mm thickness with stand-off distance as a variable, keeping charge weight constant at 3.18 gms., to study the effect of stand-off distance on profile and strain distribution of the formed blanks.

The variation of thickness strain, radial strain and deflection are plotted against radial distance in Figs. 5.17, 5.18 and 5.19 respectively
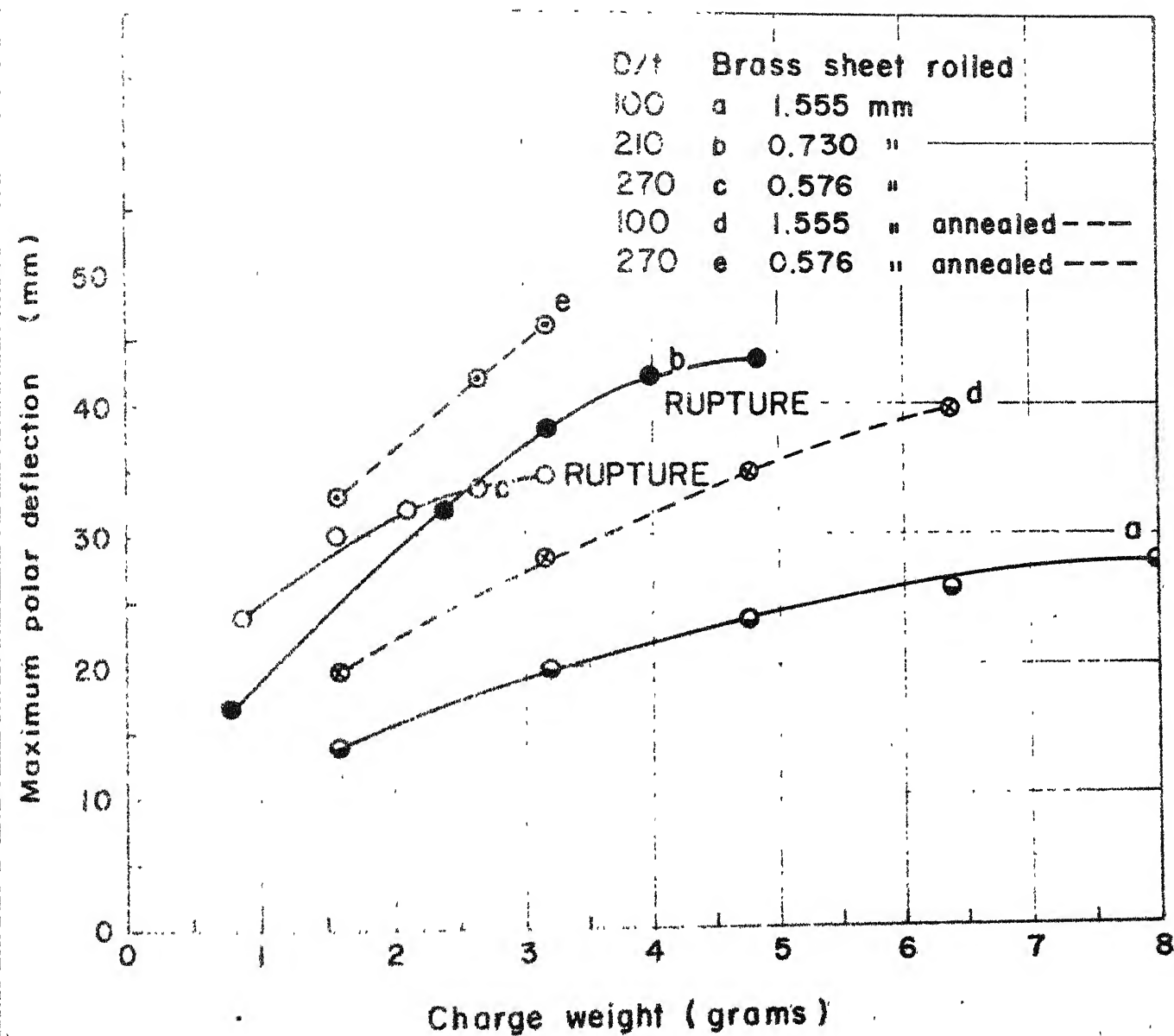
Maximum polar deflection versus charge weight
Matl. Brass, Stand-off 150 mm

Fig. 5.13

CHARGE WEIGHT GRAMS	
a	1.59
b	3.18
c	4.77
d	6.36
e	7.95
f	9.54
g	11.13
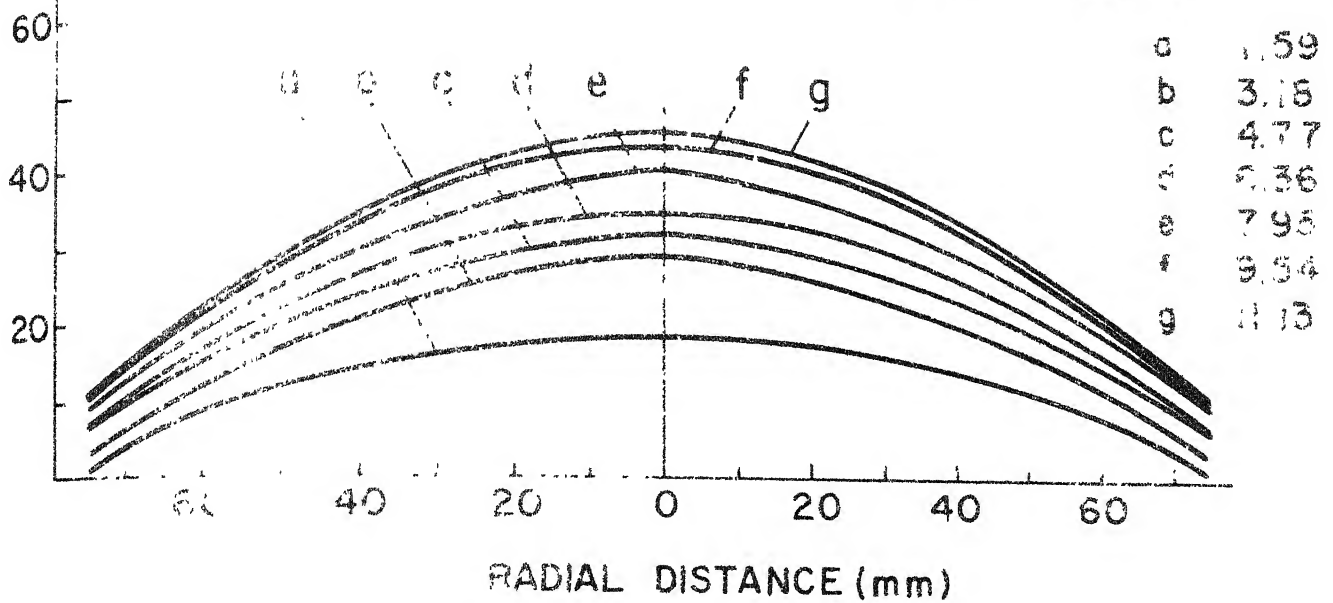
Profile of explosively formed blanks
Matl Stainless steel 304, 0.875 mm
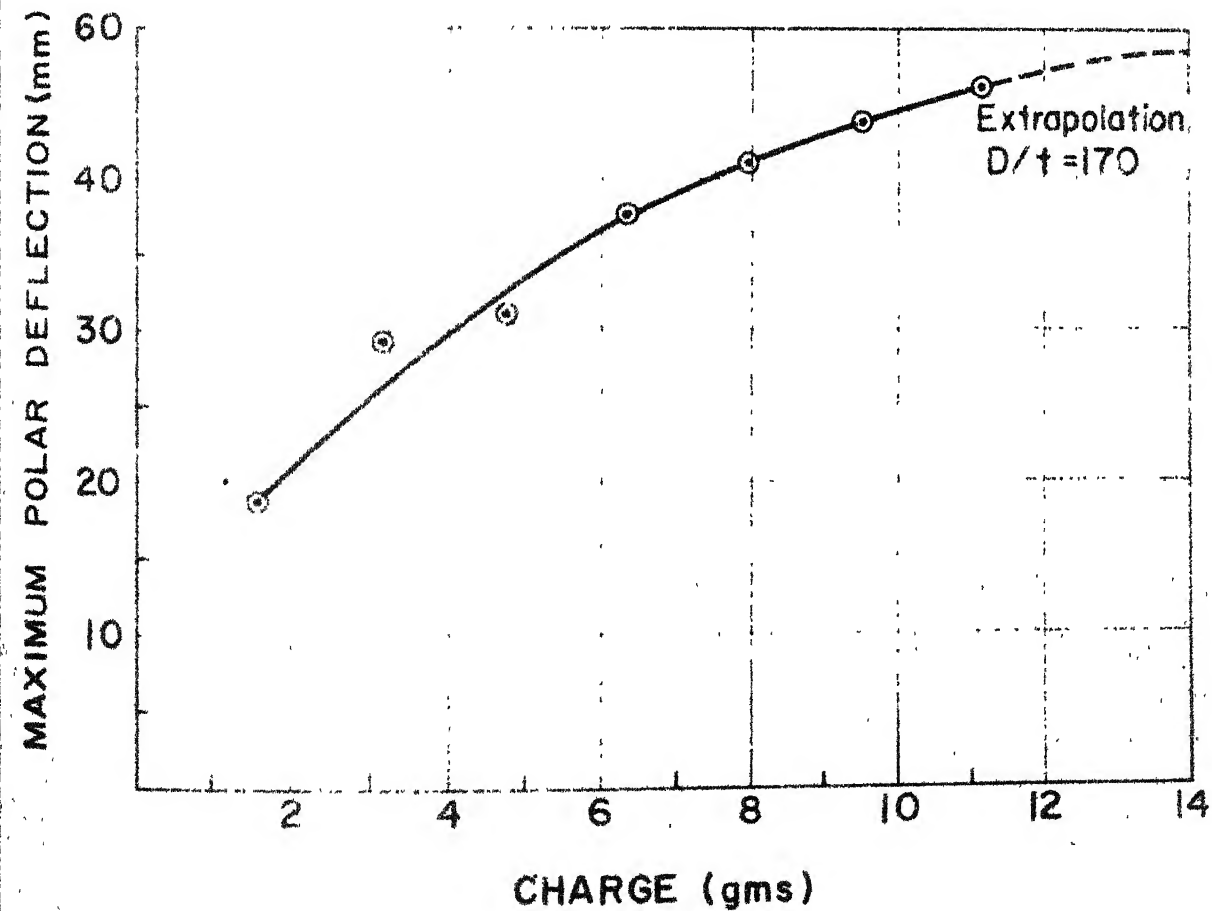
Max. Polar deflection versus charge weight
Matl. Stainless steel 304, stand-off 150 mm.

Fig. 5.14

CHARGE WEIGHT GRAMS

a	0.530
b	0.795
c	1.060
d	1.325
e	1.590

(a) Al. 1.189 mm

CHARGE WEIGHT GRAMS

a	1.06
b	1.59
c	2.12
d	2.65
e	3.18

(b) Al. 1.61 mm

Profiles of explosively formed aluminium blanks

Al. 1.189 mm   Al. 1.61 mm

Maximum deflection versus charge weight
Matl. Aluminium, Stand-off 150 mm

	CHARGE WEIGHT GRAMS
a	0.530
b	1.060
c	1.590
d	2.120
e	2.650
f	3.975
g	4.770
h	5.565
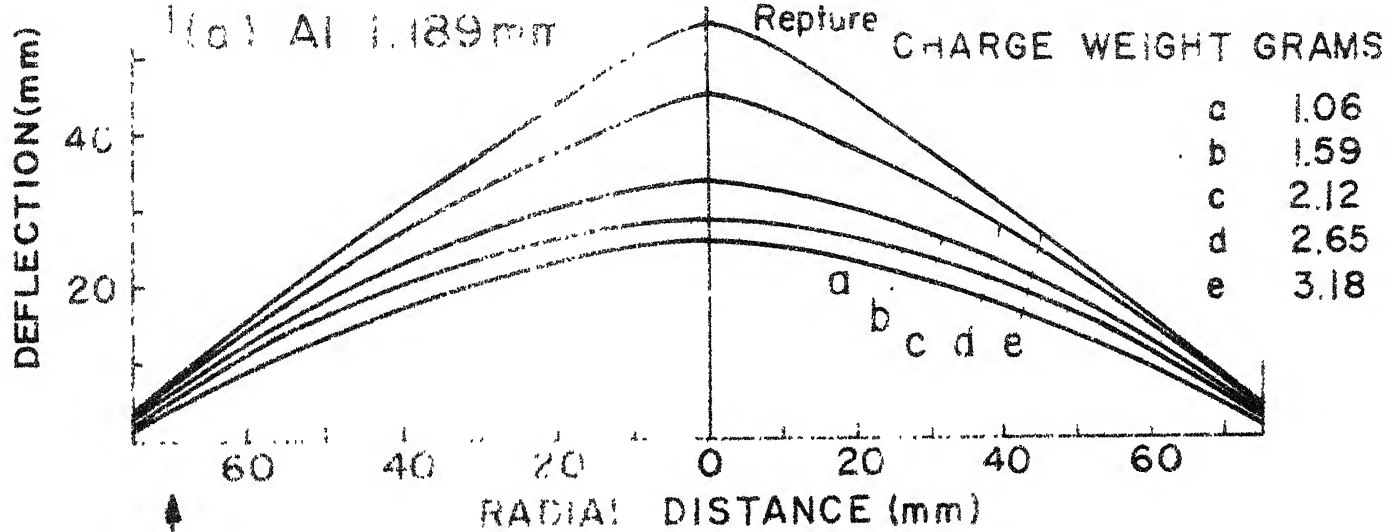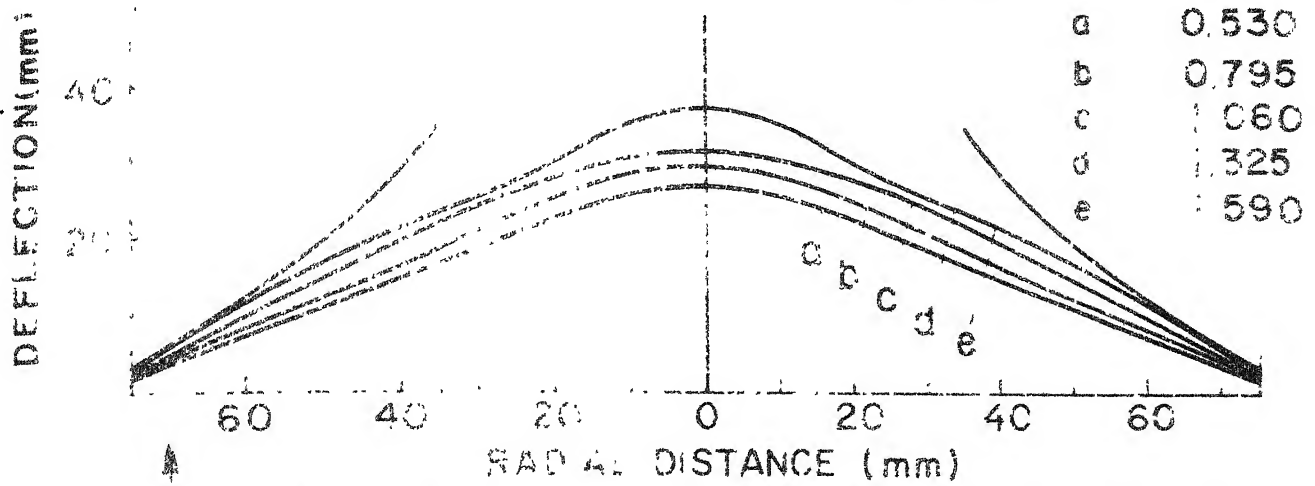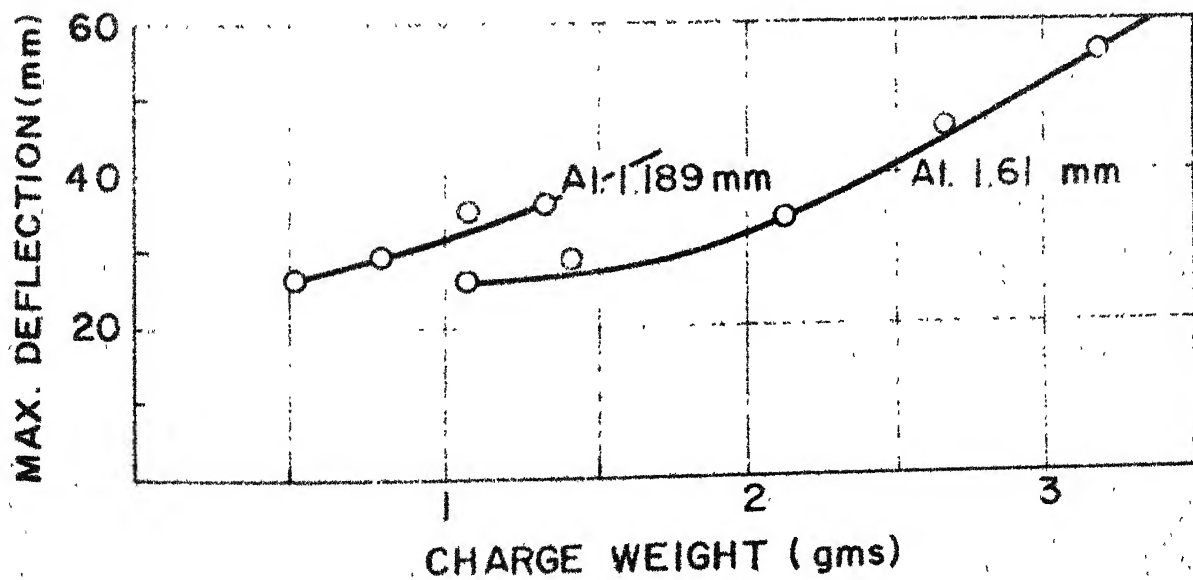
(a)   Aluminium 1.189 mm

	CHARGE WEIGHT GRAMS
a	0.795
b	1.590
c	2.385
d	2.783
e	3.180
f	3.975

(b)   Aluminium 0.671 mm

Profile of explosively formed Aluminium Blanks

THICKNESS
Al. 1.189 mm
Al. 0.67 mm

Maximum deflection   versus charge weight
Matl. Aluminium, Stand-off 300 mm   Fig. 5.16

Thickness strain versus radial distance
Matl. Brass, 0.73mm , Charge weight = 3.18 gms

Fig. 5.17

Radial strain versus radial distance
Matl. Brass 0.73 mm, Charge weight 3.18 gms

Fig. 5.18
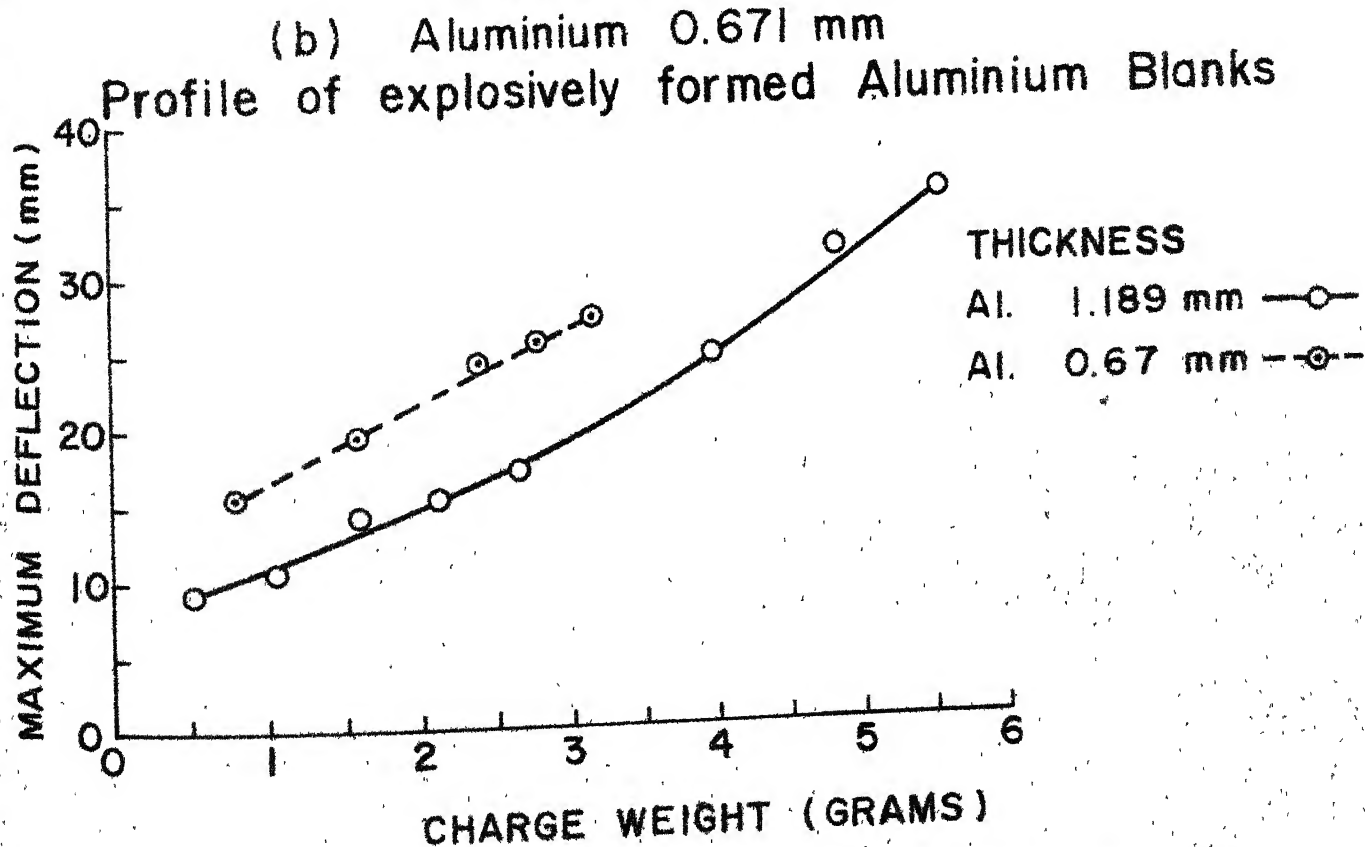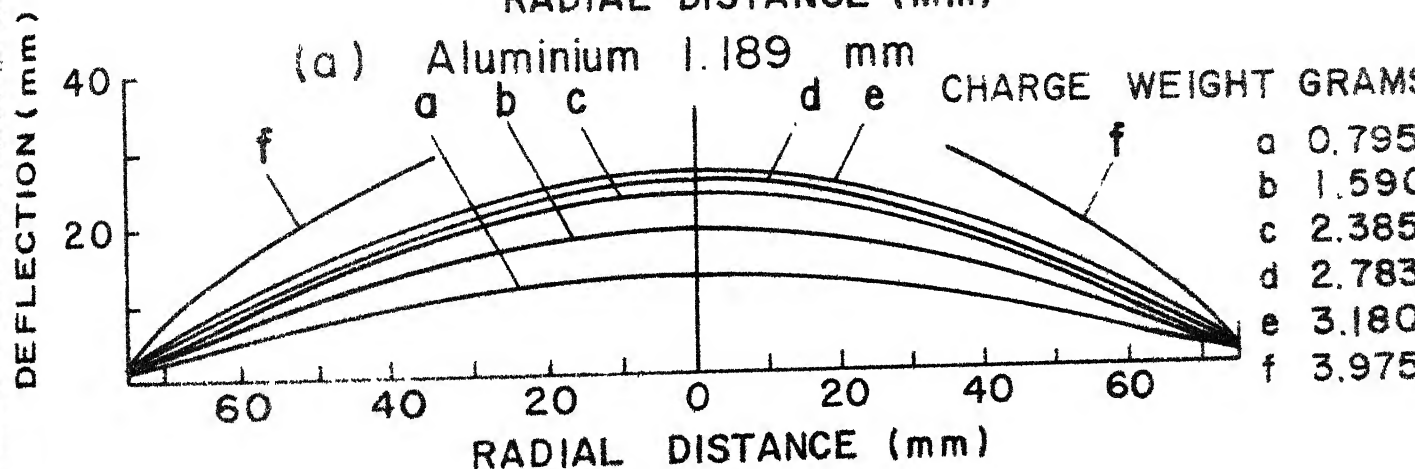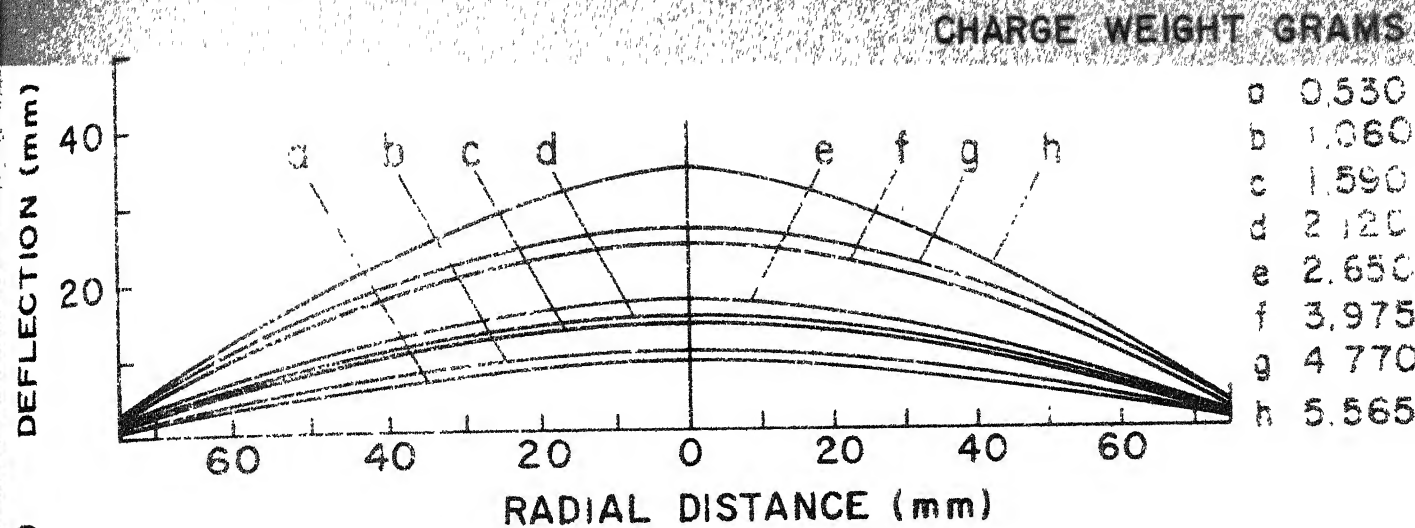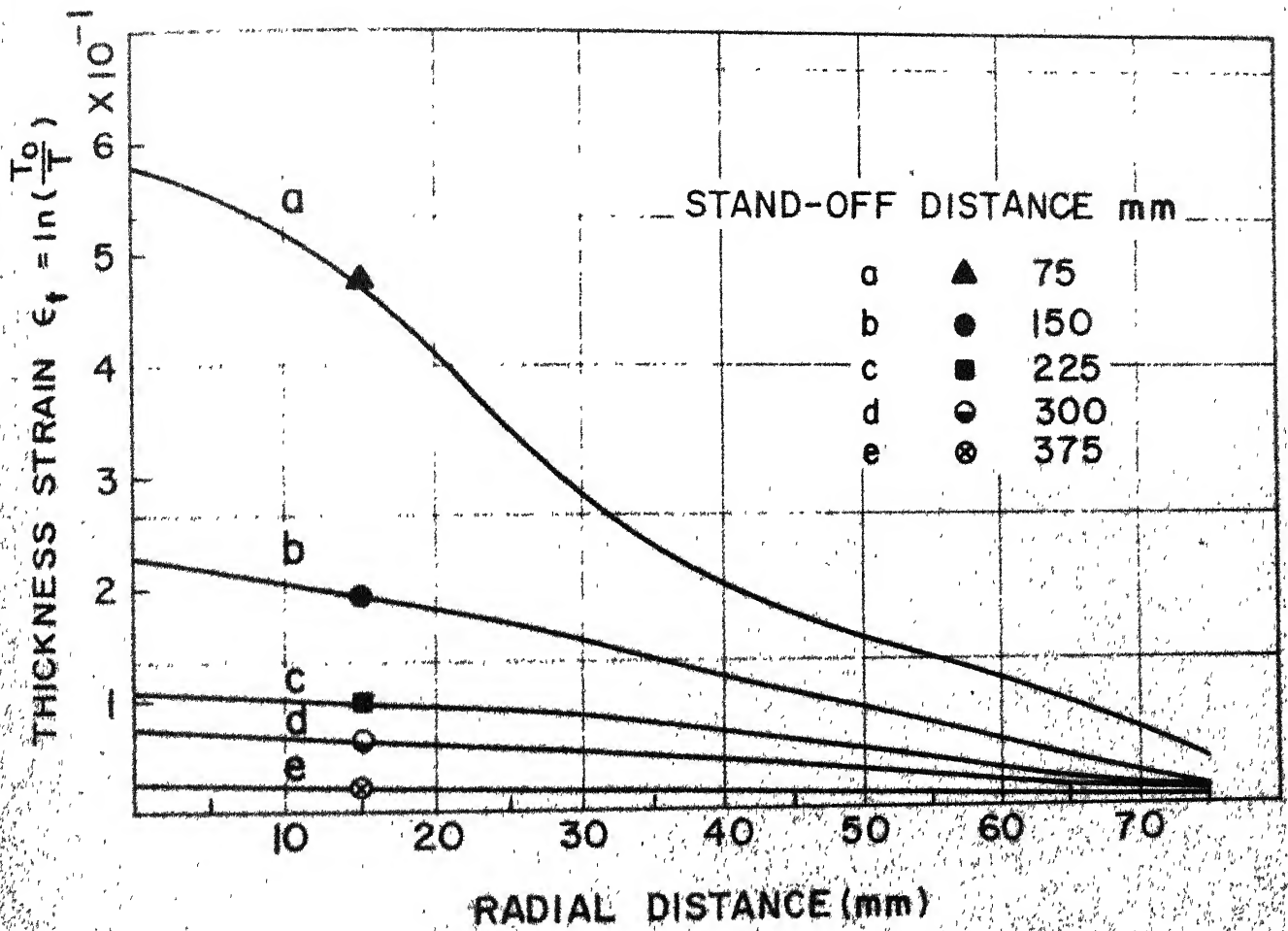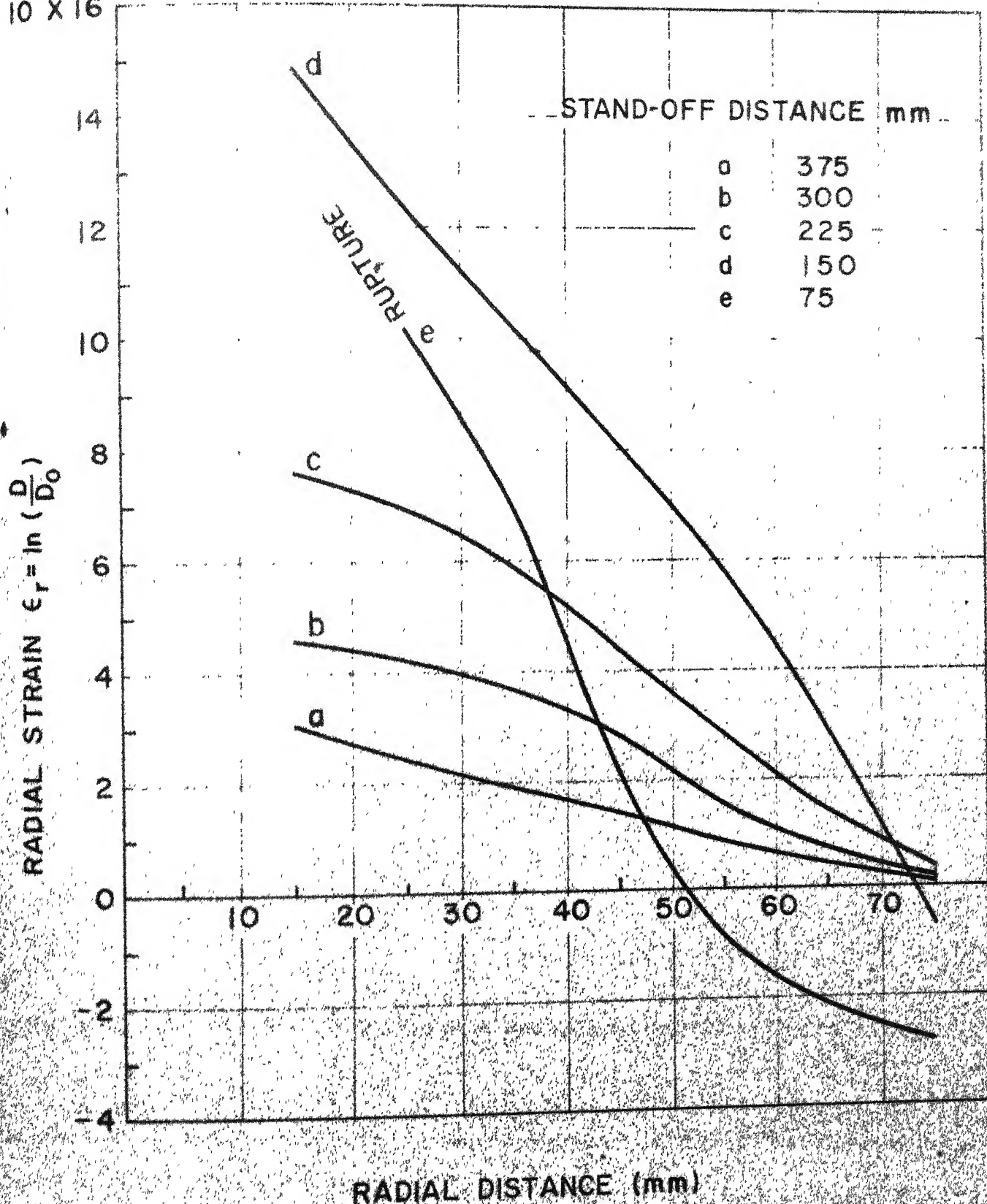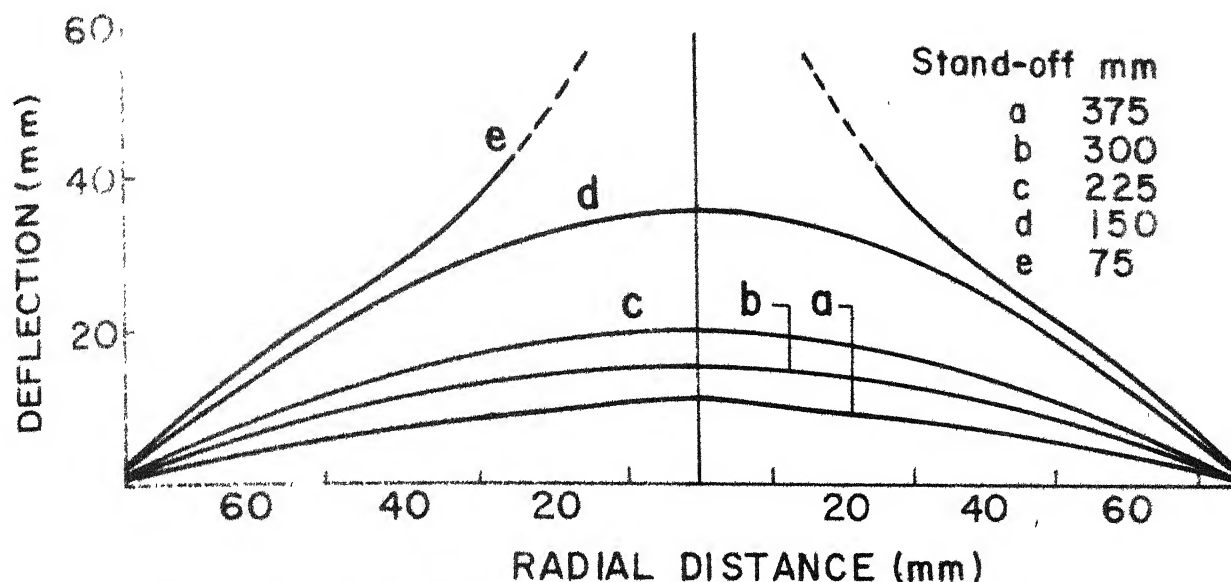
(a) Profiles of explosively formed blanks
Matl. Brass 0.73mm
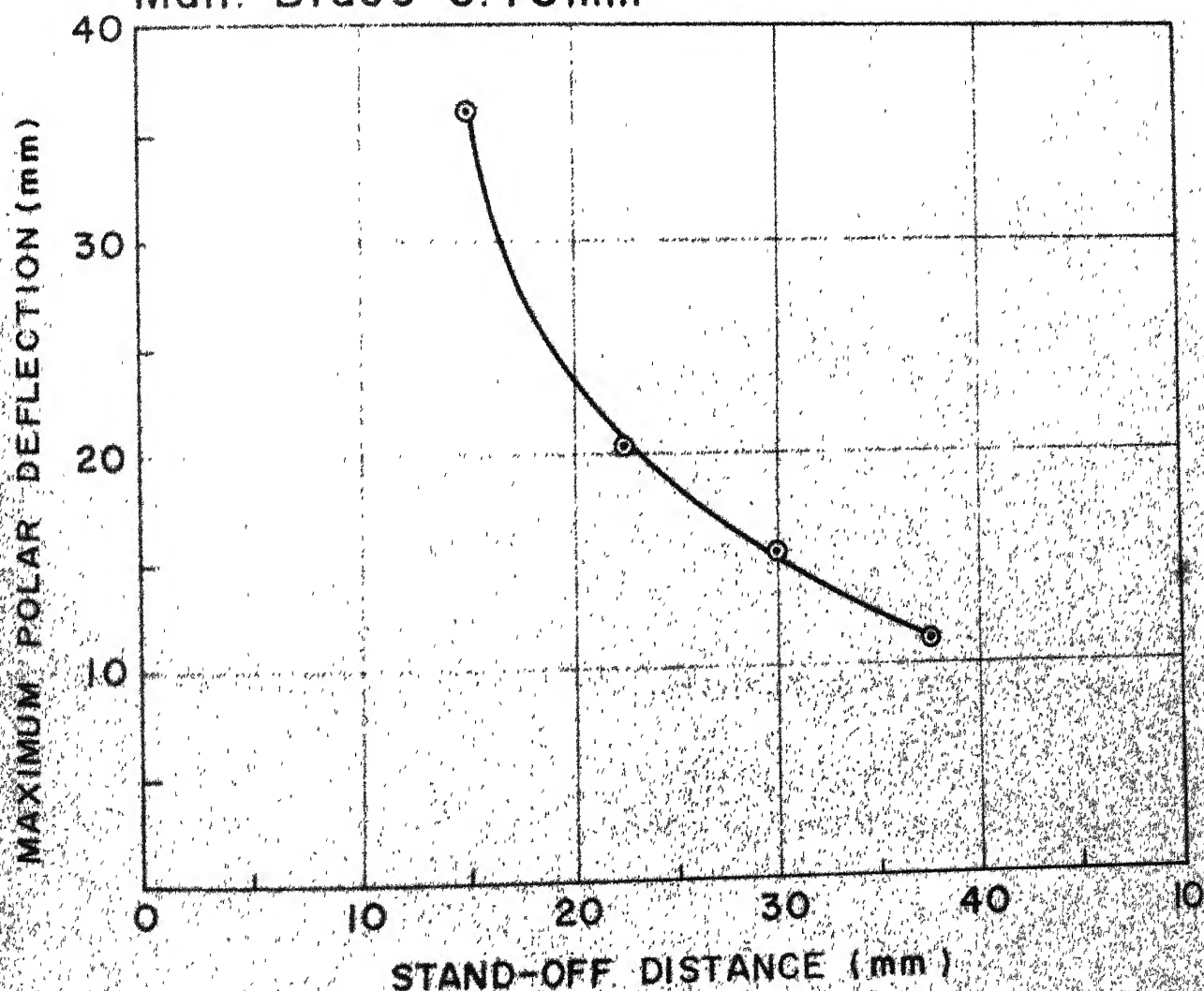
(b) Maximum deflection versus stand-off distance
Matl. Brass, 0.73mm, Constant charge 3.18gm.

Fig 5

5.3 EFFECT OF DRAW RADIUS

The effect of draw radius on the thickness strain and radial strain distribution and profile of blanks are shown in Figs. 5.20 to 5.22. Aluminium blanks of 1.189 mm thickness were formed keeping stand-off distance constant at 300 mm, charge weight constant at 5.565 gms and keeping draw radius a variable parameter.

5.3.1 Thickness Strain Distribution

Logrithmic thickness strain versus radial distance are plotted in Fig. 5.20.

5.3.2 Radial Strain Distribution

Logrithmic radial strain versus radial distance plots are shown in Fig. 5.21.

5.3.3 Maximum Deflection and Profile

Profile of explosively formed blanks and maximum deflection versus draw radius plots are shown in Fig. 5.22.

5.4 EFFECT OF ANNEALING

The effects of annealing on thickness strain distribution, radial strain distribution, and profile on Brass blanks of 1.555 and 0.571 mm thickness are shown in Fig. 5.23 to 5.26.

Thickness strain versus radial distance
Matl. Aluminium 1.189 mm
Charge weight 5.565 gms, Stand off 300 mm
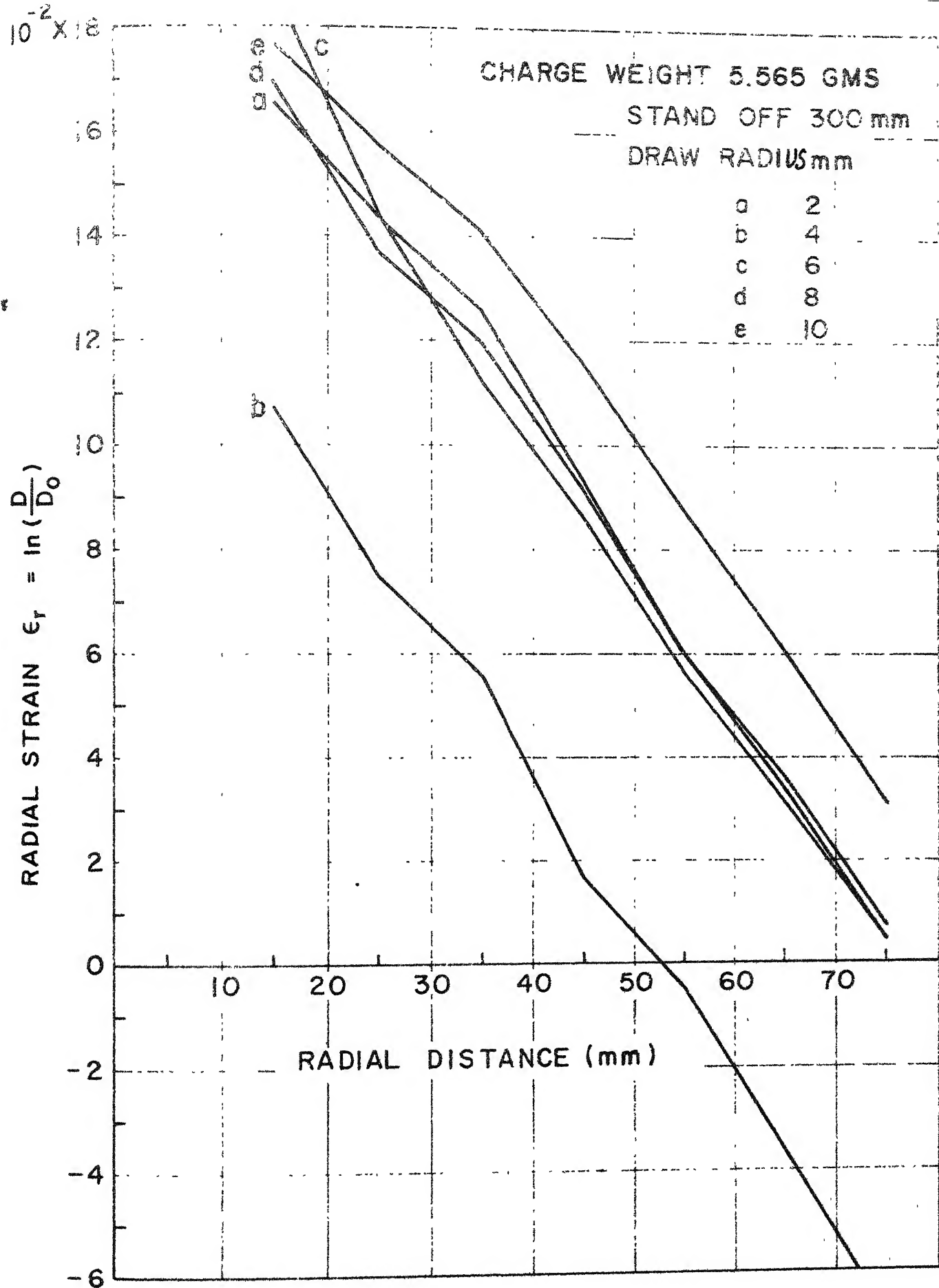
Fig. 5.20

Radial strain versus radial distance
Matl. Aluminium 1.189 mm   Fig. 5.21
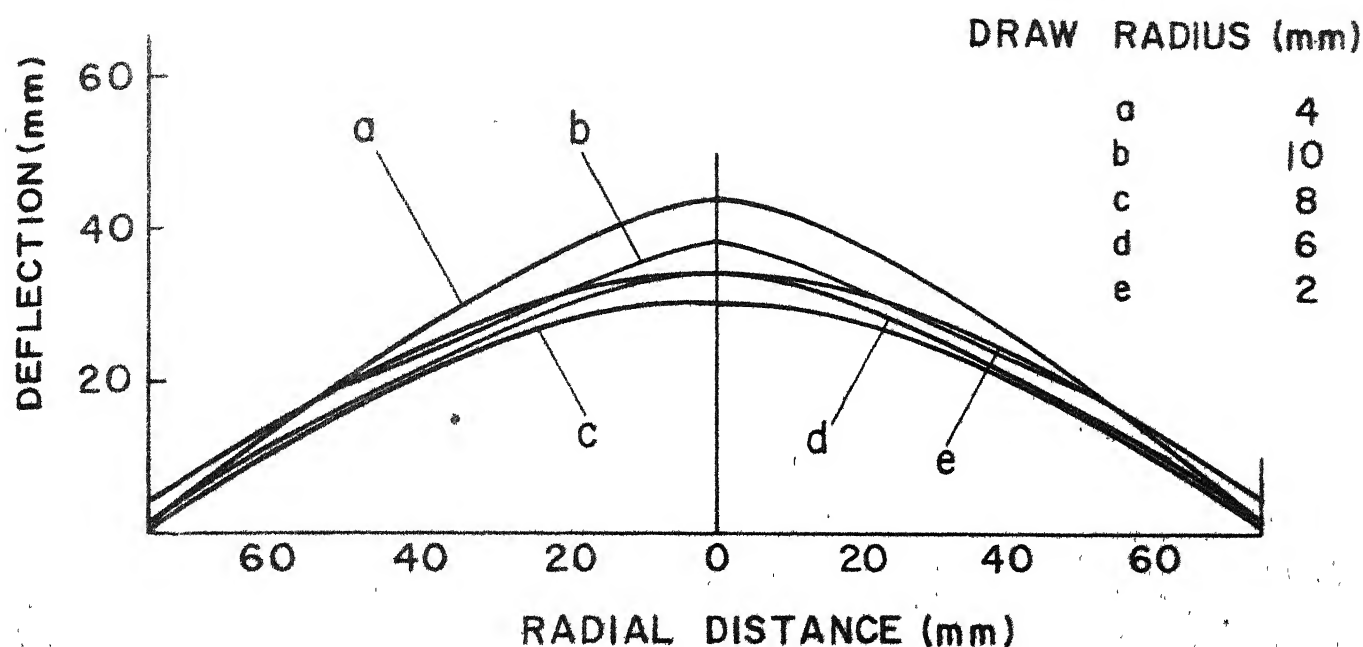
(a) Profiles of explosively formed blanks
Matl. Al. 1.189 mm, Charge weight 5.565 gms
Stand off 300 mm
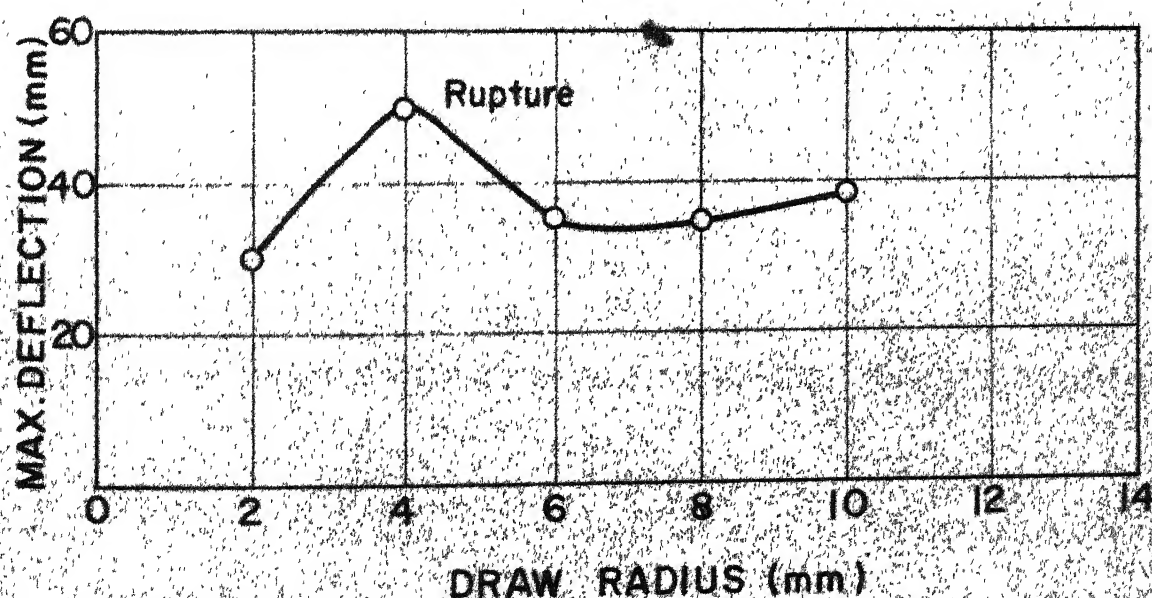
(b) Maximum polar deflection versus draw radius
Matl. Aluminium 1.189 mm, Charge weight 5.565 gm
Stand-off 300 mm
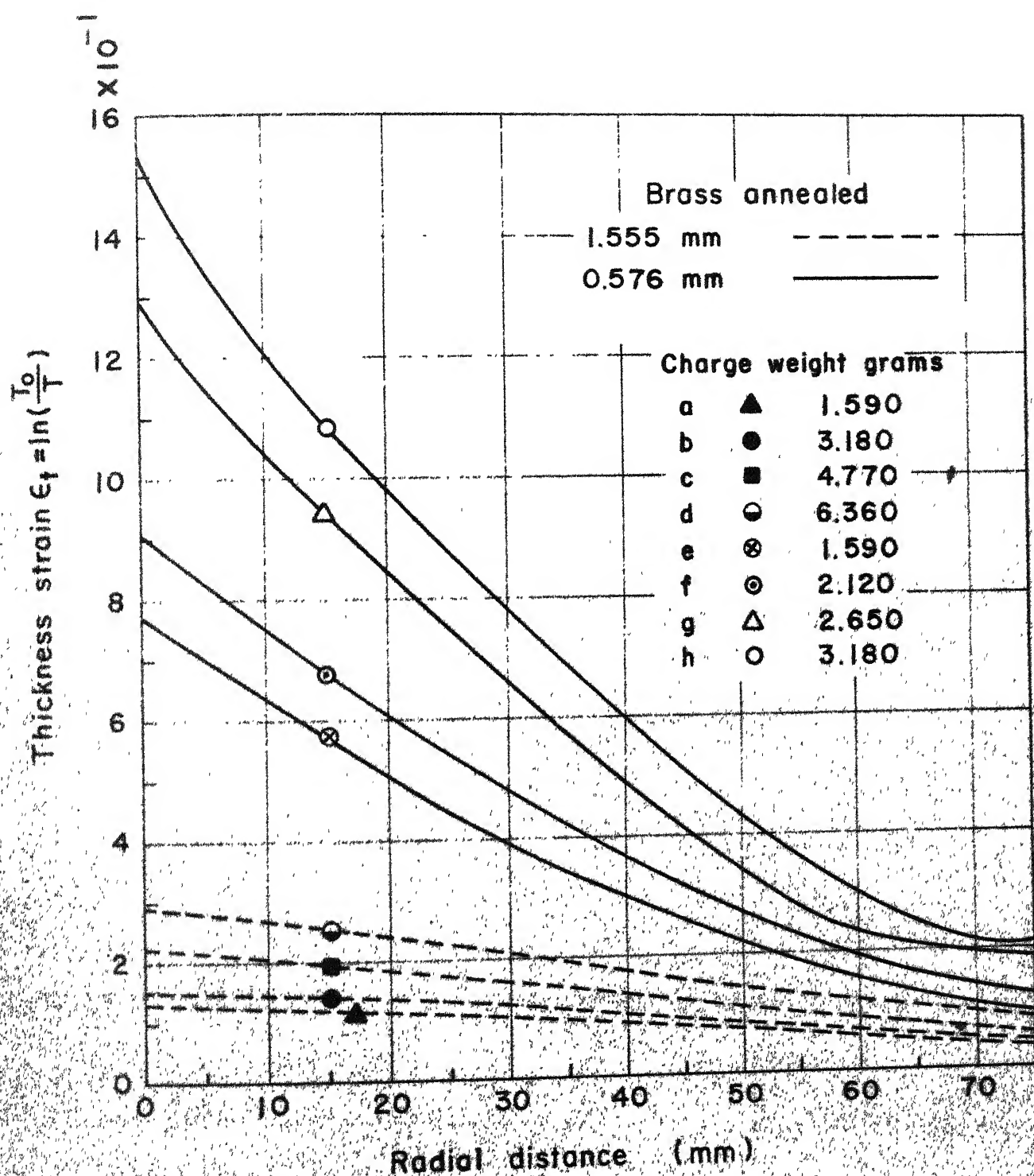
Fig. 5.22

Thickness strain versus radial distance
Matl Brass (annealed), Stand-off =150mm

Fig. 5.23
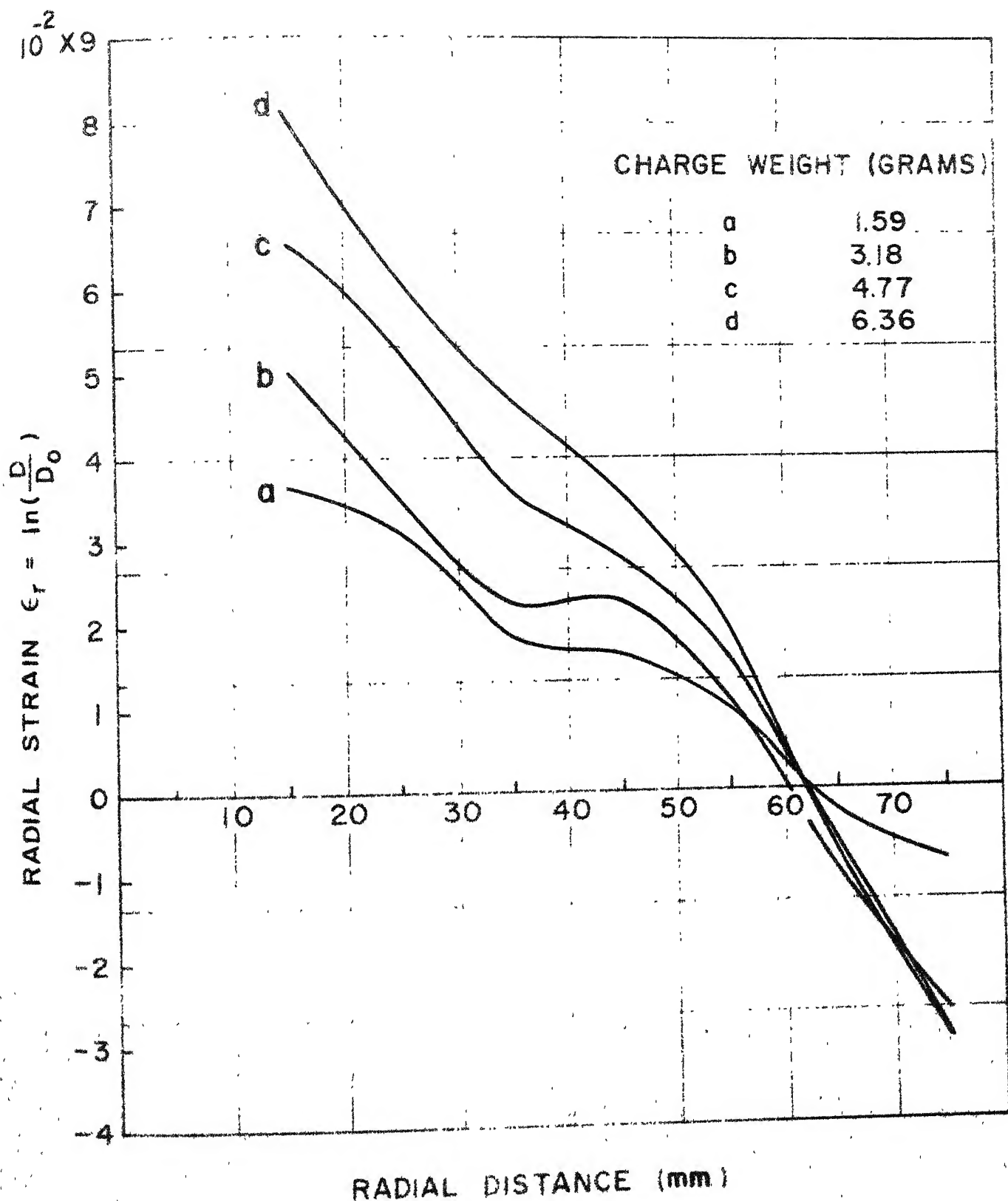
Radial strain versus radial distance
Matl. Brass (annealed)1.555mm, Stand-off 150mm

Fig 5.24

CHARGE WEIGHT GRAMS

a	1.59
b	2.12
c	2.65
d	3.18

Y-axis: RADIAL STRAIN $\epsilon_r = \ln\left(\frac{D}{D_o}\right)$, $10^{-2} \times 20$

X-axis: RADIAL DISTANCE (mm)
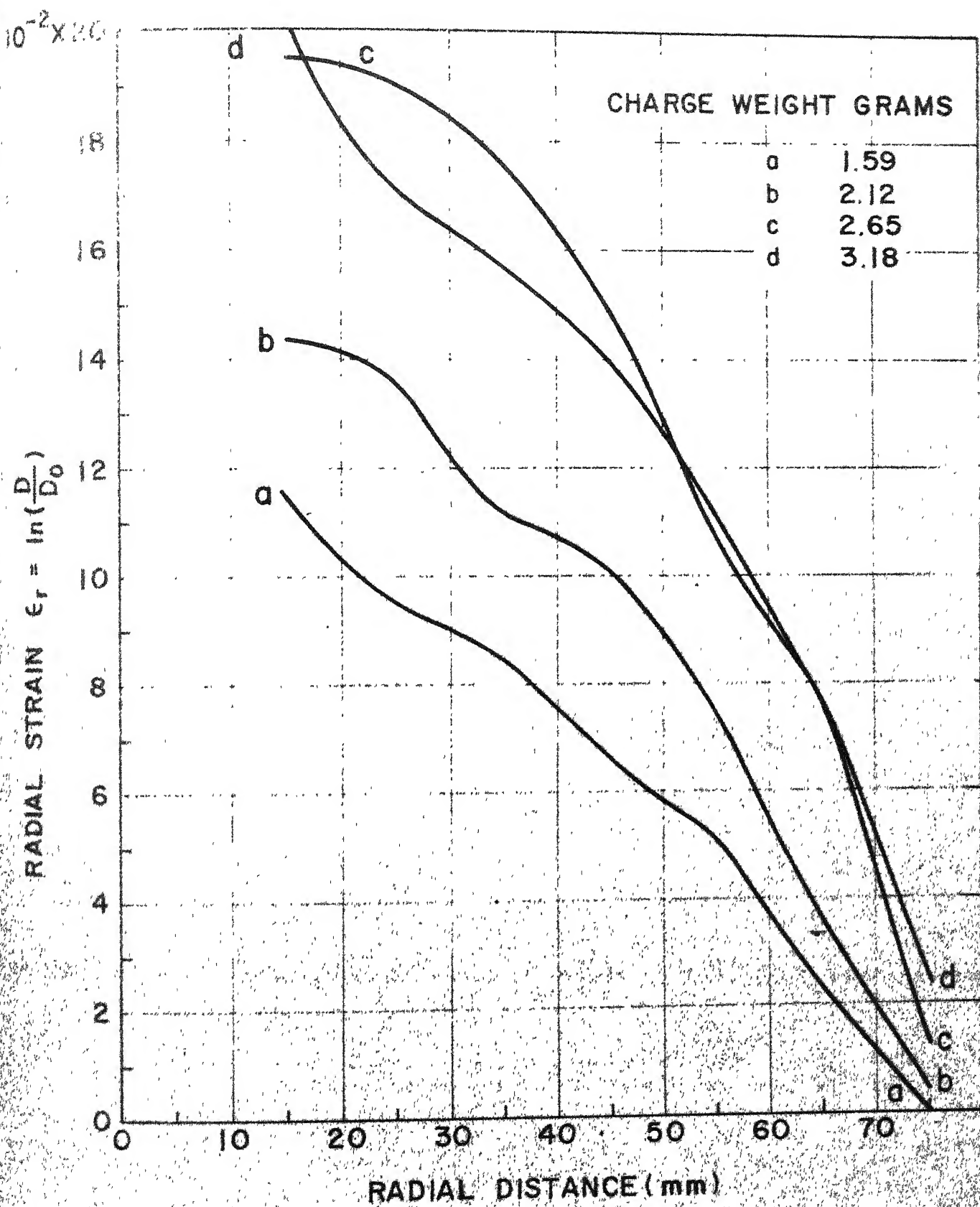
Radial strain versus radial distance
Matl. Brass (annealed) 0.576 mm, Stand-off 150 m
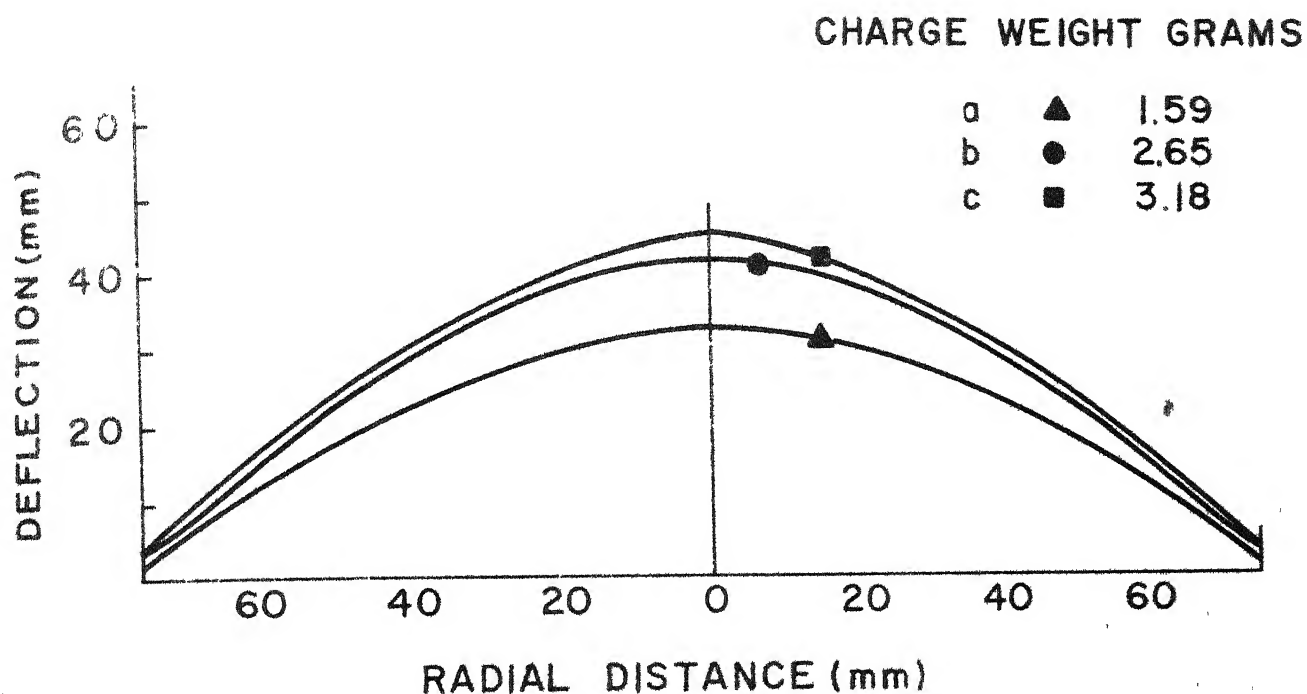
Fig. 5.25

(a)   Brass 0.576 mm (annealed)
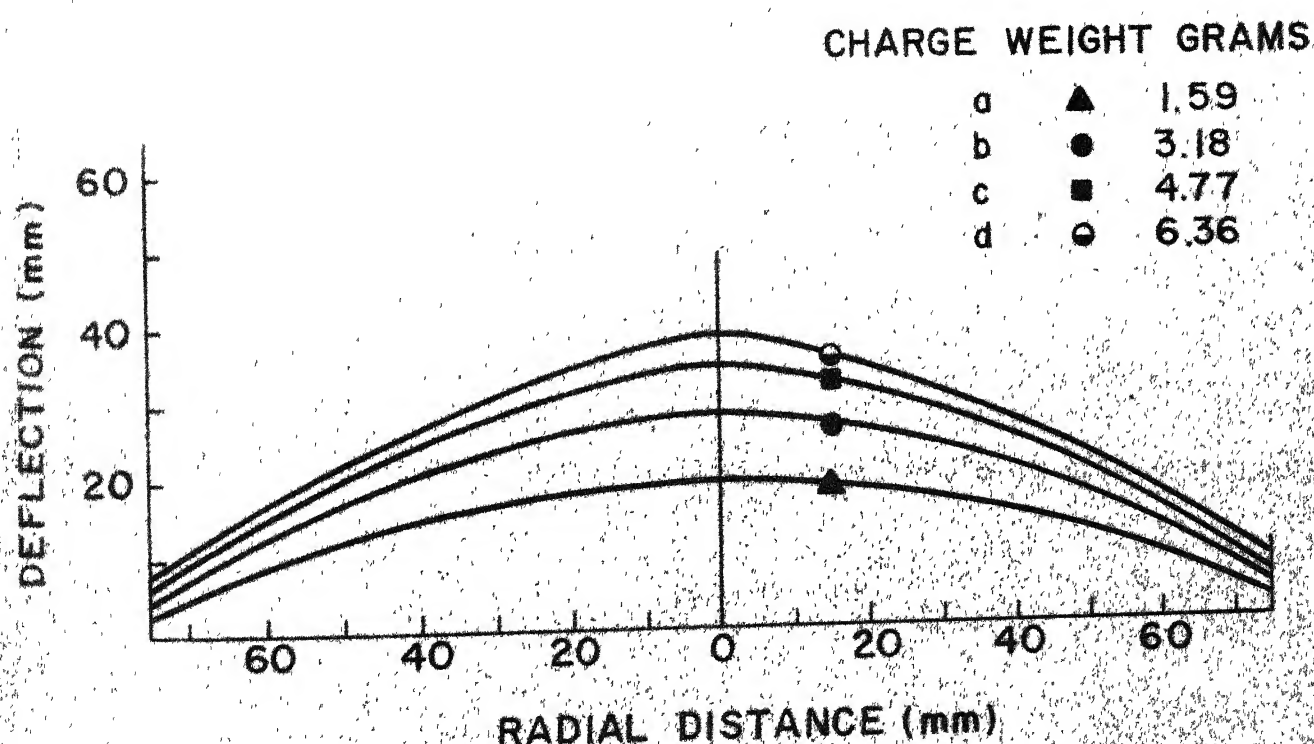
(b)   Brass 1.555 mm (annealed)

Profiles of explosively formed blanks
Matl. Brass (annealed), Stand-off 150 mm

Fig. 5.26

5.4.1 Thickness Strain Distribution

Logrithmic thickness strain versus radial distance plots are shown in Fig. 5.23.

5.4.2 Radial Strain ϵ_r

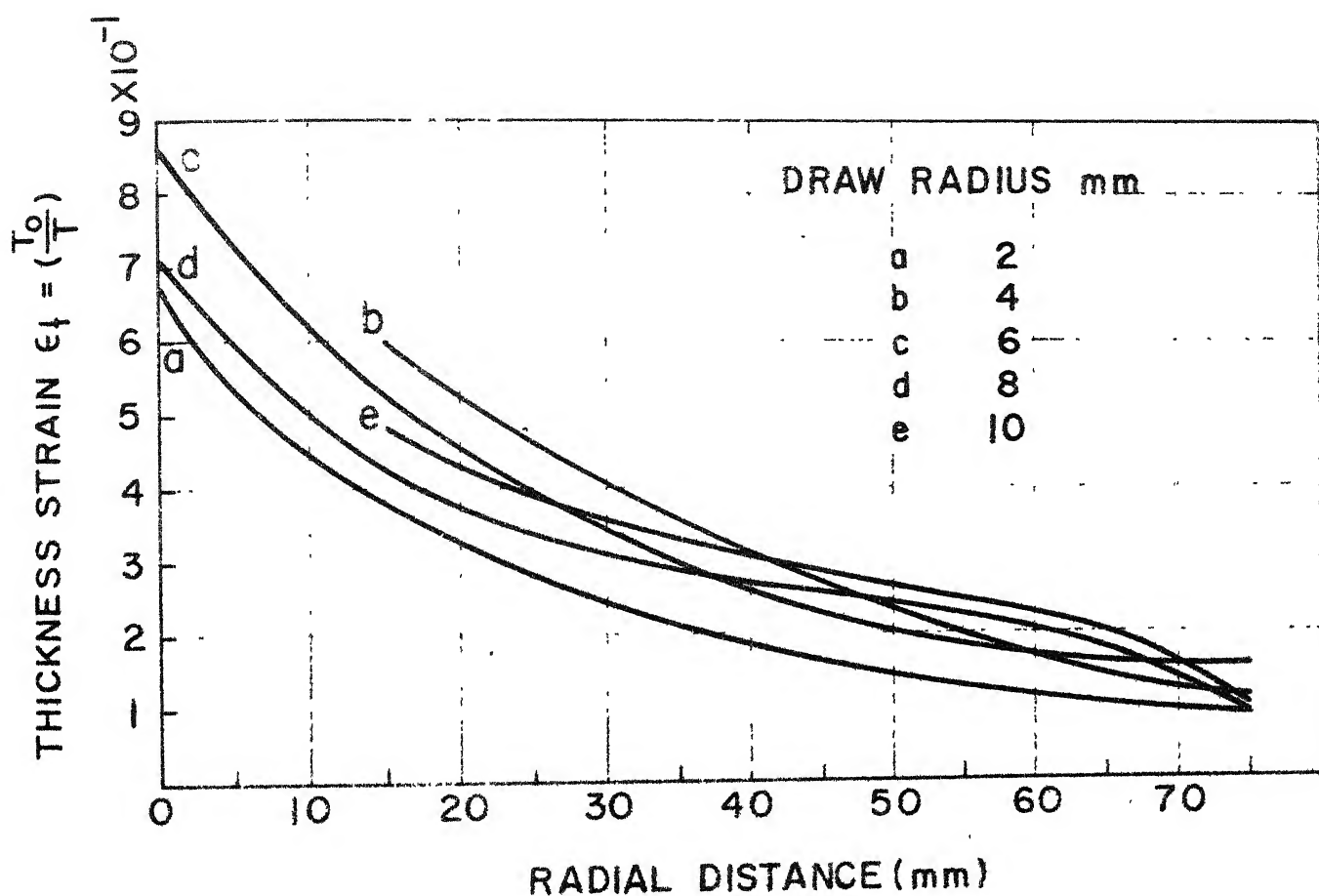Logrithmic radial strains versus radial distance plots are shown in Figs. 5.24 and 5.25.

5.4.3 Profile and Maximum Deflection

Profiles of deformed blanks are shown in Fig. 5.26 Maximum deflection versus charge weight plots are shown in Fig. 5.13.

5.5 HARDNESS

The results of hardness tests carried out on brass blanks rolled and annealed before and after deformation are shown in Table 5.1.

TABLE 5.1

RESULTS OF HARDNESS TESTS

Material thickness	Condition of blank	Stand off distance mm	Charge weight gms.	Maximum deflection h in mm	Vickers Hardness No. before forming	Vickers Hardness No. after deformation at pole	Remark
Brass 0.576 mm	normal	150 mm	1.59	30	120	137	
"	annealed	150 mm	1.59	33	91	153	
"	normal	150 mm	2.65	34	121	146	
"	annealed	150 mm	2.65	42	83	152	
"	normal	150 mm	3.18	Rupture	124	160	reading taken near rupture
"	annealed	150 mm	3.18	46	74	144	

5.6 DISCUSSIONS

5.6.1 Profile of Explosively Formed Domes

For Brass and Stainless Steel sheet (Figs. 5.12 and 5.14 (a)), the profile of the formed dome can be approximated to a parabolic shape specially for lower charge weights. This is also observed by Johnson, et al.[11] (see page 15). For softer material, such as Aluminium, (Fig. 5.15) increases in charge weight changes the shape of the profile from parabolic to a conical one with rounded apex. This was also observed by Hudson[10] who carried out experiments on thin diaphragms of Lead (Fig. 2.1 (a)). The effect of annealing of Brass blanks on the shape of the dome is shown in Fig. 5.26. The tendency of the profile to change from parabolic to a conical shape with increase in charge weight for softer Brass is clearly evident. It is also apparent from Fig. 5.22 that increase in draw radius increases the tendency towards a conical shape due to the flow of the material from the periphery. Fig. 5.19 (a) shows that the nature of profile is not affected by stand-off distance.

It can be concluded that for Brass and Stainless Steel the shape of the explosively formed domes approximates to a parabola provided that small charges are used. However, for annealed Brass and Aluminium, the shape of the dome tends to a conical one, specially with large charge weights.

5.6.2 Polar Deflection

Fig. 5.13 shows the variation of maximum polar deflection with charge weight for Brass sheets with D/t ratio varying from 100 to 270. Curves b and c pertain to cases where the higher charge weight, than the one plotted, produced ruptured dome. However, for the conditions of curves a, d, and e, experiments could not be conducted till rupture of blank. It is evident that the polar deflection increases with increase in charge weight, however, there is an optimum charge weight depending upon D/t ratio. It is also clear that annealing of brass sheets increases the formability by 20% to 50% depending upon D/t ratio.

Fig. 5.14 shows the effect of charge weight on polar deflection for Stainless Steel. Here again experiments could not be continued till rupture because of increasing edge pull-in with increase in charge weight. However, the general trend of the curves in Fig. 5.13 is valid in the case of Stainless Steel also (Fig. 5.14) where the expected optimum charge weight is at 14 gms.

It is seen from Figs. 5.15 and 5.16 (c) that polar deflection for Aluminium blank increases approximately linearly with the charge weight till rupture takes place. It is seen from Fig. 5.19 that for Brass polar deflection decreases hyperbolically with increase in stand off distance.

The effect of die radius on deflection is shown in Fig. 5.22. The maximum deflection occurs at a draw radius of 4 mm. However, there was a clear rupture as shown in Fig. 5.27 (a). It is not surprising that the fracture took place for a draw radius of 4 mm even after the experiment was repeated because the charge weight of 5.565 gms was close to the optimum charge as seen in Fig. 5.16 (c) for a blank thickness of 1.189 mm. As such no firm conclusion can be drawn as to the effect of draw radius on polar deflection.

5.6.3 Estimation of Polar Deflection-h

To establish some relationship between polar deflection 'h' and other parameters, a simple theory given by Noble and Oxley[18] (see page 19) was used. Polar deflection parameter h^2 is plotted against θ^2 W/t Y in Fig. 5.28. A linear relationship as proposed by Noble and Oxley is true to a first approximation. For the experimental conditions investigated, the efficiency of the process η is 37.8%. This also agrees with the result of Noble and Oxley, who estimated an efficiency of $\eta = 38.6\%$. It should be pointed out that the relationship proposed by Noble and Oxley[18] is valid for small value of solid angle 2θ, which implies a large stand off distance as compared to the diameter of blank. The present investigation pertains to

a value $\theta = 14°$ and $\theta = 26.6°$ for (50 mm and 300 mm stand off distance respectively.

5.6.4 Mechanism of Rupture

Typical ruptured specimens are shown in Fig. 5.27. It is observed that necking initiates in the direction of rolling at pole as shown in Fig. 5.27 (a). With higher charge weight, rupture proceeds along the direction of rolling and finally the blank opens up at about 85° inclination to the direction of rolling as shown in Fig. 5.27 (b).

5.6.5 Effect of Charge Weight on Thickness Strain, ϵ_t.

It is observed from Fig. 5.01, that for Brass the thickness strain varies almost linearly from pole to periphery of blank, specially for higher thickness of 1.555 mm corresponding to D/t ratio of 100.

Approximately linear variation of thickness strain for Stainless Steel (Fig. 5.02) is also valid for all the charge weights except for the charge weight of 11.13 gms where the strain increases sharply towards the centre.

For the case of Aluminium (Fig. 5.03) the variation of thickness strain is approximately linear with lower values of thickness and charge weight. However, with decrease in stand off distance from 300 mm to 150 mm, the rate of increase of thickness strain increases as

(a)   (b)

Rupture of blanks

Conditions:	a	b
Matl.	Al. 1.189 mm	Al. 1.189 mm
Charge weight	5.565 gms	1.59 gms
Stand off distance	300 mm	150 mm
Draw radius	10 mm	6 mm

Fig. 5.27

a STAINLESS STEEL 0.875 mm x
b BRASS   1.555 "   •
c   "   0.730 "   ⊙
d   "   0.576 "   +
e ALUMINIUM   1.610 "   ◀
f   "   1.189 "   ○
g   "   0.671 "   ■
h BRASS   0.730 "   △
     (VARIABLE STAND-OFF)

h^2 (mm^2)

θ^2 W/tY
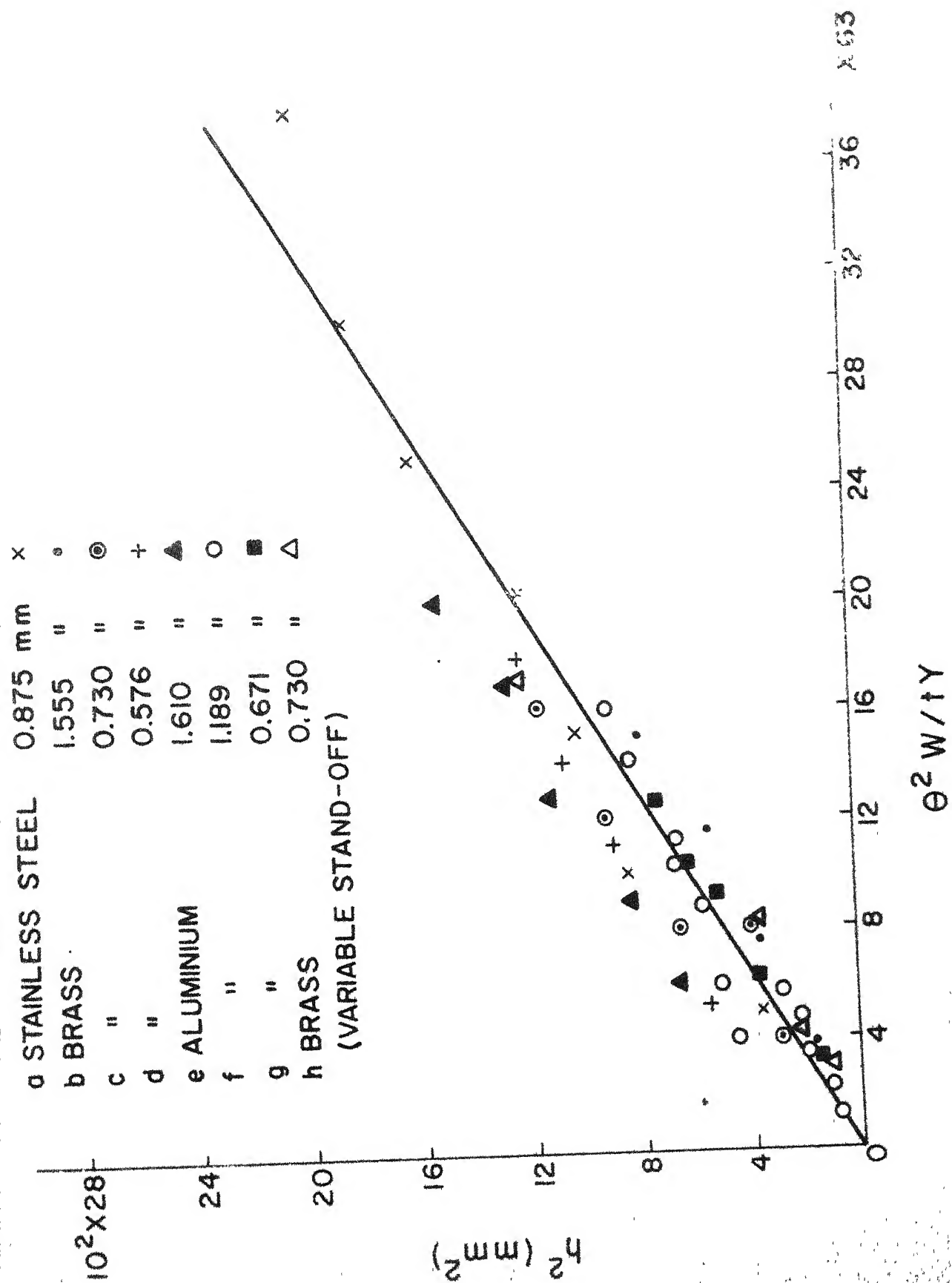
h^2 versus θ^2 W/tY (Ref. 18)

Fig. 5.28

one approaches the pole even for lower values of charge
weight (Fig. 5.04).

The effect of stand-off distance on thickness
strain for the case of Brass is clear from Fig. 5.17. It
is seen that the nature of variation of thickness strain
with radial distance changes appreciably with stand-off
distance. It is also seen from Fig. 5.23 that annealing
Brass of thickness 0.576 mm changes the nature of varia-
tion of thickness strain.

The variation of polar thickness strain with
charge weight is plotted in Fig. 5.29 for various materials
tested. It is seen that for most of cases shown, polar
thickness strain increases steeply with increase in charge
weight.

5.6.6 Radial Strain, ϵ_r

It is seen from Figs. 5.05 to 5.07, 5.24 and 5.25
for Brass that the radial strain ϵ_r decreases with
increase in radial distance, and it is maximum at the pole.
The results in Figs. 5.07 and 5.24 are erratic because
it was not possible to avoid edge pull-in as is evident
from negative radial strains at periphery even with maxi-
mum tightening of bolts.
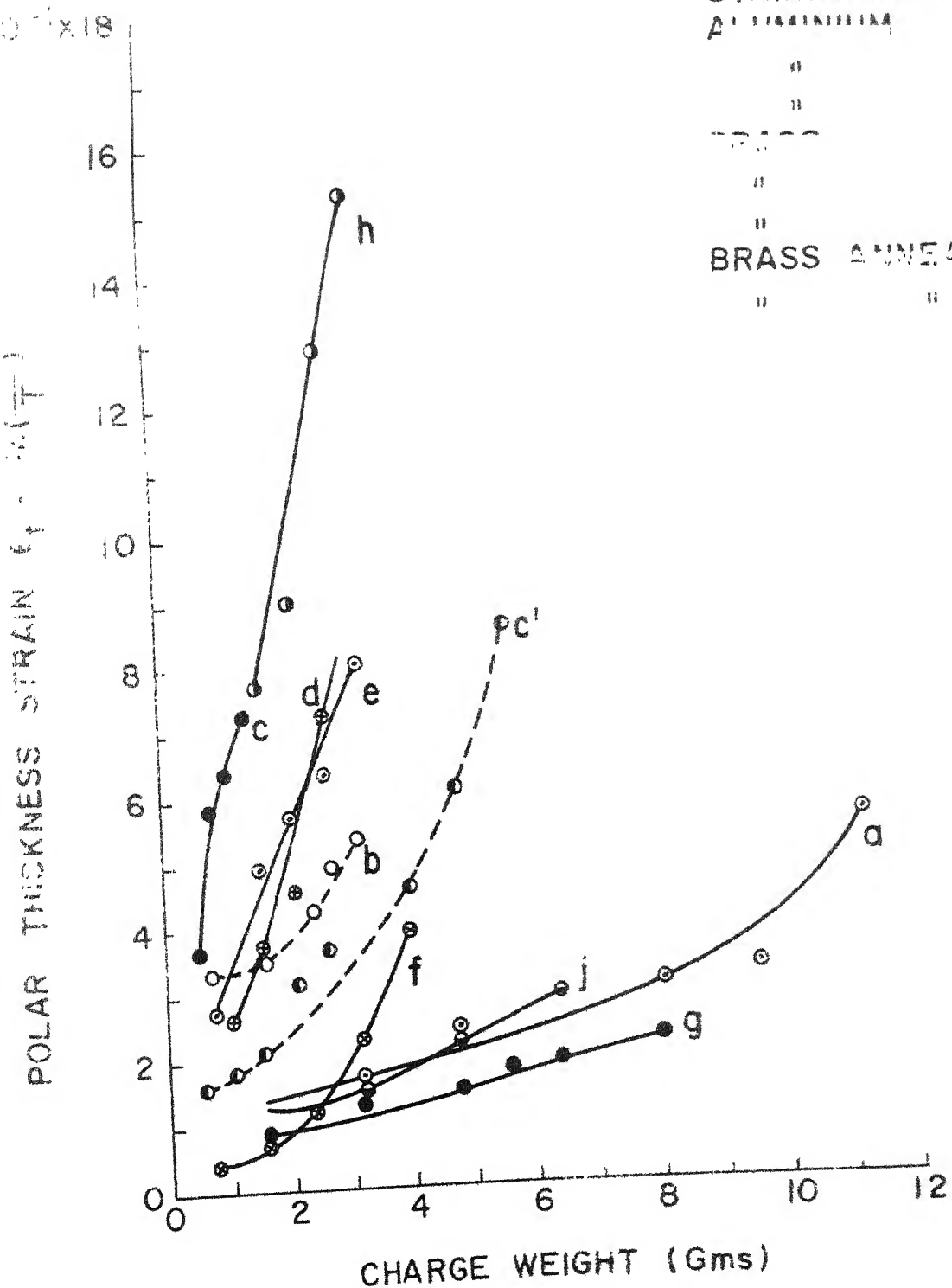
Polar thickness strain versus charge weight

Fig 5.29

For the case of Stainless Steel (Fig. 5.08), the fall in ϵ_r with radial distance is apparent and the negative values of ϵ_r are due to edge pull-in.

For the case of Aluminium (Figs. 5.09 to 5.11), the change of radial strain follows clear pattern and there is no evidence of edge pull-in.

The effect of stand-off distance on distribution of radial strain is shown in Fig. 5.18. Except for curve (e), which pertains to a ruptured specimen, the radial strain at a particular point decreases with increase in stand-off distance.

It is seen from Fig. 5.21 that the radial strain is affected, marginally, by varying the draw radius in explosively stretch forming operations (curve - b is ignored as it pertains to a ruptured blank).

Fig. 5.30 shows plots of polar radial strains against charge weight. In most of the curves, polar radial strain increases steeply with increase in charge weight. Curves 'a' and 'g' pertain to cases where large edge pull-in was observed.
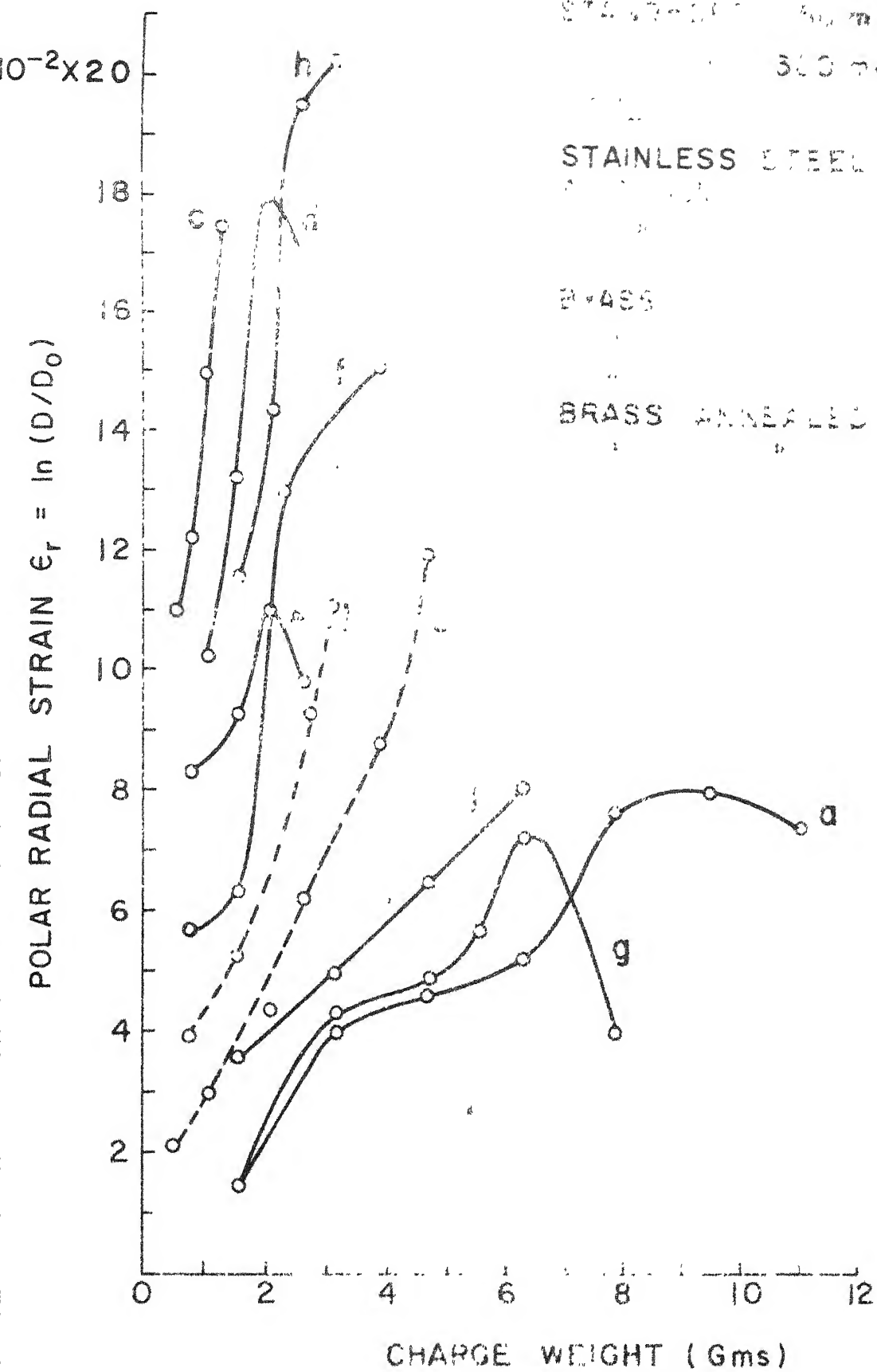
Polar radial strain versus charge weight

Fig 5.30

CHAPTER VI

CONCLUSIONS AND SUGGESTIONS FOR FURTHER WORK

6.1 CONCLUSIONS

The following broad conclusions are drawn from
the results of the experimental investigation into explosive
forming described in this work. The conclusions are valid
for the case of stretching process where the blank is
restrained at periphery.

1. For high strength strain hardening materials, such as
    Brass, the shape of the explosively formed dome
    approximates to a parabola, specially for lower charge
    weights.

2. There is a marked tendency for the profile to change to
    a conical shape with a) softer materials such as
    annealed Brass and Aluminium and b) higher charge
    weights approaching optimum values.

3. For harder materials there is an optimum charge weight
    to give maximum polar deflection depending on D/t ratio.

4. For softer materials such as Aluminium the polar deflec-
    tion increases linearly with increase in charge weight
    till rupture.

5. The polar deflection decreases hyperbolically with
    increase in stand-off distance.

6. An approximate estimation of charge weight for a given polar deflection can be made from a simple theory proposed by Noble and Oxley[18] by the following expression

$$h^2 \propto \frac{\varrho^2 \, W}{t \, Y}$$

7. The rupture of blanks initiates at the poles proceeds in the direction of rolling and finally the blank opens up at $85°$ inclination to the direction of rolling.

8. The thickness strain varies approximately linearly with radial distance, (a) with lower values of charge weight as compared to optimum charge weight and (b) with softer materials; provided the stand-off distance is large as compared to diameter of blank.

9. Thickness strain and radial strain increase steeply with increase in charge weight.

6.2 SUGGESTIONS FOR FURTHER WORK

The experimental facility outlined in this work can be used for carrying out further research work in the following aspects of explosive forming.

1. Studies of stress distribution during the movement of blank.

2. Phenomena of flange wrinkling and blank buckling
    can be studied by suitably modifying the die-
    assembly in order to apply variable pressure on
    blank.

3. Effect of shape of charge on the profile produced.

4. Explosive blanking and drawing operations can also
    be carried out by modifying the die.

REFERENCES

1. Bahrani, A.H. and B. Crossland, "Use of Explosives for Engineering Part I", Metal and Materials, Vol. 2, 1968, p. 41

2. Johnson, W. and R. Sowerby, "Experiments on Clamped Blanks Subject to an Under-water Explosive Charge", Proc. I. Mech. E., Vol. 179, Part I, No. 7, 1964-65, p. 197.

3. Rinehart, J.S. and J. Pearson, "Explosive Working of Metals," Pergamon, 1963.

4. Kolsky, H., "Stress Waves in Solids", Oxford University Press, 1953.

5. Bahrani, A.H. and B. Crossland, "Use of Explosives in Engineering Part II", Metal and Materials, Vol. 2, 1968, p. 69

6. Pearson, J., "Metal Working With Explosives", J. of Metals, Vol. 12, 1960, p. 673.

7. Munroe, C.E., "Modern Explosives", Scribber's Magazine, Vol. 3, 1888, p. 563.

8. Cole, R.H., "Under Water Explosions", Princeton University Press, Princeton, 1948.

9. Penny, W.G. et. al., "A Discussion on Detonation", Proc. of Royal Soc. of London, A 204, 1951, p. 1

10. Hudson, G.E., "A Theory of The Dynamic Deformation of Thin Diaphragm", J. of App. Phy., Vol. 22, 1951, p.1.

11. Johnson, W., J.L. Duncan, K. Kormi, R. Sowerby, and F.W. Travis, "Some Contributions to High Rate Sheet Metal Forming", Proc. 4th International MTDR Conference, Manchester, Sept. 1963, p. 237 (Pergamon)

12. Boyd, D., "Dynamic Deformation of Circular Membranes", J. of Engineering Mechanics Division, Proc. of the A.S.C.E., Vol. 92, No. EM 3, June 1966.

13. Johnson, W. and F.W. Travis, "Experiments on the Dynamic Deformation of Clamped Circular Sheets of Various Metals Subject to an Underwater Explosive Charge", Sheet Metal Industries, Vol. 39, No. 423, July 1962, p. 456.

14. Remmerswaal, J.L., "Peaceful Use of Explosives", Sheet Metal Industries, Vol. 39, No. 923, July 1962, p. 475.

15. Johnson, W., J.L. Duncan, K. Karmi, R. Sowerby, and F.W. Travis, "Some Contributions to High Rate Sheet Metal Forming", Proc. 4th International MTDR Conference, Manchester, Sept. 1963, p. 289.

16. Corbett, S.E. and A.W. Bicker, "Some Small Scale Experiments in Explosive Forming", Sheet Metal Industries, Vol. 39, No. 423, July 1962, p. 555.

17. Thurstan, G.A., "On the Effects of Edge Pull-in on the Explosive Forming of Domes", Proceedings of the 7th International MTDR Conference, Sept. 1966, Pergamon Press, p. 129.

18. Noble, C.F. and P.L.B. Oxley, "Estimating Charge Size in Explosive Forming of Sheet Metal", Proc. 5th International MTDR Conference, Birmingham, 1964, p. 329 (Pergamon).

19. Raisinghani, Murlidhar, "The Behaviour of Ferrocement Slabs Under Different Loads", Ph.D. Thesis submitted in 1976, I.I.T. Kanpur.

ME-1977-M-REK-EXP.